ANALYTICAL METHODS FOR EVALUATING TWO-DIMENSIONAL EFFECTS IN FLAT-PLATE SOLAR COLLECTORS

by

Clifford Keith Rice

Dissertation submitted to the Graduate Faculty of the
Virginia Polytechnic Institute and State University
in partial fulfillment of the requirements for the degree of

DOCTOR OF PHILOSOPHY

in

Mechanical Engineering

APPROVED:

William C. Thomas
W. C. Thomas, Chairman

Ronald J. Onega
R. J. Onega

J. R. Thomas
J. R. Thomas

Harold A. Kurstedt
H. A. Kurstedt

G. H. Beyer
G. H. Beyer

April 1978

Blacksburg, Virginia

ACKNOWLEDGMENTS

I wish to express my sincerest gratitude to Dr. William C. Thomas for his guidance throughout this work. The support from the NSF-ERG Traineeship program is gratefully acknowledged. The author would like to thank Debbie Wolfe and Carolyn Flora for their work in preparing the manuscript, M. D. Harsh for his help in preparing the figures, and John Teachman for computer assistance. Special thanks are extended to my wife for her patience and helpfulness.

TABLE OF CONTENTS

TABLE OF CONTENTS (Continued)

LIST OF TABLES

LIST OF FIGURES

LIST OF FIGURES (Continued)

NOMENCLATURE

General

a	$(W - D)/2L$
a_1, a_2, a_3	Non-dimensional parameters defined in Appendix II
$\underline{\underline{A}}$	$(M_T + 1) \times (M_T + 1)$ matrix of constant coefficients for $\underline{C}$ in Eq. 3.46; $N \times N$ coefficient matrix of the eigenvalue problem given by Eq. 4.56
A_c	Non-dimensional parameter introduced in Eq. 3.42
A_c^*	Non-dimensional parameter introduced in Eq. III.1
A_m	Non-dimensional parameter introduced in Eq. 3.43
A_m^*	Non-dimensional parameter introduced in Eq. III.2
A_n	Arbitrary constant in Eq. 3.22
A_p	Collector absorber-plate receiving area (m^2)
b_1, b_2, b_3	Non-dimensional parameters defined in Appendix II
B	$WLU_L/\dot{m}c_p$, equivalently given by $f \cdot F_{ud}$
$\underline{B}$	$N \times 1$ constant vector representing inhomogeneous part of Eq. 4.54
$B(\beta)$	Non-dimensional function representing β-dependence of $\psi_p(\eta,\beta)$ in Eq. 3.17
B_m	Non-dimensional parameter introduced in Eq. 3.43

c	$(U_L/k_p\delta_p)^{1/2}\ (W - D)/2$
c_p	Average fluid specific heat (w-s/kg-C)
$\underline{c}^j$	General eigenvector associated with the j^{th} eigenvalue of $\underline{\underline{A}}$
$\underline{C}$	$(M_T + 1) \times 1$ vector of C_n's in Eq. 3.46; $N \times 1$ constant vector introduced in Eq. 4.46
C_B	Bond conductance (w/m-C)
C_n	Series expansion coefficients introduced in Eq. 3.27
C_n^*	$C_n \cosh \gamma_n$
CEL	Acronym for conventional edge loss treatment
d	Non-dimensional parameter defined in Appendix II
d_c	Collector depth (m)
d_r	$2D/(W - D)$
d_r'	$D/(W - D)$
D	Outside diameter of flow passage (m)
$\underline{D}$	Constant vector representing inhomogeneous term in Eq. 4.62
D_i	Inside diameter of flow passage (m)
D_n	Arbitrary constant in Eq. 3.24; non-dimensional parameter introduced in Eq. 3.42
D_n^*	Non-dimensional parameter introduced in Eq. III.1

$\underline{\underline{E}}$	N × N matrix of eigenvectors for a non-symmetric $\underline{\underline{A}}$ matrix
E_c	Non-dimensional parameter introduced in Eq. 3.42
E_n	Arbitrary constant in Eq. 3.24
E_{mn}	Non-dimensional parameter introduced in Eq. 3.43
f	$L/R\dot{m}c_p$
$f(\xi_E)$	Non-dimensional function defined by Eq. 4.19
$\bar{f}$	$\int_0^1 f(\xi_E)\, d\xi_E$
f_1, f_2	Non-dimensional f-parameters for Type III geometry used in Eq. 3.16
F	Standard fin efficiency
F'	Collector efficiency factor
F_c	Non-dimensional parameter introduced in Eq. 3.42
F_d	$(F + d_r')/(1 + d_r')$
$(F_d)_n$	$(F_n + d_r')/(1 + d_r')$
F_I	Standard fin efficiency with U_L replaced by U_{LI}
F_n	$(\tanh \gamma_n)/\gamma_n$
F_R	Collector heat removal factor
F_{ud}	$(1 + d_r')/u_r d_r'$
g	$(W - D)/4k_p\delta_p R$
g_1	Non-dimensional g-parameter for Type III geometry used in Eq. 3.14

$g(\xi_E)$	Non-dimensional function defined by Eq. 4.20
$\bar{g}$	$\int_0^1 g(\xi_E)\, d\xi$
G	$N_T \dot{m}/A_p$
h	$DU_L(W - D)/4k_p\delta_p$
h_1	Non-dimensional h-parameter for Type III geometry used in Eq. 3.14
h_{ci}	Convection heat transfer coefficient for the i^{th} resistor between the absorber plate and ambient conditions (w/m^2-C)
h_f	Convection heat transfer coefficient between the coolant fluid and the flow channel (w/m^2-C)
h_{ri}	Radiation heat transfer coefficient for the i^{th} resistor between the absorber plate and ambient conditions (w/m^2-C)
H	Non-dimensional parameter introduced in Eq. 4.32
HR	Insolation per unit time per unit area (w/m^2-C)
i	Integer variable
$\underline{I}$	N × 1 vector with each element equal to 1
$\underline{\underline{I}}$	N × N identity matrix
k	Integer variable
$k_{ins,B}$	Thermal conductivity of the collector bottom insulation (w/m-C)
$k_{ins,E}$	Thermal conductivity of the collector edge insulation (w/m-C)

k_p	Thermal conductivity of the absorber plate (w/m-C)
K	Non-dimensional parameter introduced in Eq. 4.27
j	Integer variable
L	Length of the absorber plate (m)
L_c	External length of the collector (m)
LEL	Acronym for localized edge loss treatment
m	Integer variable; $(U_L/k_p\delta_p)^{1/2}$
m_E	$(U_{LE}/k_p\delta_p)^{1/2}$
m_I	$(U_{LI}/k_p\delta_p)^{1/2}$
$\dot{m}$	Mass flow rate through each flow channel (kg/s)
M	$k_p\delta_p/L^2U_L$, equivalently given by $(a/c)^2$
M_T	Integer truncation value
n	Integer variable
n_E	$(U_{LE}/k_p\delta_p)^{1/2}$ (W - D)
n_I	$(U_{LI}/k_p\delta_p)^{1/2}$ (W - D)
N	Integer variable given by N_T, $N_T/2$, or $(N_T + 1)/2$
N_T	Number of collector tubes
$N(\eta)$	Non-dimensional function representing the η-dependence of $\psi_p(\eta,\beta)$ in Eq. 3.17
P_c	Length around the perimeter of the collector (m)

q_a	$-k_p \delta_p \frac{d^2\bar{T}_p}{dy^2}$
q_b	Net energy collected on the tube base surface per unit time per differential length in the flow direction (w/m)
q_c	Net energy collected, per unit time per differential length in the flow direction, on the surface of the absorber-plate and tube regions (w/m)
q_{EC}	Transverse conduction heat loss rate from the edge absorber plate (w/m)
q_{fb}	Heat flow rate into the tube base region per differential length in the flow direction (w/m)
q_j	Sum of q_j^+ and q_j^-
q_j^+	Heat flow rate per differential length in the flow direction entering the left tube base of plate segment j in the positive x-direction (w/m)
q_j^-	Same as above except in the negative x-direction
q_u	Useful energy gain for the fluid per channel per unit time per differential length in the flow direction (w/m)
q_{uj}	Value of q_u for the j^{th} flow channel (j = 1,2,...,N)
$\underline{q}_u$	N × 1 vector with elements given by q_{uj}
$\underline{q}_{um}$	$\int_0^1 \underline{q}_u(\beta)\, d\beta$
Q_B, Q_E, Q_T	Heat loss rate through the bottom, edge, and top of the collector, respectively (w)

Q_L	Sum of Q_B, Q_E, and Q_T
r	$a^2 W_b d_r / 2D$
r_1, r_2, r_3	Non-dimensional parameters defined in Appendix II
r_m, r_n	$r(\lambda_m^*)^2$, $r(\lambda_n^*)^2$
R	General notation for the resistance per unit tube length between the tube base region and the coolant fluid (m-C/w)
R_1	$1/(h_f \pi D_i) + 1/C_B$
R_2	$1/(h_f \pi D_i)$
R_i	The i^{th} resistance between the absorber plate and ambient conditions (m-C/w), i = 1,2,...,6
s	Entropy per unit mass (w-s/kg)
S	$HR(\tau\alpha)_e$ -- the net solar energy absorbed per unit time per unit area on the surface of the absorber plate (w/m^2)
S_E	Edge structure shape factor
t_B, t_E	Insulation thickness on the bottom and edge of the collector, respectively (m)
u_r	$1/RDU_L$
$\underline{u}^j$	Orthogonal unit eigenvector associated with the j^{th} eigenvalue of a symmetric $\underline{\underline{A}}$ matrix
$\underline{\underline{U}}$	N × N matrix with columns given by $\underline{u}^j$

U_B, U_E, U_T	Collector bottom, edge, and top loss coefficients based on A_p -- CEL model (w/m^2-C)
U_{BE}, U_{EE}, U_{TE}	Collector bottom, edge, and top loss coefficients for the edge absorber plates -- LEL model (w/m^2-C)
U_{BI}, U_{EI}, U_{TI}	Collector bottom, edge, and top loss coefficients for the interior absorber plates -- LEL model (w/m^2-C)
U_E'	Local edge loss coefficient given by Eq. I.10
U_G	Collector useful energy gain coefficient (w/m^2-C)
U_L	Collector overall loss coefficient, sum of U_B, U_E, and U_T
U_{LE}	Sum of U_{BE}, U_{EE}, and U_{TE}
U_{LI}	Sum of U_{BI}, U_{EI}, and U_{TI}
$U_{L,equiv}$	Collector equivalent overall loss coefficient -- LEL model (w/m^2-C)
U_o	Transverse heat conductance between the coolant fluid and ambient conditions (w/m^2-C)
V	Non-dimensional parameter introduced in Eq. 4.32
$\underline{\underline{V}}$	$N_T \times N_T$ matrix introduced in Eq. 4.69
V_w	Wind velocity (m/s)
W	Tube-to-tube spacing (m)
$\underline{\underline{W}}$	$N_T \times N_T$ matrix introduced in Eq. 4.69
W_b	Arc length of the tube base region (m)

W_c	External width of the collector (m)
W_{eff}	Effective tube-to-tube spacing defined by Eq. 4.87
W_I	$WN_T - (W - D)$
W_p	$W_I + (W - D)(1 + \delta_E)$
x	Transverse dimension normal to the flow channels (m)
y	Axial (flow) dimension (m)
$\underline{Y}$	$N_T \times 1$ vector introduced in Eq. 4.69
z	Dimension normal to the plane of the collector (m)
$\underline{Z}$	$N_T \times 1$ vector introduced in Eq. 4.69
$\underline{\ }$	Notation for an N × 1 column vector
$=$	Notation for an N × N matrix
$( )_A, ( )_E,$ $( )_{1-D}$	Parenthetical quantity to be evaluated by the averaging, exact, or 1-D fin method, respectively
$( )_{CEL},$ $( )_{LEL}$	Parenthetical quantity to be evaluated by the CEL or LEL method, respectively

Temperature variables

P	$(T - T_{fi})/(S/U_L + T_a - T_{fi})$
T	Primary temperature variable (C)
$\bar{T}_{fo}$	Arithmetic average of outlet fluid temperatures -- LEL model, parallel-flow (C)

$\bar{T}_p$	$\frac{W-D}{W}\int_0^1 T_p(\eta,\beta)\,d\eta + \frac{D}{W}T_b(\beta)$
Θ	$T - T_a - S/U_L$ (U_L is replaced by U_{LE} or U_{LI} if Θ has the subscript E or I, respectively)
ϕ_{fj}	Θ_{fj}/Θ_{fi}
Φ	$T - T_a$ (C)
ψ_f	Θ_f/Θ_{fi} -- non-dimensional fluid temperature used in Chapter III
ψ_p	Θ_p/Θ_{fi} -- non-dimensional plate temperature used in Chapter III
ψ_{fj}	Non-dimensional fluid temperature in the j^{th} flow channel, used in the variable change $\underline{\phi}_f = \underline{\underline{E}}\,\underline{\psi}_f$ in Chapter IV
ψ_{pj}	Θ_{pj}/Θ_{bj} ($j = 1,2,\ldots,N_T-1$), non-dimensional plate temperature used in Chapter IV

Temperature subscripts

a	Ambient
b	Tube base region
E	Edge absorber plate region
f	Coolant fluid
i	Inlet
I	Internal absorber-plate region

j	Integer variable
m	Mean value
o	Outlet
p	Absorber-plate region
s	Dummy subscript
t	Tube region

Superscripts

I	Notation for replacement of S/U_{LE} in Θ_{pm_E} by S/U_{LI}
T	Matrix transpose
-1	Matrix inverse

Greek symbols

α	Non-dimensional parameter defined in Appendix II
α_E	Non-dimensional parameter introduced in Eq. 4.15
β	Non-dimensional axial coordinate -- y/L
γ	Non-dimensional parameter introduced in Eq. 4.31
γ_m, γ_n	$(\lambda_m^2 + c^2)^{1/2}$, $(\lambda_n^2 + c^2)^{1/2}$
$\underline{\underline{\Gamma}}$	N × N matrix introduced in Eq. 4.46 -- Type I and II geometries
$\underline{\underline{\Gamma}}^*$	Complement of $\underline{\underline{\Gamma}}$ valid for Type III geometry
δ_E	Non-dimensional factor which accounts for variable edge

	plate widths, e.g., $W_p = WN_T + \delta_E(W - D)$
δ_{jk}	Kronecker delta function
δ_p	Absorber-plate thickness (m)
$\underline{\underline{\Delta}}$	$N_T \times N_T$ diagonal matrix introduced in Eq. 4.67
ΔF_R	$(F_R)_{1-D} - (F_R)_E$
$\varepsilon_1, \varepsilon_2$	Long-wave emissivities of parallel plates 1 and 2, respectively
η	Non-dimensional transverse coordinate -- $2x/(W - D)$
η_c	Instantaneous collector efficiency
η_T	Instantaneous thermodynamic collector efficiency
λ	Arbitrary separation constant
λ_m, λ_n	$m\pi a$, $n\pi a$
λ_m^*, λ_n^*	$m\pi$, $n\pi$
$\underline{\underline{\Lambda}}$	$N \times N$ diagonal matrix with diagonal entries equal to the eigenvalues of the $\underline{\underline{A}}$ matrix
μ	Non-dimensional parameter defined in Appendix II
ν	Non-dimensional parameter defined by Eq. 4.45
ξ_E	Non-dimensional transverse coordinate for the left side edge absorber plate defined by Eq. 4.9
ξ_j	Non-dimensional transverse coordinate for the j^{th} interior absorber plate defined by Eq. 4.6

$\P$	Non-dimensional parameter introduced in Eq. 4.68
σ	Stefan-Boltzmann constant -- 5.6697×10^{-8} $w/m^2\text{-}K^4$
$(\tau\alpha)_e$	Effective transmittance-absorptance product
ψ	Non-dimensional parameter defined in Appendix II
ω	Non-dimensional parameter introduced in Eq. 4.31
$\Omega_1,\Omega_2,\Omega_3$	Options for mid-tube symmetry, full-plate, or mid-plate symmetry calculations, respectively, introduced in Eq. 4.38

I. INTRODUCTION

Purpose of Research

Recent public interest in solar energy as a viable energy option has stimulated growth in the solar collector industry. Within the industry, flat-plate collectors are currently the most economical means of solar energy utilization. At this time, however, there exist significant discrepancies in thermal performance predictions between the experimental and theoretical results with the latter generally overestimating performance. Since a theoretical analysis is the basis for most competitive designs, the uncertainties make it difficult for designers of flat-plate solar collectors to maximize the net collection of energy vs cost. Thus there is considerable incentive in attempting to identify both those areas of analysis which need improvement as well as those which are already adequate.

Two new methods of analysis which can be used within the framework of existing theory are developed in the present investigation. The first method uses the separation of variables technique in a unique manner to solve exactly for the coupled axial and transverse temperature distributions in an absorber plate-tube assembly. The conventional assumption of an overall uniform loss coefficient U_L is used in the analysis. The second method uses two sectionally uniform loss coefficients, U_{LI} for internal collector sections and U_{LE} for edge sections, to evaluate collector performance. The first new method is practical only for parallel-flow collectors, while the second is applicable for

both parallel-flow and serpentine configurations.

The validity of two assumptions commonly made in flat-plate collector analysis is investigated using the new methods. The first assumption is that axial conduction within the absorber plates has a negligible effect on the local plate conductance for transverse heat flow; thus, axial conduction is either totally neglected [1] or treated by an averaging technique [2]. By solving for the coupled axial and transverse temperature distributions, the validity of existing axial conduction treatments can be evaluated. The second assumption deals with the manner in which heat losses from the collector edges are taken into account. Conventionally, the edge losses are calculated assuming one-dimensional heat flow through the collector sides and bottom. The resulting edge losses are then distributed over the entire collector surface by means of an overall uniform loss coefficient U_L. By sectionalizing the loss coefficient, the applicability of conventional edge loss treatment is analyzed.

The emphasis of the investigation is on the development of new methods of collector analysis which serve two purposes. First, the methods developed can be used for absorber plate-tube thermal analyses in place of existing methods. Secondly, the degree of approximation incurred by existing models is quantitatively determined.

For a fuller appreciation of the new approaches, a presentation of the conventional theories is necessary. The remaining part of this chapter deals with the basic overall equations and assumptions. Chapter II deals with the details of the existing models which are

compared in Chapters III and IV with the subject methods.

Background

The conventional theory of flat-plate collectors is the collective work of Hottel and Woertz, Whillier, Bliss, Tabor, and Duffie and Beckman [3,4,5,6,1]. Figure 1 shows a typical parallel-flow collector assembly (without the transparent cover system). An overall energy balance on the entire absorber plate-tube assembly, taken to be a steady-state control volume, yields the following relation.

$$HR\ (\tau\alpha)_e\ A_p = Q_u + Q_L \tag{1.1}$$

where HR is the total energy available to the collector per unit area per unit time, $(\tau\alpha)_e$ is the effective transmittance-absorptance product, and A_p is the area of the collector exposed to solar radiation. The term $(\tau\alpha)_e$ is the ratio of the net energy absorbed onto the absorber plate-tube assembly to the energy received on the collector outer surface. The term Q_L represents the heat loss rate from the collector cover and structure assembly to the environment by conduction, convection, and (longwave) radiation. The loss term, Q_L, is composed of top, bottom, and edge losses, i.e.,

$$Q_L = Q_T + Q_B + Q_E \tag{1.2}$$

The useful heat gain rate, Q_u, is the rate of increase in enthalpy of the coolant fluid between collector inlet and outlet, i.e.,

$$Q_u = N_T\ \dot{m}\ c_p\ (T_{fo} - T_{fi}) \tag{1.3}$$

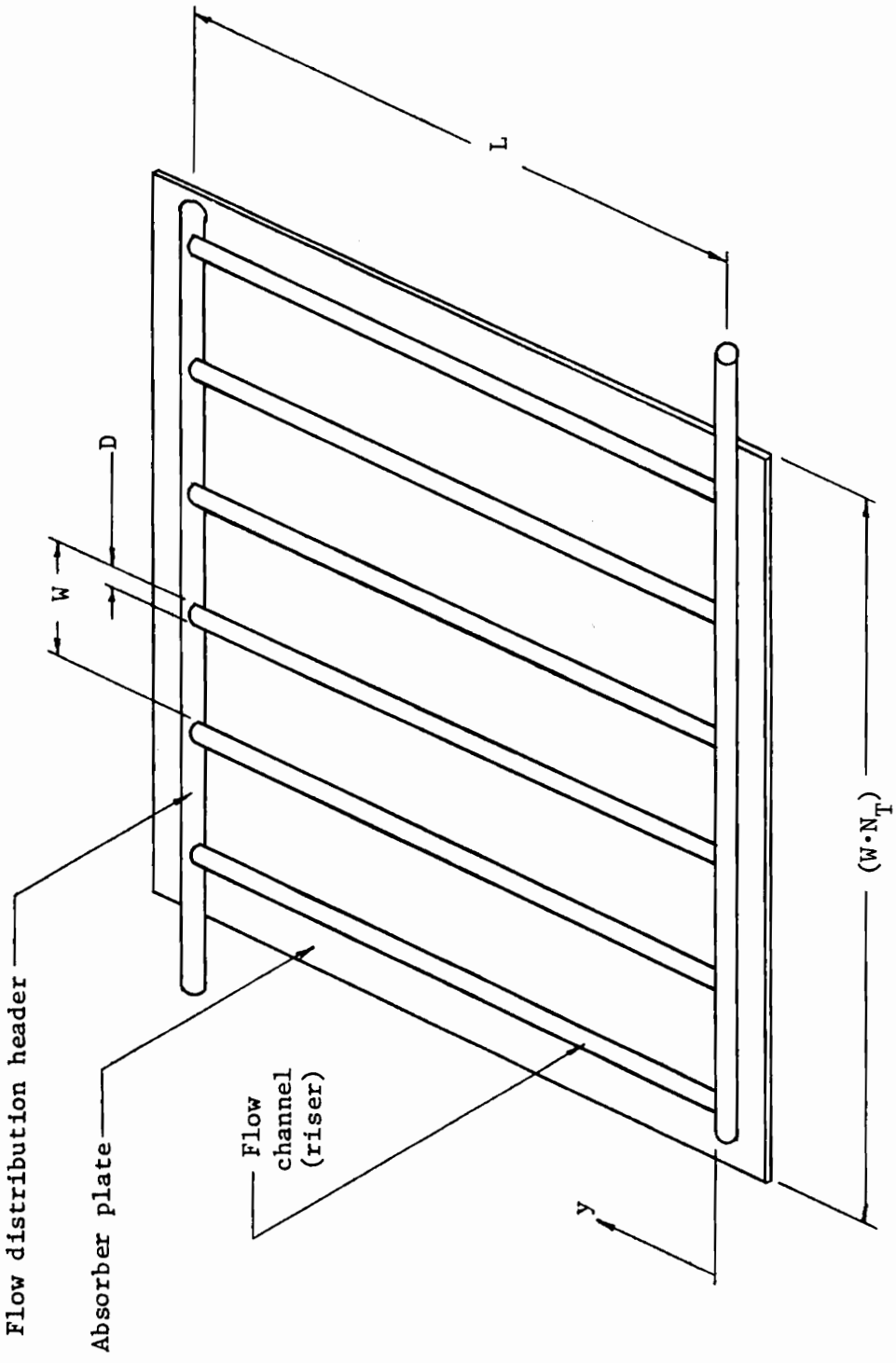

Figure 1. Typical Parallel-Flow Absorber-Plate Assembly

where N_T is the number of parallel flow channels.

The overall loss coefficient U_L is based on collector absorber area and is defined as

$$U_L = \frac{Q_T + Q_B + Q_E}{A_p (T_{pm} - T_a)} \tag{1.4}$$

where T_{pm} and T_a are mean plate temperature and ambient temperature, respectively. Conventionally, the overall loss coefficient is taken as the sum of three separate loss coefficients, i.e.,

$$U_L = U_T + U_B + U_E \tag{1.5}$$

where each component is defined by the corresponding term in Eq. 1.4. The evaluation of the Q_L term in Eq. 1.1, consequently, consists of evaluating each loss coefficient in Eq. 1.5. However, as a result of the various convection, conduction, and radiation mechanisms involved in Q_L, U_L is a rather involved function of collector heat transfer and geometrical properties as well as environmental and operating conditions. A more complete discussion of the overall loss coefficient is presented in Appendix I. A major consideration, however, is that U_L is a strong non-linear function of T_{pm}.

The evaluation of Q_u, from Eq. 1.3, requires a thermal analysis of the absorber plate-tube assembly to obtain: (1) the outlet fluid temperature, T_{fo}, and (2) the coolant specific heat, c_p, which is dependent on the mean fluid temperature, T_{fm}. The analysis involves property and geometrical characteristics of both the absorber plates

and the plate-tube-fluid interfaces and is highly dependent on the value of U_L. The present study concentrates on this area of collector analysis.

Since the evaluation of Q_L and Q_u are necessarily coupled through U_L, T_{pm}, and T_{fm} in a manner which does not have a closed form solution, iterative techniques must be used to evaluate these quantities. The computational procedure can be separated into three sets of iterations. The procedure starts with the Q_L iteration. A reasonable guess is made for T_{pm}, which leads to a first estimate of U_L and $(\tau\alpha)_e$ by an internal iterative process. Iteration for Q_u involves using the U_L and $(\tau\alpha)_e$, so obtained, to evaluate T_{fm} through calculations of c_p and h_f, the tube wall-to-fluid convective heat transfer coefficient. Both c_p and h_f are dependent on T_{fm}. The value of T_{fm} is then used to calculate a new estimate of T_{pm}, etc.

Once T_{fo}, c_p, U_L, and $(\tau\alpha)_e$ are known, all the quantities in Eq. 1.1 may be evaluated. For comparison purposes, however, two generalized collector factors have been defined* which give information

---

*Another generalized collector efficiency factor has been defined by Phillips [2]. He defines a thermodynamic efficiency factor based on the rate of change in thermodynamic availability of the outlet fluid, relative to the inlet.

$$\eta_T = \frac{Q_u - N_T \dot{m} T_{fi}(s_{fo} - s_{fi})}{HR A_p}$$

where s denotes entropy.

about individual collector thermal performance in a more convenient fashion. The collector heat removal factor, F_R, is defined as the ratio of the useful energy gain rate of the collector, Q_u, to the useful gain rate had the entire absorber surface temperature been T_{fi}, i.e.,

$$F_R = \frac{Q_u}{A_p[HR(\tau\alpha)_e - U_L(T_{fi} - T_a)]} \tag{1.6}$$

The instantaneous collector efficiency, η_c, is defined as

$$\eta_c = \frac{Q_u}{HR\ A_p} \tag{1.7}$$

These efficiency factors are generalized in that these factors are applicable for all types of collectors and collector analyses. Two additional efficiency factors will be introduced in Chapter II. These factors, however, are not as general as F_R and η_c.

II. EXISTING ANALYTICAL METHODS USED IN ABSORBER PLATE THERMAL ANALYSES

Introduction

Existing methods for predicting the temperature distribution in the absorber plate are presented and the important simplifications are reviewed. The results are presented in a form which allows direct comparison with the new methods presented in the following chapters. The development is essentially taken from Duffie and Beckman [1] and from Phillips [2]. The material in Chapter II serves as the basis for comparison with the important extensions taken into account by the new methods.

Several simplifying assumptions common to both of the existing methods have been made [1] as follows:

1. Operating conditions are steady-state.
2. Construction is of sheet and tube type with parallel flow.
3. The effect of the flow headers is negligible, i.e., the headers cover a small area of the collector.
4. Heat transfer through the side and bottom insulation is one dimensional.
5. Heat losses through the sides of the collector may be uniformly distributed over the entire collector surface.
6. The overall loss coefficient U_L may be treated as independent of position.

7. The temperature gradient across the absorber plate thickness is negligible.
8. The tube base region has a uniform temperature in the x-direction.
9. Flow properties may be evaluated at a mean fluid temperature.
10. Shading of the collector absorber plate by the sides and ends is negligible.
11. The tube spacing is constant with the edge tube located inward a distance of one-half the spacing.
12. Axial conduction in the absorber plate does not affect the local plate conductance for transverse heat flow.

There are more assumptions relating to the evaluation of U_L. These assumptions, however, affect the quantitative results rather than the absorber plate analysis and are noted in Appendix I.

The validity of assumption 12 is the major consideration in Chapters II and III. The assumption has been introduced to circumvent the necessity of solving a two-dimensional partial differential equation with intractable boundary conditions to obtain an analytical solution. The solution of such a system is the subject of Chapter III. Also, the two methods given in Chapter II differ only in the application of assumption 12. In the first method, axial conduction is neglected entirely. In the second method, axial conduction is included by use of an averaging technique.

In either case, axial conduction is not considered to affect the local plate conductance for transverse heat flow. The first method is adequate for collectors in which both the tube spacing to length ratio and the axial fluid temperature gradient are small. The second method is a good approximation when the plate conductance is large. For other situations, however, the two existing methods may fail to give accurate results.

The methods reviewed are also useful as a basis for comparison with the new analysis presented in Chapter IV where assumptions 5 and 6 are critically examined while axial conduction is assumed negligible. In this way, the effects of the various assumptions are treated independently to establish applicability.

The One-Dimensional Fin Method

In the one-dimensional fin method [1], axial conduction in the absorber plate is neglected. Thus, within the absorber plate, the model assumes one-dimensional heat flow from the absorber plate to the tube base. The first step in a thermal analysis of the absorber plate-tube assembly is to obtain expressions for the temperature distributions in the region between tubes. Using the previously noted assumptions for parallel-flow collectors, symmetry can be used to separate the individual tube-sheet sections by insulated boundary conditions at locations midway between tubes. Within each separated section, symmetry again exists for each half-width region. Figure 2 shows one such region, on which a one-dimensional thin-fin thermal analysis will be made. Applying an energy balance

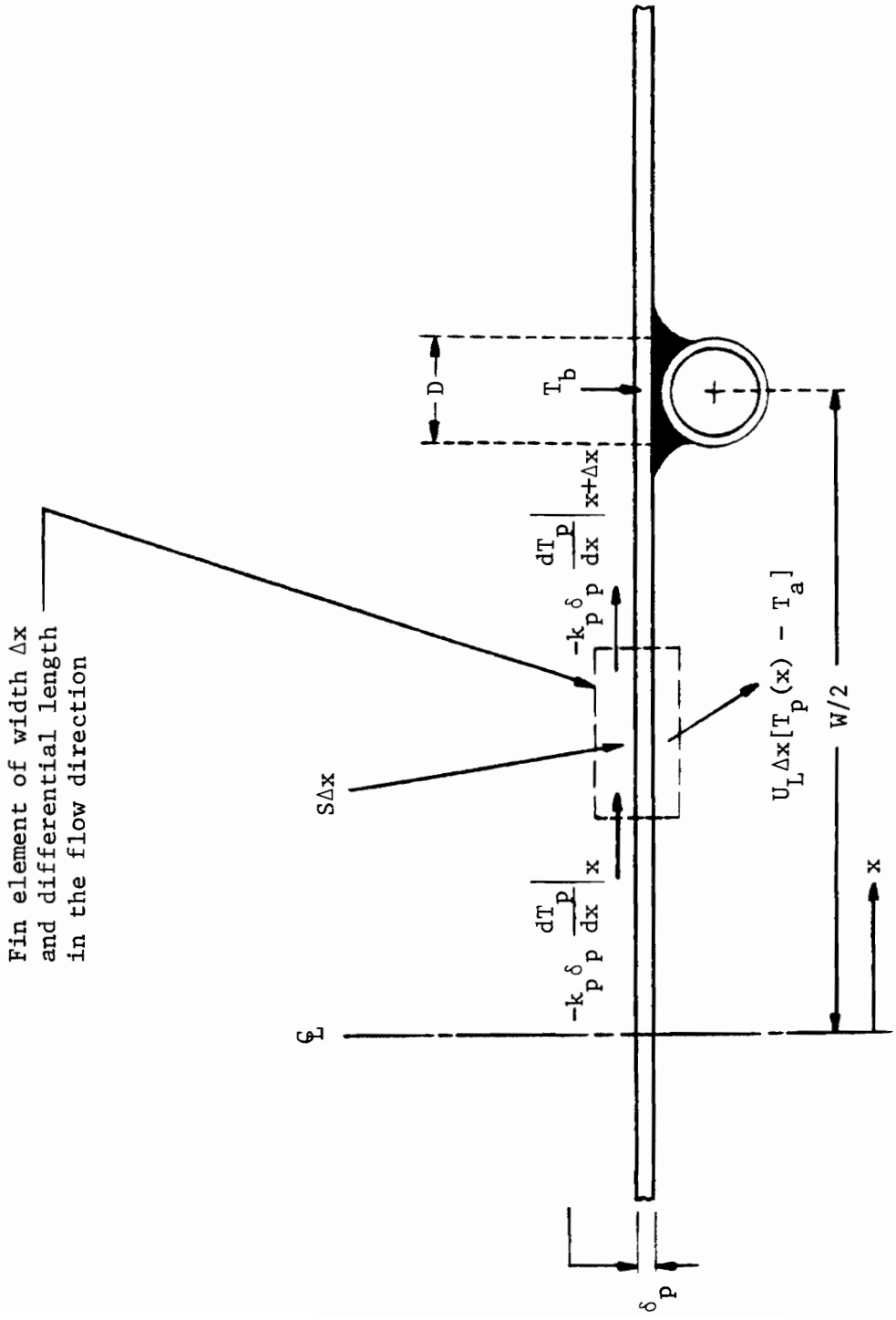

Figure 2. One-Dimensional Thin Fin Model

on the fin element gives the following differential equation applicable for $0 \leq x \leq \frac{W - D}{2}$.

$$k_p \delta_p \frac{d^2T_p}{dx^2} - U_L(T_p - T_a) + S = 0 \qquad (2.1)$$

with boundary conditions

$$\left.\frac{dT_p}{dx}\right|_{x=0} = 0 \quad \text{and} \quad \left.T_p\right|_{x = \frac{W-D}{2}} = T_b$$

where $T_p = T_p(x)$, $T_b = T_b(y)$, and $S = HR(\tau\alpha)_e$. The subscripts "p" and "b" refer to the absorber plate ($0 \leq x \leq \frac{W - D}{2}$) and the tube base region ($\frac{W - D}{2} \leq x \leq \frac{W}{2}$), respectively. Note that the tube base temperature, $T_b(y)$, is assumed uniform in the x-direction. Equation 2.1 can be rewritten as

$$\frac{d^2\Theta_p}{dx^2} - m^2\Theta_p = 0 \qquad (2.2)$$

where $\Theta_p = T_p - T_a - S/U_L$ and $m^2 = U_L/k_p\delta_p$.

Equation 2.2 is a second-order linear ordinary differential equation with the solution [1, 4]

$$\Theta_p = \Theta_b \frac{\cosh(mx)}{\cosh(m[W - D]/2)} \qquad (2.3)$$

where $\Theta_b = T_b - T_a - S/U_L$. Throughout Chapter II, the subscripted variable Θ_s will denote $T_s - T_a - S/U_L$, where s is a dummy subscript.

The heat flow from the absorber plates into the tube base region, per differential length in the flow direction, can be evaluated from

$$q_{fb} = -2\, k_p \delta_p \left.\frac{dT_p}{dx}\right|_{x = (W-D)/2} \tag{2.4}$$

where the factor of 2 results from heat flow into both sides of the tube base. Using Eq. 2.3, Eq. 2.4 may be written as

$$q_{fb} = -(W - D)FU_L\Theta_b \tag{2.5}$$

where F is the standard fin efficiency given by

$$F = \frac{\tanh[m(W - D)/2]}{m(W - D)/2} \tag{2.6}$$

At this point, the specific analysis depends on the type of tube-sheet assembly chosen [5]. Figure 3 shows three types of assemblies. Type II can be considered a limiting case of either Type I or III since the Type I and III cases revert to Type II when the absorber plate-tube bond conductance C_B becomes large. The methods discussed in Chapter II have more generality than the methods discussed in Chapters III and IV in that although the specifics of the analysis are different for the Type I and III

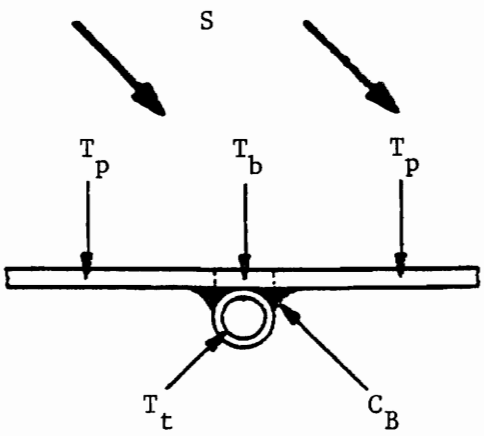

Type I

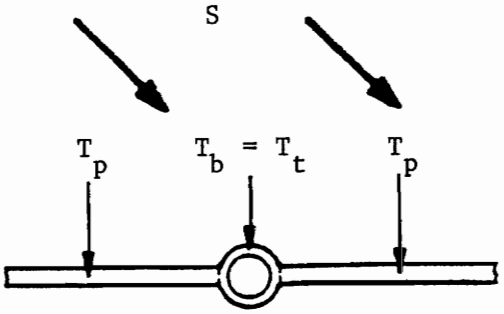

Type II

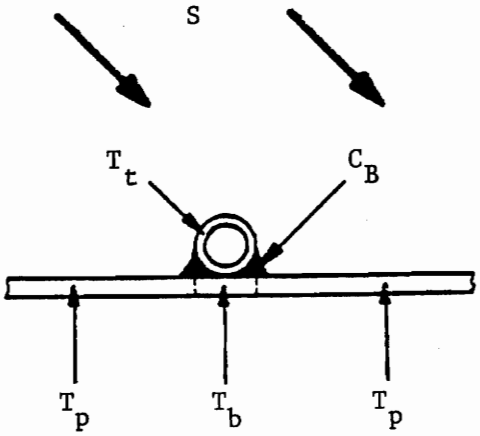

Type III

Figure 3. Basic Types of Tube-Sheet Assemblies

cases, the methods in Chapter II can account for the differences in terms of a single parameter. The methods in Chapters III and IV require significant changes in order to achieve the same generality. The advantage is small, however, in practical applications since the difference between T_b and T_t is not significant for usual values of C_B.

The procedure that will be followed for all methods will be to show the specifics for Type I geometry, which in the limiting case includes Type II, (since most commercial flat-plate collector assemblies are of these two types) and to outline the changes to account for the Type III case.

For the Type I case, the net energy collected on the tube base surface per unit time per differential length in the flow direction is given by

$$q_b = D[S - U_L(T_b - T_a)] \tag{2.7}$$

which in terms of Θ_b becomes

$$q_b = -DU_L\Theta_b \tag{2.8}$$

Summing q_{fb} and q_b, from Eqs. 2.5 and 2.8, respectively, yields an expression for the total useful energy gain, i.e.,

$$q_u = q_{fb} + q_b = -U_L[(W - D)F + D]\,\Theta_b \tag{2.9}$$

The useful energy gain, q_u, collected at the tube base is transferred

to the fluid through a resistance R, which is the sum of the resistances of the tube bond, the tube thickness, and the inner tube wall-to-fluid convection film. The resistance resulting from the tube thickness is negligible in practice so the total resistance R is given by

$$R_1 = 1/(h_f \pi D_i) + 1/C_B$$

for Type I designs and by

$$R_2 = 1/(h_f \pi D_i)$$

for Type II designs. In terms of R, q_u is given by

$$q_u = (T_b - T_f)/R \tag{2.10}$$

which may be written in terms of Θ_b and Θ_f as

$$q_u = (\Theta_b - \Theta_f)/R \tag{2.11}$$

Eliminating Θ_b by solving for Θ_b in Eq. 2.11, substituting the result into Eq. 2.9, and solving the final result for q_u gives

$$q_u = -WU_L F' \Theta_f \tag{2.12}$$

where F', known as the collector efficiency factor, is given by

$$F' = \frac{1/U_L}{W\{\frac{1}{U_L[D + (W - D)F]} + R\}} \tag{2.13}$$

for Type I and II geometries. The collector efficiency factor, F',

is the parameter noted earlier which, for Chapter II methods, alone accounts for analysis differences between Type I and Type III designs. For the Type III case, F' is given [5] as

$$F' = \frac{1/U_L}{W\left\{\frac{1}{DU_L + \frac{1}{\frac{1}{C_B} + \frac{1}{U_L(W - D)F}}} + R_2\right\}} \tag{2.14}$$

Note that as $C_B \to \infty$, Eq. 2.14 reverts to Eq. 2.13. The parameter F' may be physically interpreted as a heat transfer resistance ratio, i.e.,

$$F' = \frac{\text{heat transfer resistance from absorber plate to ambient air}}{\text{heat transfer resistance from the fluid to ambient air}}$$

Denoting these resistances as $1/U_L$ and $1/U_o$, F' is given by

$$F' = U_o/U_L \tag{2.15}$$

A thermal resistance network is useful for visualizing the various heat transfer processes involved in tube-sheet designs. Figure 4 shows the thermal networks resulting from the one-dimensional fin analysis for Type I and Type III designs as well as the general network valid for all parallel-flow designs. These networks are also used later to compare the one-dimensional fin method to the method developed by Phillips.

Once the useful energy gain per differential length in the flow

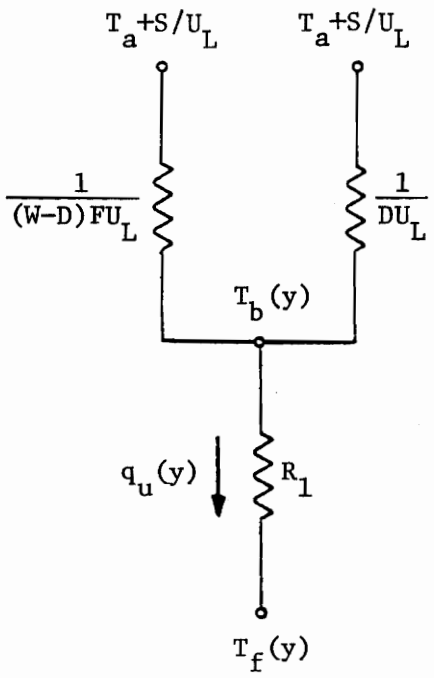

(a) Type I Design Network

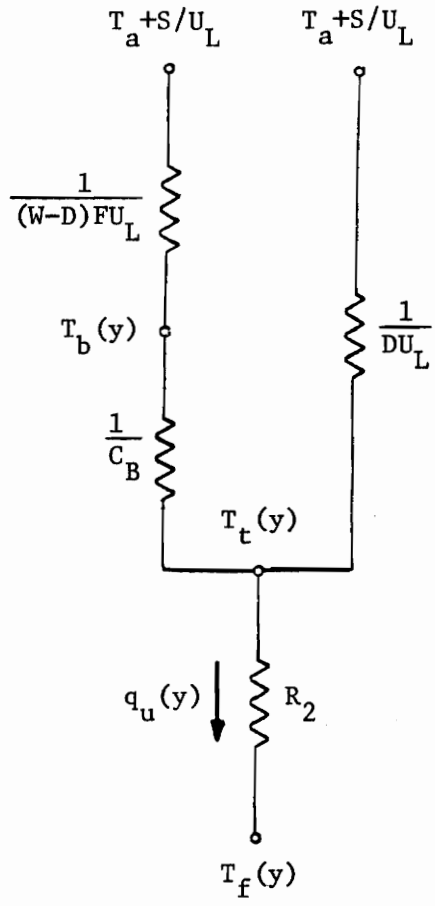

(b) Type III Design Network

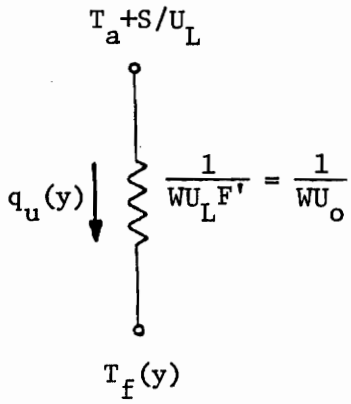

(c) Generalized 1-D Fin Analysis Network

Figure 4. 1-D Thin Fin Thermal Networks

direction has been evaluated, an energy balance can be made on the corresponding differential fluid element. Figure 5 shows a typical fluid element and the terms involved in the energy balance. Axial conduction within the fluid is neglected. The differential equation which results is given in terms of Θ_f by

$$\dot{m}c_p \frac{d\Theta_f}{dy} + WF'U_L\Theta_f = 0 \tag{2.16}$$

with the boundary condition

$$\Theta_f(0) = \Theta_{fi}$$

Equation 2.16 has the solution

$$\Theta_f(y) = \Theta_{fi} \exp(- U_L WF'y/\dot{m}c_p) \tag{2.17}$$

Once the fluid temperature distribution has been found, the collector heat removal factor, F_R, defined by Eq. 1.6, can be evaluated. In terms of Θ_f, Eq. 1.6 may be written as

$$F_R = \frac{N_T \dot{m} c_p}{U_L A_p} [1 - \Theta_f(L)/\Theta_{fi}] \tag{2.18}$$

Using Eq. 2.17, Eq. 2.18 becomes

$$F_R = \frac{G c_p}{U_L} [1 - \exp(- U_L F'/Gc_p)] \tag{2.19}$$

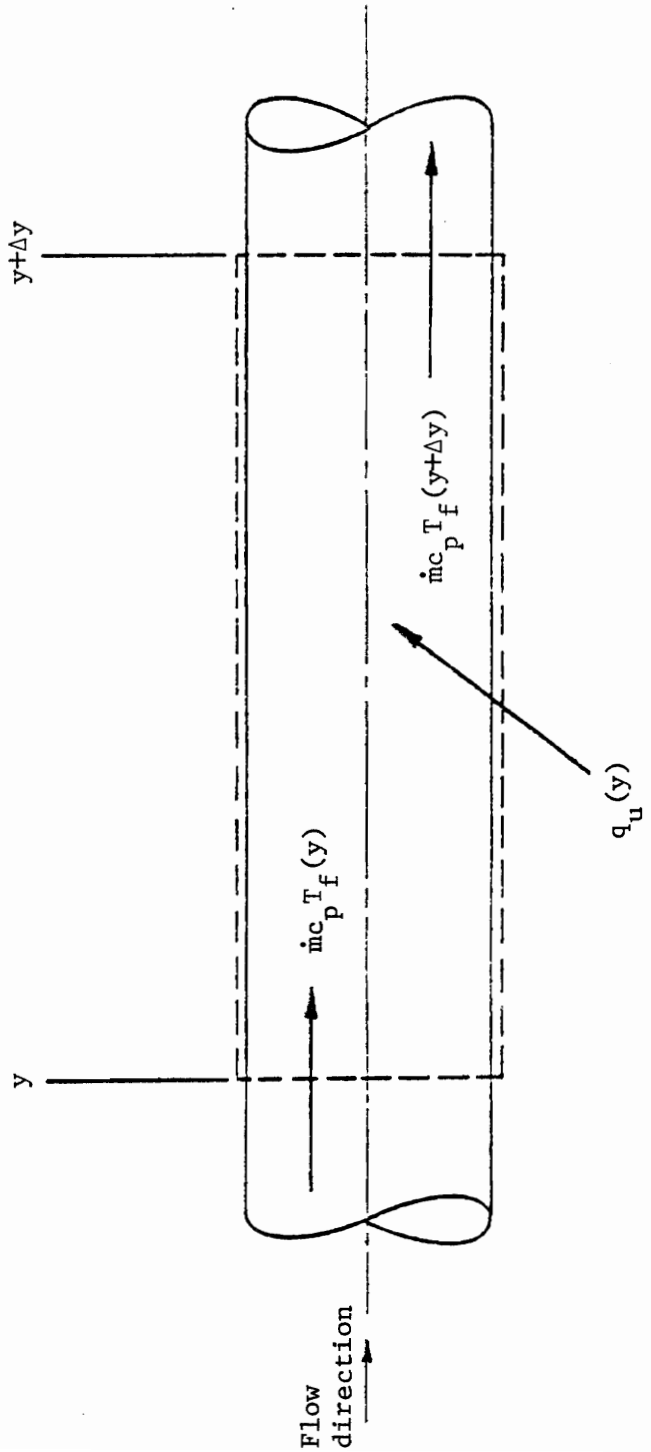

Figure 5. Energy Balance on a Typical Fluid Element

where G is the mass flow rate per unit of collector area given by $G = N_T\dot{m}/A_p$.

Introducing F_R, the total useful energy gain, Q_u, can be found from Eq. 1.3 by

$$Q_u = A_p F_R[S - U_L(T_{fi} - T_a)] \tag{2.20}$$

Equation 1.7 can then be used to calculate the collector efficiency η_c.

The absorber plate thermal analysis is not complete until expressions have been obtained for the mean plate and fluid temperatures. These temperatures, as noted in Chapter I, are needed for the evaluation of U_L, S, and c_p. Note that the expression for Q_u given by Eq. 2.20 is dependent on F_R, S, and U_L -- each must be evaluated by an iterative procedure.

By integrating Eq. 2.17 from 0 to L and using Eqs. 2.19 and 2.20, the mean fluid temperature has been shown [7] to be

$$T_{fm} = T_{fi} + \frac{Q_u(1 - F_R/F')}{U_L F_R A_p} \tag{2.21}$$

For later comparison, Eq. 2.21 can be written in a more convenient form as

$$\frac{\Theta_{fm}}{\Theta_{fi}} = \frac{F_R}{F'} \tag{2.22}$$

Equation 2.22 follows from Eq. 2.21 when the expression for Q_u from

Eq. 2.20 is substituted and the result written in terms of Θ_{fm} and Θ_{fi}. Equations 2.21 and 2.22 give the mean fluid temperature exactly within the assumption of the one-dimensional fin model.

While expressions for the mean fluid temperature are both "exact" and general (due to the F' factor), this generality has not, to the author's knowledge, been extended to "exact" expressions for the mean plate temperature. An approximate method for obtaining T_{pm} has conventionally been used to provide the desired generality. Reference 1 gives the following relation between the mean plate and fluid temperatures.

$$T_{pm} - T_{fm} = (Q_u/N_T L)\ R_2 \tag{2.23}$$

It can be shown that T_{pm} in this equation is actually the mean tube temperature. Reference 1 notes that Eq. 2.23 is a good approximation for T_{pm} only when the bond conductance, C_B, and the fin efficiency, F, are high.

Since Chapter III will be concerned with comparisons between T_{pm} for all three methods considered, the use of an approximate method for evaluating T_{pm} in any of the methods would obscure the objective of comparing plate axial conduction effects. Therefore T_{pm} will be evaluated "exactly" for Type I geometry and any differences with the result for the Type III case will be noted.

The relevant equations in evaluating T_{pm} "exactly" are Eqs. 2.3, 2.11, 2.12, 2.13, and 2.22. By weighting the absorber plate and tube base temperatures by their respective x-dimensions, T_{pm} is given in

terms of Θ_{pm} as

$$\Theta_{pm} = \left\{ \frac{(W-D) \int_0^L \Theta_b(y) \int_0^{\frac{W-D}{2}} \cosh mx \, dx \, dy}{(\frac{W-D}{2}) L \cosh m(\frac{W-D}{2})} + \frac{D \int_0^L \int_{\frac{W-D}{2}}^{\frac{W+D}{2}} \Theta_b(y) dy \, dx}{DL} \right\} /W \tag{2.24}$$

Performing the required integration, Eq. 2.24 becomes

$$\Theta_{pm} = [(W - D)F + D] \, \Theta_{bm}/W \tag{2.25}$$

where Θ_{bm} is given by

$$\Theta_{bm} = \frac{1}{L} \int_0^L \Theta_b(y) \, dy \tag{2.26}$$

From Eq. 2.11, $\Theta_b(y)$ may be written as

$$\Theta_b(y) = \Theta_f(y) + R \, q_u(y) \tag{2.27}$$

Substituting Eq. 2.12 into Eq. 2.27 and integrating the result according to Eq. 2.26 gives

$$\Theta_{bm} = \Theta_{fm}(1 - RWU_L F') \tag{2.28}$$

Using Eq. 2.13 for F' and Eq. 2.22 for Θ_{fm}, Eq. 2.28 becomes, after algebraic simplification,

$$\Theta_{bm} = \frac{W F_R \Theta_{fi}}{[(W - D)F + D]} \tag{2.29}$$

Substitution of Eq. 2.29 into Eq. 2.25 yields the result

$$\frac{\Theta_{pm}}{\Theta_{fi}} = F_R \tag{2.30}$$

Using comparable equations for the Type III design yields the same result for Θ_{pm}. Further investigation of Eq. 2.30 shows that the relation is valid not only for the one-dimensional fin method but also for any absorber plate analysis which makes the assumption of a uniform overall loss coefficient U_L. Expanding Eq. 2.30 by using the definition of F_R from Eq. 1.6 gives

$$\frac{\Theta_{pm}}{\Theta_{fi}} = \frac{\dot{m} c_p N_T (\Theta_{fo} - \Theta_{fi})}{- A_p U_L \Theta_{fi}} \tag{2.31}$$

Rearranging Eq. 2.31 gives

$$SA_p - U_L A_p (T_{pm} - T_a) = \dot{m} c_p N_T (T_{fo} - T_{fi}) \tag{2.32}$$

Equation 2.32 represents the overall energy balance for any absorber plate-tube assembly analysis under the assumption of a uniform loss coefficient U_L. Equation 2.30 is therefore valid for all the methods discussed in Chapters II and III. The per cent error between the mean plate temperature values obtained from the approximate and exact equations, i.e., Eqs. 2.23 and 2.30, is given, for large values of C_B, by

$$\frac{\Theta_{pm(1\text{-D approx})} - \Theta_{pm(1\text{-D exact})}}{\Theta_{pm(1\text{-D exact})}} = \left[\frac{1}{\frac{D}{W} + (1 - \frac{D}{W})F} - 1 \right] \cdot 100\% \tag{2.33}$$

For cases where $1/C_B$ is significant, the error is larger than that given by Eq. 2.33.

The expression for the mean fluid temperature, Eq. 2.22, can be combined with Eq. 2.30 to give a relation between Θ_{pm} and Θ_{fm}, i.e.,

$$\Theta_{pm} = F' \Theta_{fm} \tag{2.34}$$

Equation 2.22, 2.30, and 2.34 are all general expressions with respect to geometry types. However, only Eq. 2.30 has been shown to be a general expression for the range of analysis methods discussed in Chapters II and III. The derivations of Eqs. 2.22 and 2.34 were dependent on the specifics of the one-dimensional fin analysis.

Figure 6 shows a mean temperature network analogy for the one-dimensional fin method. Figure 6a was obtained by integrating the general network of Fig. 4c over the dimensions of a single absorber plate-tube section. Figure 6b is an expanded version which includes a mean plate temperature node. Figures 6a and 6b can be used to identify the physical basis for Eq. 2.34. Each side of Eq. 2.34, when multiplied by the term WLU_L, yields equivalent expressions for Q_u/N_T, the useful heat gain per tube. The equivalence of the two expressions for Q_u/N_T can be seen from Figs. 6a and 6b. Note that the useful heat gain per tube is also given by

$$Q_u/N_T = \dot{m}c_p(T_{fo} - T_{fi}) \tag{2.35}$$

The results given by Eqs. 2.22 and 2.30 for Θ_{fm}/Θ_{fi} and Θ_{pm}/Θ_{fi} are useful in design procedures since graphs of F' and F_R/F' are currently available [1]. Existing F_R/F' graphs can be directly

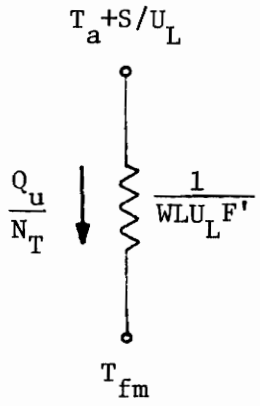

(a) Integrated Form of Fig. 4c

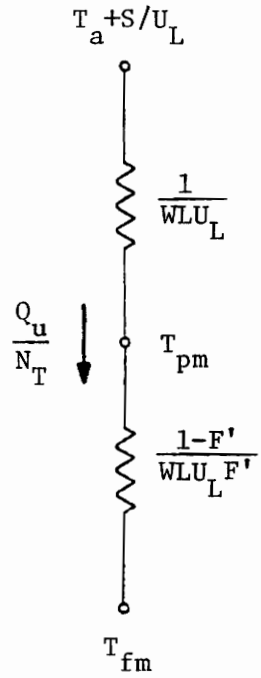

(b) Expanded Form

Figure 6. Mean Temperature Network Analogy

relabeled in terms of Θ_{fm}/Θ_{fi}. The value of Θ_{pm}/Θ_{fi} follows from the use of the F' graph.

The Averaging Method

A method of accounting for axial conduction within the absorber plate has recently been given by Phillips [2]. The method will be referred to as the averaging method. The averaging method uses an average transverse temperature in a lumped formulation of the absorber plate governing equation. In the lumped formulation, axial conduction in the absorber plate is included as an averaged quantity. Transverse heat flow is treated approximately by using one-dimensional fin results. By eliminating the transverse coordinate, the averaging method yields an absorber-plate governing differential equation in y alone. The equation is second-order, ordinary, and linear. The second-order absorber-plate equation is coupled to a first-order ordinary linear differential equation in y for the fluid temperature. Thus the averaging method uses an average transverse temperature distributed in the axial direction to account for plate axial conduction effects. All other assumptions made for the one-dimensional fin analysis are retained.

An energy balance on a control volume of incremental length Δy, taking axial conduction into consideration, is shown in Fig. 7. The energy balance can be written as

$$S W \Delta y + k_p \delta_p W \left[\left. \frac{d\bar{T}_p}{dy} \right|_{y+\Delta y} - \left. \frac{d\bar{T}_p}{dy} \right|_{y} \right] - U_L W \Delta y \left[\bar{T}_p - T_a \right] - q_u(y) \Delta y = 0 \quad (2.36)$$

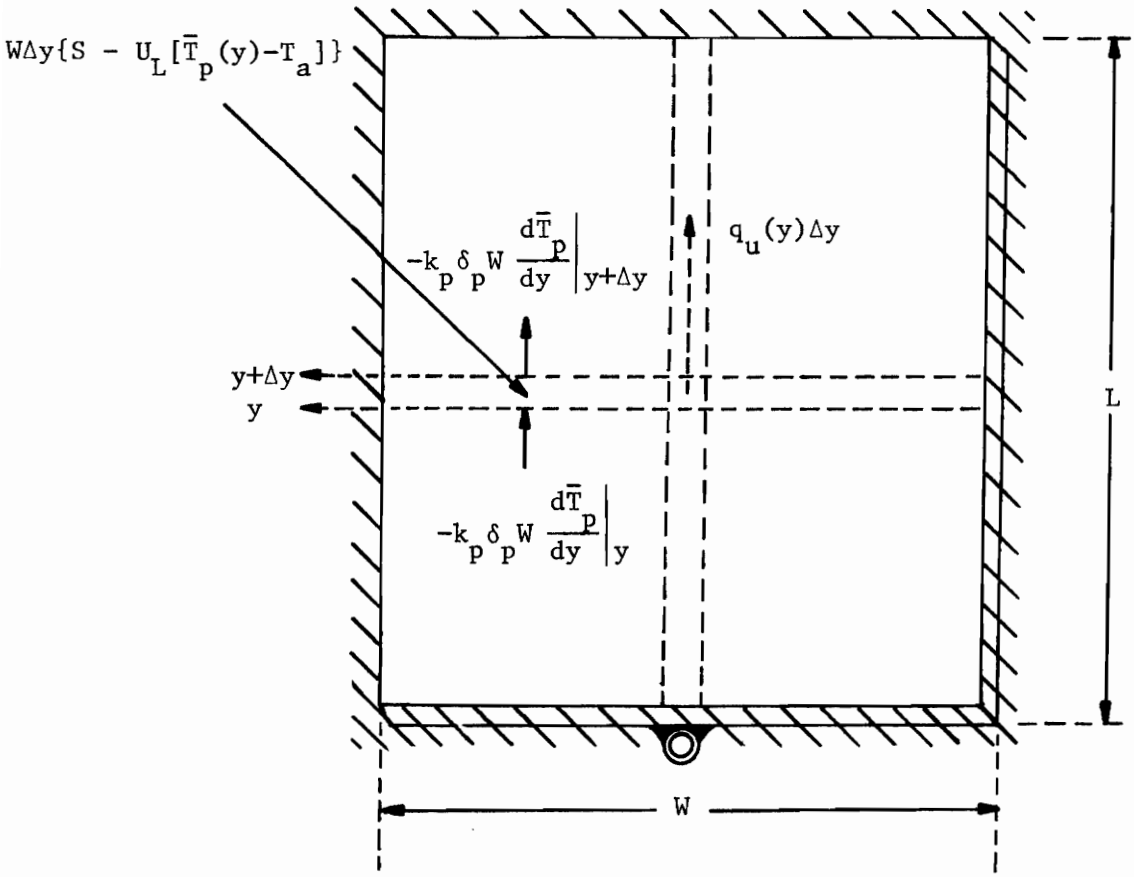

Figure 7. The Averaging Model

The term $q_u(y)$ in Eq. 2.36 represents the net heat flow, per differential length in the y-direction, from the absorber plate to the fluid when axial conduction effects are considered. Dividing Eq. 2.36 by Δy and taking the limit as Δy goes to zero gives

$$k_p \delta_p W \frac{d^2\bar{T}_p}{dy^2} - WU_L(\bar{T}_p - T_a - S/U_L) - q_u(y) = 0 \qquad (2.37)$$

Under the assumption of a uniform loss coefficient U_L, the second term on the left side of Eq. 2.37 is an exact expression for the net energy collected, per unit time per differential length in the y-direction, on the surface of the absorber-plate and tube regions. Denoting the term by $q_c(y)$, Eq. 2.37 may be rewritten as

$$k_p \delta_p W \frac{d^2\bar{T}_p}{dy^2} + q_c(y) - q_u(y) = 0 \qquad (2.38)$$

By rearranging Eq. 2.38 as

$$q_u(y) = q_c(y) - \left[-k_p \delta_p W \frac{d^2\bar{T}_p}{dy^2}\right] \qquad (2.39)$$

it is seen that $q_u(y)$, the local useful heat gain for the averaging method, is equal to $q_c(y)$ minus the net axial heat flow out of the differential control volume. Note that for the one-dimensional fin method $q_c(y) = q_u(y)$.

The term $q_u(y)$ is next expressed in terms of $\bar{T}_p(y)$ and $T_f(y)$ in order to achieve the necessary coupling between the plate and fluid governing equations. The expression for $q_u(y)$ is obtained from the one-dimensional fin analysis. The form of the appropriate expression

for $q_u(y)$ is more easily shown from a thermal network analysis. Type I geometry is assumed for the analysis. The procedure, however, is valid for Type II and III geometries also. Figure 8a shows the Type I design network introduced in Chapter II for the one-dimensional fin method. The network in Fig. 8a can be reduced to the equivalent network given by Fig. 8b. Using the general equality

$$q_c(y) = -WU_L[\bar{T}_p - T_a - S/U_L] \tag{2.40}$$

Fig. 8b can be expanded as in Fig. 8c to include $\bar{T}_p(y)$. The resistance value between $\bar{T}_p(y)$ and $T_b(y)$ in Fig. 8c is obtained by extracting the series resistance $1/U_L W$ from the net resistance between $T_b(y)$ and $T_a + S/U_L$ in Fig. 8b. Next, in Fig. 8d, the resistances on both sides of $T_b(y)$ in Fig. 8c are combined to give the equivalent resistance $1/U_G W$. Also, an axial heat flow term, $q_a(y)$, is included. The $q_a(y)$ term is the basic difference between the averaging method and the one-dimensional fin method. The resulting network in Fig. 8d is based on the assumption that axial conduction does not affect the local plate conductance for transverse heat flow. The plate transverse conductance is given by the term U_G. From Fig. 8d, the term $q_u(y)$ can be written as

$$q_u(y) = U_G W\,[\bar{T}_p(y) - T_f(y)] \tag{2.41}$$

where for a Type I design U_g is given by

$$U_G = \left[\frac{(W - D)(1 - F)}{U_L[(W - D)F + D]} + R_1 W\right]^{-1} \tag{2.42}$$

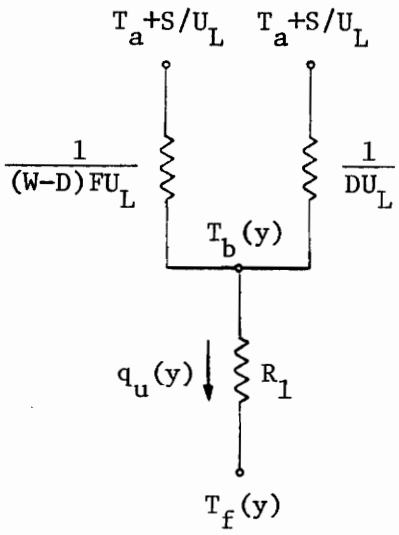

(a) Type I Design Network

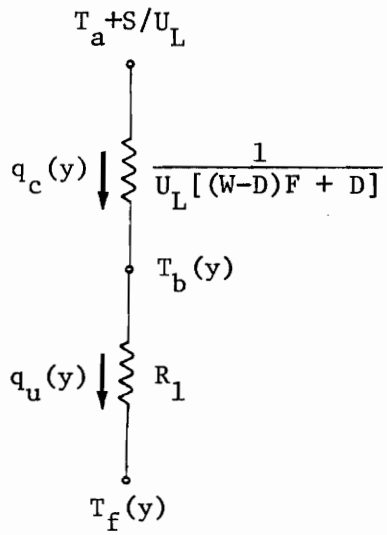

(b) Equivalent Type I Network

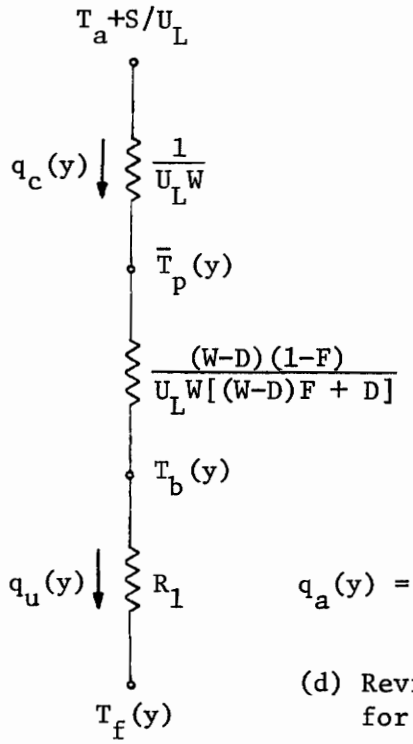

(c) Expanded Equivalent Network for a Type 1 Design

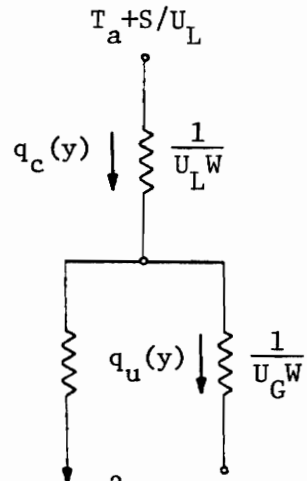

$$q_a(y) = -k_p \delta_p \frac{d^2\bar{T}_p}{dy^2}$$

(d) Revised Axial Conduction Network for the Averaging Method

Figure 8. Thermal Network Development for the Averaging Method

Substitution of Eq. 2.41 for $q_u(y)$ into the governing equation for $\bar{T}_p$, Eq. 2.37, yields

$$k_p \delta_p \frac{d^2\bar{T}_p}{dy^2} - U_L(\bar{T}_p - T_a) - U_G(\bar{T}_p - T_f) + S = 0 \qquad (2.43)$$

An energy balance on the fluid gives

$$\dot{m}c_p \frac{dT_f}{dy} + U_G W(T_f - \bar{T}_p) = 0 \qquad (2.44)$$

when q_u in Fig. 5 is replaced by Eq. 2.41. Equations 2.43 and 2.44 are coupled linear ordinary differential equations. Phillips non-dimensionalizes these equations by choosing the following variable substitutions. Let

$$P_s = \frac{T_s - T_{f,i}}{S/U_L + T_a - T_{f,i}}$$

where the dummy subscript s is replaced by either "p" or "f". Also the following dimensionless variables are defined:

$$M = \frac{\delta_p k_p}{L^2 U_L}, \qquad B = \frac{WLU_L}{\dot{m}c_p}, \qquad \beta = y/L$$

Noting that $F' = U_G/(U_L + U_G)$, Eqs. 2.43 and 2.44 become

$$M(1 - F') \frac{d^2\bar{P}_p}{d\beta^2} - \bar{P}_p + F'P_f + (1 - F') = 0 \qquad (2.45)$$

and

$$(1 - F')\frac{dP_f}{d\beta} + F'B(P_f - \bar{P}_p) = 0. \tag{2.46}$$

Although Eqs. 2.45 and 2.46 were derived for a Type I case, the equations are valid for any type of flat-plate assembly through the generality of the F' term. Note also that when M = 0, the equations reduce to the one-dimensional fin model.

In terms of the dimensionless parameters, the boundary conditions are given by

$$\left.\frac{d\bar{P}_p}{d\beta}\right|_{\beta=0} = 0, \quad \left.\frac{d\bar{P}_p}{d\beta}\right|_{\beta=1} = 0, \quad P_f(0) = 0$$

These conditions correspond to insulated boundaries for the plate and an inlet fluid temperature of T_{fi}, respectively.

The simultaneous solution of Eqs. 2.45 and 2.46 gives the following results.

$$\bar{P}_p(\beta) = 1 - \frac{a_1 e^{r_1\beta} + a_2 e^{r_2\beta} + a_3 e^{r_3\beta}}{d(b_1 + b_2 + b_3)} \tag{2.47}$$

and

$$P_f(\beta) = 1 - \frac{b_1 e^{r_1\beta} + b_2 e^{r_2\beta} + b_3 e^{r_3\beta}}{b_1 + b_2 + b_3} \tag{2.48}$$

where all the numerically subscripted variables (and d) are constants. The expressions for these constants are given in Appendix II. The relation between P_s and Θ_s is given by

$$P_s = 1 - \Theta_s / \Theta_{fi} \tag{2.49}$$

where s again denotes a dummy subscript. The heat removal factor, F_R, is obtained through the use of Eqs. 2.18, 2.48, and 2.49 and is given by

$$F_R = P_f(1)/B \tag{2.50}$$

The mean plate and fluid temperatures can be evaluated by integrating Eqs. 2.47 and 2.48 over β from 0 to 1. However, as noted earlier in Chapter II, the mean plate temperature can be more easily evaluated by use of the generalized expression given by Eq. 2.30, i.e.,

$$\frac{\Theta_{pm}}{\Theta_{fi}} = F_R \tag{2.30}$$

The mean fluid temperature can also be obtained more easily from Eq. 2.22, i.e.,

$$\frac{\Theta_{fm}}{\Theta_{fi}} = \frac{F_R}{F'} \tag{2.22}$$

The proof that Eq. 2.22 is valid for the averaging method analysis can be made as follows. Note that when the thermal network in Fig. 8d is integrated over all y, the net axial heat flow is equal to zero

due to the insulated y-direction boundary conditions, i.e.,

$$\int_0^L q_a(y)\, dy = 0 \tag{2.51}$$

Using Eq. 2.51, integration of Eq. 2.40 over y yields the result

$$\int_0^L q_u(y)\, dy = \int_0^L q_c(y)\, dy \tag{2.52}$$

Therefore the integrated form of the network given by Figure 8d is equivalent to the mean temperature network of Fig. 6, for which Eq. 2.22 is valid. Equation 2.52 can be rewritten as $Q_u = Q_c$. Note, however, that Q_u and Q_c will have a value in the averaging method that is different from the value in the one-dimensional fin method. The difference is due to the inclusion of the axial conduction term in the averaging method. Therefore, while Eqs. 2.22 and 2.30 are valid for both methods, the values of F_R, Θ_{pm}, and Θ_{fm} will be different for the two methods.

The averaging method yields some useful graphs and analytical limiting cases. One of these limiting cases, as noted earlier, is the one-dimensional fin method which results when M = 0. For M = ∞, axial conduction is very large and the absorber plate approaches a uniform temperature in the y direction. The M = ∞ case is given analytically by Phillips in terms of $P_f(1)$ as

$$P_f(1) = \frac{B\{1 - \exp[-F'B/(1 - F')]\}}{1 + B - \exp[-F'B/(1 - F')]} \tag{2.53}$$

as compared to

$$P_f(1) = 1 - \exp(- F'B) \tag{2.54}$$

when M = 0.

Another limiting case occurs when F' = 1; this case is given in Appendix II. Phillips notes differences in F_R values of as much as 25 per cent between the M = ∞ and the M = 0 limiting cases when the values of B range between 1 and 5.

The averaging method represents an improvement over the one-dimensional fin method. The improvement results from the inclusion of an averaged axial-conduction term in the absorber-plate governing equation. The question left unanswered by both methods is the amount of approximation incurred by the assumption of constant U_G values for local transverse plate conductance. If axial-transverse coupling significantly affects the local values of plate transverse conductance (i.e., if $U_G(y) \neq U_G$), the concept of constant U_G and F' values may fail to give accurate results. In Chapter III, the coupling between the transverse and axial temperature distributions is investigated.

III. AN ANALYTICAL METHOD FOR INCLUDING ABSORBER-PLATE AXIAL-TRANSVERSE COUPLING

Development of Basic Equations

The subject of Chapter III is the development and solution of equations which more accurately account for the two-dimensional nature of absorber-plate heat flow. For reference purposes, the analysis in Chapter III will be referred to as the exact method. All the assumptions used in Chapter II analyses are retained for the exact analysis except assumption 12, i.e., the assumption that axial conduction in the absorber plate does not affect the plate conductance for transverse heat flow. In eliminating assumption 12, a two-dimensional partial differential equation with intractable boundary conditions must be solved. The exact method which follows is a novel way of handling such difficult boundary conditions. The solution technique used has the potential of application to many types of conduction-convection problems.

Figure 9 shows a two-dimensional control volume on the absorber plate, valid for $0 \leq x \leq (W - D)/2$ and $0 \leq y \leq L$. An energy balance on the control volume yields the following governing equation, i.e.,

$$k_p \delta_p \frac{\partial^2 T_p}{\partial x^2} + k_p \delta_p \frac{\partial^2 T_p}{\partial y^2} + S - U_L (T_p - T_a) = 0 \qquad (3.1)$$

where $T_p = T_p(x,y)$. In terms of $\Theta_p(x,y)$, Eq. 3.1 becomes

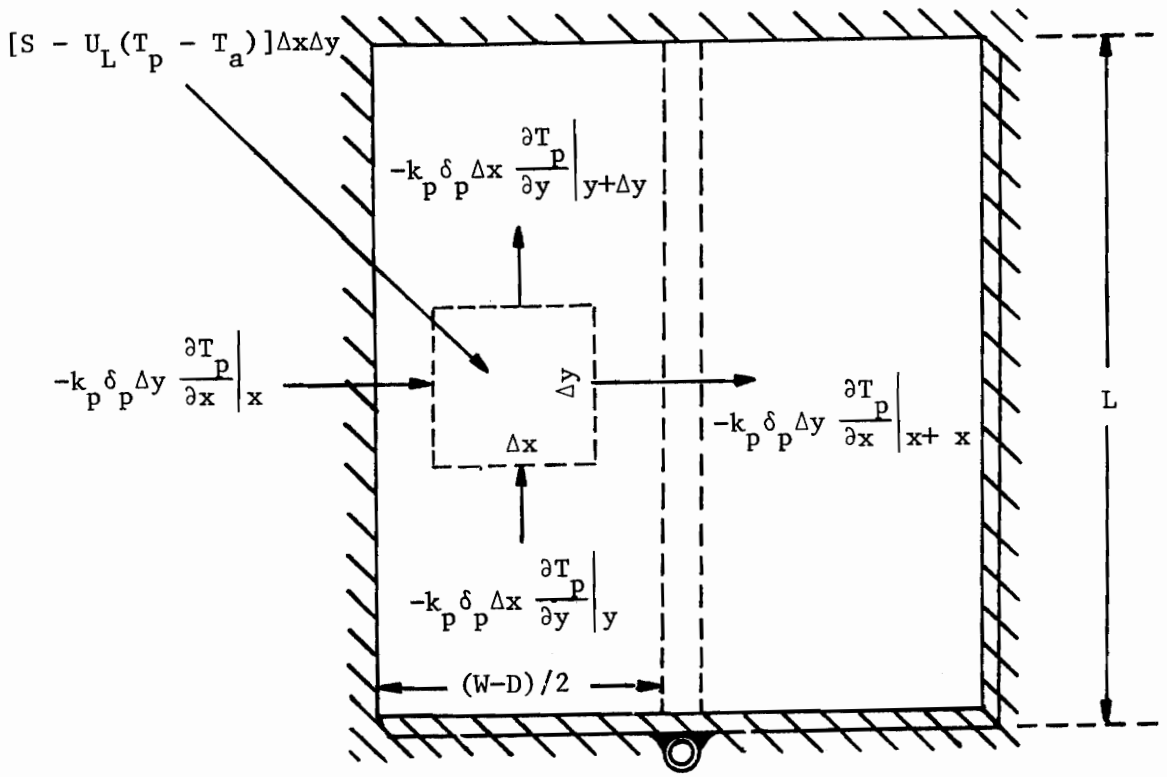

Figure 9. The Exact Model

$$\frac{\partial^2 \Theta_p}{\partial x^2} + \frac{\partial^2 \Theta_p}{\partial y^2} - \frac{U_L \Theta_p}{k_p \delta_p} = 0 \tag{3.2}$$

An energy balance on the fluid for Type I and II geometries yields

$$\dot{m} c_p \frac{dT_f}{dy} = [T_p(\frac{W-D}{2}, y) - T_f]/R \tag{3.3}$$

where $T_f = T_f(y)$. In terms of Θ_f and Θ_p, Eq. 3.3 becomes

$$\dot{m} c_p \frac{d\Theta_f}{dy} = [\Theta_p(\frac{W-D}{2}, y) - \Theta_f]/R. \tag{3.4}$$

By non-dimensionalizing the coordinate system, Eqs. 3.2 and 3.4 may be written as

$$\frac{\partial^2 \Theta_p}{\partial \eta^2} + a^2 \frac{\partial^2 \Theta_p}{\partial \beta^2} - c^2 \Theta_p = 0 \tag{3.5}$$

and

$$\frac{d\Theta_f}{d\beta} + f\ \Theta_f = f\ \Theta_p(1,\beta) \tag{3.6}$$

where

$$\eta = \frac{x}{(W-D)/2}\ , \quad \beta = y/L$$

$$a = \frac{W-D}{2L}\ , \quad c^2 = \frac{U_L(\frac{W-D}{2})^2}{k_p \delta_p}\ , \quad f = \frac{L}{R\dot{m}c_p}$$

Equations 3.5 and 3.6 constitute a set of coupled linear differential equations. The appropriate boundary conditions must next be applied. For the absorber plate region, there are three homogeneous and one non-homogeneous boundary conditions. The homogeneous conditions are given by the three insulated boundaries, i.e.,

$$\left.\frac{\partial \Theta_p(\eta,\beta)}{\partial \beta}\right|_{\beta=0} = \left.\frac{\partial \Theta_p(\eta,\beta)}{\partial \beta}\right|_{\beta=1} = 0 \tag{3.7}$$

for the y-direction boundaries and

$$\left.\frac{\partial \Theta_p(\eta,\beta)}{\partial \eta}\right|_{\eta=0} = 0 \tag{3.8}$$

for the mid-plate symmetry condition. The non-homogeneous boundary condition is given, for Type I-II geometries, by an energy balance on the tube base region, i.e.,

$$-2\,k_p\delta_p \left.\frac{\partial T_p(x,y)}{\partial x}\right|_{x=\frac{W-D}{2}} + D\{S - U_L[T_p(\tfrac{W-D}{2}, y) - T_a]\} =$$

$$-k_p\delta_p W_b \left.\frac{\partial^2 T_p(x,y)}{\partial y^2}\right|_{x=\frac{W-D}{2}} + [T_p(\tfrac{W-D}{2}, y) - T_f(y)]/R \tag{3.9}$$

where W_b is the effective width of the tube base region, given by D for Type I geometry and by one-half the average tube circumference for Type II geometry.*

*Note, in Eq. 3.9, that axial conduction along the tube base region is included by means of the second-partial derivative term. Axial

In terms of Θ, η, and β, Eq. 3.9 becomes

$$-\frac{r\,\partial^2\Theta_p(1,\beta)}{\partial\beta^2}+\frac{\partial\Theta_p(1,\beta)}{\partial\eta}+(g+h)\,\Theta_p(1,\beta)=g\Theta_f(\beta) \tag{3.10}$$

where

$$r=\frac{a^2\,W_b\,d_r}{2D},\qquad d_r=\frac{D}{(W-D)/2}$$

$$g=\frac{W-D}{4k_p\,\delta_p\,R},\qquad h=\frac{DU_L(W-D)}{4k_p\,\delta_p}$$

The fluid boundary condition is given by specifying the inlet fluid temperature, i.e.,

$$\Theta_f(0)=\Theta_{fi} \tag{3.11}$$

The analysis differences for Type III geometry occur in the absorber-plate non-homogeneous boundary condition and in the fluid governing equation. The absorber-plate non-homogeneous boundary condition for Type III geometry is obtained by energy balances on the tube base and tube regions. For the tube base region, the

---

*continued. . .

conduction along the tube region, however, is assumed negligible for Type I geometry to prevent unmanageable differential coupling between T_b, T_t, and T_f; i.e., the last term on the right side of Eq. 3.9 is valid for Type I geometry only under this assumption. For Type II geometry the tube base region and the tube region are the same; thus, no axial conduction is neglected. The averaging method in Chapter II also inherently neglects axial conduction in the tube region and includes axial conduction in the tube base region for Type I geometry. Therefore any difference between the exact and averaging model results for Type I geometry will not be obscured by the neglection of axial conduction in the tube region.

balance gives

$$\frac{-2k_p\delta_p}{(W-D)/2}\frac{\partial\theta_p(\eta,\beta)}{\partial\eta}\bigg|_{\eta=1} = \frac{-k_p\delta_p D}{L^2}\frac{\partial^2\theta_p(\eta,\beta)}{\partial\beta^2}\bigg|_{\eta=1} + C_B[\theta_p(1,\beta)-\theta_t(\beta)] \quad (3.12)$$

An energy balance on the tube region, neglecting axial conduction along the tube, yields

$$C_B[\theta_p(1,\beta) - \theta_t(\beta)] - DU_L\theta_t(\beta) = [\theta_t(\beta) - \theta_f(\beta)]/R_2 \quad (3.13)$$

Solving Eq. 3.13 for $\theta_t(\beta)$ and using the result to eliminate $\theta_t(\beta)$ from Eq. 3.12 gives

$$\frac{-a^2 d_r}{2}\frac{\partial^2\theta_p}{\partial\beta^2} + \frac{\partial\theta_p(1,\beta)}{\partial\eta} + (g_1 + h_1)\,\theta_p(1,\beta) = g_1\theta_f(\beta) \quad (3.14)$$

where

$$g_1 = \frac{W-D}{4k_p\delta_p}\cdot\frac{C_B/R_2}{C_B + DU_L + 1/R_2}$$

and

$$h_1 = \frac{W-D}{4k_p\delta_p}\cdot\frac{C_B DU_L}{C_B + DU_L + 1/R_2}\cdot$$

Note the equivalent forms of Eqs. 3.14 and 3.10. For the Type III case, the exact method again includes axial conduction in the tube base region and neglects axial conduction in the tube region. The corresponding Type III equations for the averaging method,

however, inherently include axial conduction in both the tube and the tube base regions. Therefore the effect of axial-transverse coupling cannot be independently shown for the case of Type III geometry but must be inferred from Type I results. The fluid equation for Type III geometry is given by

$$\frac{\dot{m}c_p}{L}\frac{d\Theta_f(\beta)}{d\beta} = [\Theta_t(\beta) - \Theta_f(\beta)]/R_2 \tag{3.15}$$

Using Eq. 3.13 to eliminate Θ_t from Eq. 3.15 gives

$$\frac{d\Theta_f(\beta)}{d\beta} + (f_1 + f_2)\,\Theta_f(\beta) = f_1\Theta_p(1,\beta) \tag{3.16}$$

where

$$f_1 = \frac{L}{\dot{m}c_p R_2} \cdot \frac{C_B}{C_B + DU_L + 1/R_2}$$

and

$$f_2 = \frac{L}{\dot{m}c_p R_2} \cdot \frac{DU_L}{C_B + DU_L + 1/R_2}$$

Equations 3.16 and 3.6 have the same form except for the f_2 term in Eq. 3.16. Since, however, the differential forms of the Type I-II and Type III equations are the same, the solution technique which follows is valid in either case.

Separation of Variables Solution

Equations 3.5 and 3.6 are to be solved subject to the boundary

conditions given by Eqs. 3.7, 3.8, 3.10, and 3.11. For later convenience, the equations may be totally non-dimensionalized by dividing through each equation by Θ_{fi}. The new equations are given by replacing "Θ" throughout by "ψ".

An expression for the plate temperature distribution, $\psi_p(\eta,\beta)$, can be found by an extension of the separation of variables techniques. The conventional difficulty arises in the evaluation of the resulting Fourier series expansion coefficients. The difficulty is due to the coupling between the second-order partial differential absorber-plate equation, Eq. 3.5, and the first-order ordinary differential fluid equation, Eq. 3.6. The situation is analogous to a two-dimensional heat conduction problem with a convective boundary condition in which the ambient temperature is coupled to the boundary temperature. The following analysis yields a separation of variables solution for the coupled boundary condition problem.

Assume a separable solution of the form

$$\psi_p(\eta,\beta) = N(\eta) \cdot B(\beta) \tag{3.17}$$

Substitution of Eq. 3.17 into Eq. 3.5 gives

$$\frac{1}{N(\eta)} \frac{d^2N(\eta)}{d\eta^2} - c^2 = \frac{-a^2}{B(\beta)} \frac{d^2B(\beta)}{d\beta^2} = \pm \lambda^2 \tag{3.18}$$

where $\pm \lambda^2$ is an arbitrary constant. Since β is the homogenous direction, the plus sign for λ^2 is chosen [8]. From Eq. 3.18, the

governing equation for $B(\beta)$ is

$$\frac{d^2B}{d\beta^2} + \lambda^{*2} B = 0 \tag{3.19}$$

where $\lambda^* = \lambda/a$.

The general solution of Eq. 3.19 is given by

$$B(\beta) = A \cos \lambda^* \beta + C \sin \lambda^* \beta \tag{3.20}$$

where A and C are arbitrary constants. The boundary conditions for Eq. 3.20, from the separable form of Eq. 3.7, are

$$\left.\frac{dB}{d\beta}\right|_{\beta=0} = \left.\frac{dB}{d\beta}\right|_{\beta=1} = 0 \tag{3.21}$$

Application of the boundary conditions to Eq. 3.20 yields a family of particular solutions, i.e.,

$$B_n(\beta) = A_n \cos \lambda_n^* \beta \qquad n = 0,1,2,\ldots \tag{3.22}$$

where $\lambda_n^* = \lambda_n/a = n\pi$ and A_n is an arbitrary constant. Next, from Eq. 3.19, the governing equation for $N(\eta)$ is given by

$$\frac{d^2N_n(\eta)}{d\eta^2} - \gamma_n^2 N_n(\eta) = 0 \tag{3.23}$$

where $\gamma_n^2 = \lambda_n^2 + c^2$ and $\lambda_n = n\pi a$. The general solution to Eq. 3.23 is given by

$$N_n(\eta) = D_n \sinh \gamma_n \eta + E_n \cosh \gamma_n \eta \tag{3.24}$$

where D_n and E_n are arbitrary constants. The homogenous boundary condition for Eq. 3.24, obtained from the separable form of Eq. 3.8, is given by

$$\left.\frac{dN_n}{d\eta}\right|_{\eta=0} = 0 \tag{3.25}$$

Applying Eq. 3.25 to Eq. 3.24 yields

$$N_n(\eta) = E_n \cosh \gamma_n \eta \tag{3.26}$$

Substitution of Eqs. 3.22 and 3.26 into Eq. 3.18 and summing over n from 0 to ∞ yields the general solution for $\psi_p(\eta,\beta)$, i.e.,

$$\psi_p(\eta,\beta) = \sum_{n=0}^{\infty} C_n \cosh \gamma_n \eta \cos \lambda_n^* \beta \tag{3.27}$$

where $C_n = B_n E_n$. The non-homogenous boundary condition, Eq. 3.10, may be rewritten in terms of $\psi_p(\eta,\beta)$ and $\psi_f(\beta)$ as

$$\frac{-r\,\partial^2\psi_p(1,\beta)}{\partial\beta^2} + \frac{\partial\psi_p(1,\beta)}{\partial\eta} + (g + h)\,\psi_p(1,\beta) = g\psi_f(1,\beta). \tag{3.28}$$

From Eq. 3.27,

$$\frac{\partial\psi_p(1,\beta)}{d\eta} = \sum_{n=0}^{\infty} C_n\gamma_n \sinh \gamma_n \cos \lambda_n^* \beta \tag{3.29}$$

and

$$\frac{\partial^2\psi_p(1,\beta)}{\partial\beta^2} = -\sum_{n=0}^{\infty} C_n(\lambda_n^*)^2 \cosh \gamma_n \cos \lambda_n^* \beta \tag{3.30}$$

Substituting Eqs. 3.29 and 3.30 into Eq. 3.28 gives

$$\sum_{n=0}^{\infty} C_n[\gamma_n \sinh \gamma_n + (g + h + r_n) \cosh \gamma_n] \cos \lambda_n^* \beta = g\psi_f(\beta) \quad (3.31)$$

where $r_n = r(\lambda_n^*)^2$.

Multiplying both sides of Eq. 3.31 by $\cos \lambda_m^* \beta$, integrating over β from 0 to 1, and using the orthogonality relations

$$\int_0^1 \cos \lambda_m^* \beta \cos \lambda_n^* d\beta = 0 \text{ for } m \neq n \quad (3.32)$$

$$= 1/2 \text{ for } m = n,\ n \neq 0$$

$$= 1 \text{ for } m = n,\ n = 0$$

yields the following expressions for the expansion coefficients C_n.

$$C_o = \frac{g \int_0^1 \psi_f(\beta) d\beta}{c \sinh c + (g + h)\cosh c} \quad (3.33)$$

and

$$C_m = \frac{2g \int_0^1 \psi_f(\beta) \cos \lambda_m^* \beta \, d\beta}{\gamma_m \sinh \gamma_m + (g + h + r_m)\cosh \gamma_m},$$

$$(m = 1, 2, \ldots) \quad (3.34)$$

To evaluate the integrals within Eqs. 3.33 and 3.34, an appropriate expression for $\psi_f(\beta)$ must be found. The fluid governing equation, Eq. 3.6, and the corresponding boundary condition, Eq. 3.11, when written in terms of $\psi_f(\beta)$ and $\psi_p(1,\beta)$, become

$$\frac{d\psi_f(\beta)}{d\beta} + f\ \psi_f(\beta) = f\ \psi_p(1,\beta) \tag{3.35}$$

and

$$\psi_f(0) = 1 \tag{3.36}$$

Using Eq. 3.30 in Eq. 3.35 gives

$$\frac{d\psi_f(\beta)}{d\beta} + f\ \psi_f(\beta) = f \sum_{n=0}^{\infty} C_n \cosh \gamma_n \cos \lambda_n^* \beta \tag{3.37}$$

Multiplying both sides of Eq. 3.37 by the integrating factor $e^{f\beta}$ gives

$$d(e^{f\beta}\psi_f(\beta)) = fe^{f\beta}[C_o \cosh c + \sum_{n=1}^{\infty} C_n \cosh \gamma_n \cos \lambda_n^* \beta] \tag{3.38}$$

Multiplying both sides of Eq. 3.38 by $d\beta$ and integrating over β from 0 to 1 yields, after algebraic simplification,

$$\psi_f(\beta) = e^{-f\beta} + (1 - e^{-f\beta})C_o \cosh c + \sum_{n=1}^{\infty} \frac{C_n \cosh \gamma_n}{1 + (\lambda_n^*/f)^2} \cdot$$

$$(\cos \lambda_n^* \beta + \frac{\lambda_n^*}{f} \sin \lambda_n^* \beta - e^{-f\beta}) \tag{3.39}$$

The integrals within Eqs. 3.33 and 3.34 can now be evaluated through the use of Eq. 3.39 and standard integration formula tables. From Eq. 3.34,

$$\int_0^1 \psi_f(\beta)d\beta = \frac{1}{f} \{1 - e^{-f} + [f - (1 - e^{-f})]C_o \cosh c -$$

$$\sum_{n=1}^{\infty} [(-1)^n - e^{-f}] \frac{C_n \cosh \gamma_n}{1 + (\lambda_n^*/f)^2} \tag{3.40}$$

From Eq. 3.33,

$$\int_0^1 \psi_f(\beta) \cos \lambda_m^* \beta \, d\beta = \frac{1}{f} \frac{[1 - (-1)^m e^{-f}]}{1 + (\lambda_m^*/f)^2} \{1 - C_o \cosh c -$$

$$\sum_{n=1}^{\infty} \frac{C_n \cosh \gamma_n}{1 + (\lambda_n^*/f)^2} \} + \frac{C_m \cosh \gamma_m}{2[1 + (\lambda_m^*/f)^2]} +$$

$$\frac{2}{f} \sum_{n=i,i+2,..}^{\infty} \frac{C_n \cosh \gamma_n}{[1 + (\lambda_n^*/f)^2][1 - (m/n)^2]} \tag{3.41}$$

where i = 1 when m is even ($m \neq 0$) and i = 2 when m is odd. Substituting Eqs. 3.40 and 3.41 into the respective expansion coefficient expressions, Eqs. 3.33 and 3.34, yields equations for each expansion coefficient in terms of all the expansion coefficients; i.e., the right side of the resulting expressions for C_o and C_m contain all C_n's (n = 0, 1, 2, 3, ...) including the specific C_o or C_m given on the left side. Solving for the specific C_o and C_m gives the results

$$C_o = [E_c(1 - \sum_{n=2,4,..}^{\infty} C_n D_n) + F_c \sum_{n=1,3,..}^{\infty} C_n D_n]/A_c \tag{3.42}$$

and

$$C_m = [B_m(1 - C_o \cosh c - \sum_{\substack{n=1,2,.. \\ n \neq m}}^{\infty} C_n D_n) + 2 \sum_{n=i,i+2,..}^{\infty} C_n D_n E_{mn}]/A_m \tag{3.43}$$

where

$$A_c = \frac{fc}{g} \sinh c + (fh/g + E_c) \cosh c$$

$$A_m = \frac{f\gamma_m}{2g} \sinh \gamma_m + f(h + g + r_m) \cosh \gamma_m/2g - D_m(f - 2B_m)/2$$

$$B_m = \frac{1 - (-1)^m e^{-f}}{1 + (\lambda_m^*/f)^2}$$

$$D_n = \frac{\cosh \gamma_n}{1 + (\lambda_n^*/f)^2}$$

$$E_c = 1 - e^{-f}$$

$$E_{mn} = \frac{1}{1 - (m/n)^2}$$

$$F_c = 1 + e^{-f}$$

Equations 3.42 and 3.43 express C_o and C_m, respectively, in terms of all the remaining C_n's. By collecting all the expansion coefficients on one side, Eqs. 3.42 and 3.43 can be rewritten, respectively, as

$$\sum_{n=2,4,..}^{\infty} C_n D_n - \frac{F_c}{E_c} \sum_{n=1,3,..}^{\infty} C_n D_n + C_o A_c/E_c = 1 \qquad (3.44)$$

and

$$\sum_{n=i,i+2,..}^{\infty} C_n D_n (1 - 2E_{mn}/B_m) + \sum_{\substack{n=j,j+2,.. \\ n\neq m}}^{\infty} C_n D_n + C_m A_m/B_m + C_o \cosh c = 1 \qquad (3.45)$$

where j = 1 when m is odd and j = 2 when m is even ($m \neq 0$). Note that Eq. 3.45 is an infinite set of equations (m = 1, 2, ...). Equations 3.44 and 3.45 therefore constitute a complete infinite set of linear algebraic equations for C_n (n = 0, 1, ...). By truncating the complete infinite set of equations at $m = M_T$ and the interior summations at $n = M_T$, a solvable finite set of $M_T + 1$ linear algebraic equations is obtained. The finite set can be cast in the form

$$\underline{\underline{A}}\ \underline{C} = \underline{I} \tag{3.46}$$

where $\underline{\underline{A}}$ is a $(M_T + 1) \times (M_T + 1)$ matrix of constant coefficients for the C_n's given by the truncated form of Eqs. 3.44 and 3.45, $\underline{C}$ is a column vector with elements given by C_o, C_1, ..., C_{M_T}, and $\underline{I}$ is a column vector with each element equal to 1. From Eq. 3.46, the solution for $\underline{C}$ is given by

$$\underline{C} = \underline{\underline{A}}^{-1}\ \underline{I} \tag{3.47}$$

The values of the expansion coefficients so obtained are approximate values as a result of the truncation necessary for solution. However, the predominant coefficient C_o converges rapidly to within 0.01 per cent for $M_T = 10$. Later in Chapter III it will be shown that only C_o is needed to calculate the values of F_R, ψ_{pm}, and ψ_{fm}. Further discussion of the computational procedure used to evaluate the expansion coefficients is given in Appendix III. A listing of the FORTRAN program is also provided.

The series solutions for $\psi_p(\eta,\beta)$ and $\psi_f(\beta)$ as given by Eqs. 3.27

and 3.39 are functions of eight dimensionless variables -- η, β, a, c, f, g, h, and r. The variables g and h may be conveniently rewritten as

$$g = u_r d_r' c^2 \tag{3.48}$$

and

$$h = d_r' c^2 \tag{3.49}$$

where the variables d_r' and u_r are also dimensionless quantities given by

$$d_r' = d_r/2 = D/(W - D)$$

and

$$u_r = 1/RDU_L$$

The variable r may be rewritten as

$$r = a^2 d_r' (W_b/D) \tag{3.50}$$

From Eqs. 3.48, 3.49, and 3.50, a new set of eight dimensionless variables can be obtained, i.e., the set of η, β, a, c, f, d_r', u_r, and W_b/D. For later convenience, the variables B, M, and F' from Chapter II can be written in terms of the new set of variables as follows:

$$B = \frac{f(1 + d_r')}{u_r d_r'} \tag{3.51}$$

$$M = a^2/c^2 \tag{3.52}$$

$$F' = \frac{1}{\frac{1 + d_r'}{F + d_r'} + \frac{1 + d_r'}{u_r d_r'}} \tag{3.53}$$

where

$$F = (\tanh c)/c \tag{3.54}$$

Evaluation of F_R, ψ_{pm}, and ψ_{fm} and Comparison with Existing Models

The heat removal factor F_R is given, in terms of ψ_f, by

$$F_R = [1 - \psi_f(1)]/B \tag{3.55}$$

Using Eq. 3.39 with $\beta = 1$, Eq. 3.55 becomes

$$(F_R)_E = [(1 - e^{-f}) - \sum_{n=0}^{M_T} [(-1)^n - e^{-f}] C_n D_n]/B \tag{3.56}$$

where the subscript E denotes the exact method. Using the general relation between Θ_{pm} and F_R derived in Chapter II, i.e., Eq. 2.40, F_R is alternately given by

$$(F_R)_E = (\psi_{pm})_E \tag{3.57}$$

An expression for $(\psi_{pm})_E$ can be obtained from

$$(\psi_{pm})_E = \frac{W-D}{W} \int_0^1 \int_0^1 \psi_p(\eta,\beta) d\beta d\eta + \frac{D}{W} \int_0^1 \psi_p(1,\beta)\, d\beta \tag{3.58}$$

Using the series solution for $\psi_p(\eta,\beta)$ given by Eq. 3.27, Eq. 3.58 becomes

$$(\psi_{pm})_E = F_d C_o \cosh c \tag{3.59}$$

where

$$F_d = \frac{F + d_r'}{1 + d_r'}$$

From Eqs. 3.57 and 3.59, $(F_R)_E$ is alternately given by

$$(F_R)_E = F_d C_o \cosh c \tag{3.60}$$

Equation 3.60 is more accurate than Eq. 3.56 since the value of C_o converges more rapidly than the truncated series in Eq. 3.56. Equation 3.60 is also preferable by reason of simplicity since for any given set of parameters, C_o is the only unknown.

An expression for $(\psi_{fm})_E$ is given by Eq. 3.40 because, by definition

$$\psi_{fm} = \int_0^1 \psi_f(\beta)\, d\beta \tag{3.61}$$

Using Eqs. 3.56 and 3.60, Eq. 3.40 can be rewritten as

$$(\psi_{fm})_E = (F_R)_E\ (F_{ud} + 1/F_d) \tag{3.62}$$

where

$$F_{ud} = \frac{1 + d_r'}{u_r d_r'}$$

From the definitions of F_d and F_{ud}, Eq. 3.53 can be rewritten as

$$F' = \frac{1}{1/F_d + F_{ud}} \tag{3.63}$$

Substitution of Eq. 3.63 into Eq. 3.62 gives the result

$$(\psi_{fm})_E = \frac{(F_R)_E}{F'} \tag{3.64}$$

Equation 3.64 can be shown to be valid for Type III geometry also. The form of Eq. 3.64 is the same as the ψ_{fm} equations derived in Chapter II.* Therefore, for each of the three methods, ψ_{pm} and ψ_{fm} are given by the relations

$$\psi_{pm} = F_R \tag{3.65}$$

and

$$\psi_{fm} = \frac{F_R}{F'} \tag{3.66}$$

Equations 3.65 and 3.66 can be combined to give another relation, i.e.,

$$\psi_{pm} = F'\psi_{fm} \tag{3.67}$$

Equations 3.65 and 3.66 are two equations in the three unknowns F_R, ψ_{pm}, and ψ_{fm}. For the evaluation of all three quantities, one of the three must be evaluated independently. In the one-dimensional fin and averaging methods, F_R is most conveniently evaluated from the value of

---

* Note, however, that a derivation specific to the particular method is necessary in each case.

$\psi_f(1)$. In the exact method F_R is evaluated from knowledge of C_o. The value of F_R will, in general, be different for each method. From Eqs. 3.65 and 3.66, different F_R values result in different ψ_{pm} and ψ_{fm} values.

The equivalence of Eq. 3.67 for all three methods does not imply that the concept of constant F' and U_G values is valid for local transverse heat-flow evaluation. Equation 3.67 indicates that the mean value of transverse plate conductance is given by U_G. The differences in local transverse heat-flow relations between methods will be noted later in Chapter III.

Since ψ_{pm} and ψ_{fm} values are directly related to F_R values, only F_R comparisons between methods need be made. The exact method relation for F_R, Eq. 3.60, is a function of a, c, f, d_r', u_r, and W_b/D for the general Type I-II case. For Type I geometry specifically, the variable W_b/D is equal to 1. The exact analysis has therefore increased the number of dimensionless variables needed to represent F_R, ψ_{pm}, and ψ_{fm} to five or greater. This compares with two (B and F') for the one-dimensional fin model and three (B, F', and M) for the averaging method.

The largest differences between the exact and the averaging-method results for F_R are to be expected when axial conduction becomes large relative to transverse conduction. This extreme situation corresponds, for the averaging method, to the $M = \infty$ limiting case. From Eq. 2.53, for $M = \infty$, F_R is given by

$$(F_R)_A^{\infty} = \frac{1 - \exp\,[-BF'/(1 - F')]}{B + 1 - \exp\,[-BF'/(1 - F')]} \tag{3.68}$$

where the subscript A denotes the averaging method and the superscript ∞ denotes the $M = \infty$ case when used with "A". Equation 3.67 is to be compared with the corresponding limiting case for the exact method. The analogous case for the exact method occurs when $a = \infty$. From Eq. 3.43, as $a \to \infty$, the expansion coefficients $C_n (n \neq 0) \to 0$. More importantly, the $C_n \cosh \gamma_n$ terms of the series expansion solution for $\psi_p(\eta,\beta)$, Eq. 3.27, also go to zero as $a \to \infty$. Note that γ_n is defined as $\gamma_n = [c^2 + (n\pi a)^2]^{1/2}$. As $a \to \infty$, $C_n \to 0$ more quickly than $\cosh \gamma_n \to \infty$. With $C_n \cosh \gamma_n = 0$ $(n \neq 0)$, Eq. 3.42 reduces to

$$C_o = E_c/A_c \tag{3.69}$$

Substituting Eq. 3.69 into Eq. 3.60 and using the definitions of E_c and A_c yields, after algebraic simplification, the result

$$(F_R)_E^{\infty} = \frac{(1 - e^{-f})\, F_d}{BF_d + (1 - e^{-f})} \tag{3.70}$$

where the superscript ∞ denotes the $a = \infty$ case when used with the subscript E. Noting the identity

$$f = BF_dF'/(F_d - F') \tag{3.71}$$

Eq. 3.70 becomes

$$(F_R)_E^{\infty} = \frac{\{1 - \exp\,[-BF_dF'/(F_d - F')]\}\, F_d}{BF_d + 1 - \exp\,[-BF_dF'/(F_d - F')]} \tag{3.72}$$

The form of Eq. 3.72 was chosen to facilitate comparisons between the exact and averaging methods. Equation 3.72 is a function of B, F', and F_d. The $(F_R)_A^\infty$ equation, Eq. 3.68, is a function of B and F'. Therefore the exact method requires one additional dimensionless parameter, i.e., F_d, to specify F_R in the limiting case of large axial conduction.

When $F_d = 1$, $(F_R)_E^\infty = (F_R)_A^\infty$. This case occurs when F = 1 or when $d_r' \to \infty$. The value of F_d can range from $F' \leq F_d \leq 1$. The range of F_d values can be seen by rewriting Eq. 3.63 as

$$F_{ud} = \frac{1}{F'} - \frac{1}{F_d} \tag{3.73}$$

Since $F_{ud} \geq 0$, $F' \leq F_d$. Also, since $F' \leq 1$ and $F_{ud} \geq 0$, $F_d \leq 1$. The maximum differences between $(F_R)_A^\infty$ and $(F_R)_E^\infty$ occur when $F_d = F'$. Taking the limit as $F_d \to F'$, Eq. 3.72 reduces to

$$(F_R)_E^\infty = \frac{F'}{BF' + 1} \tag{3.74}$$

Figure 10 through 15 show F_R vs B for values of F' from 0.5 to 1.0. The shaded region in each figure is bounded above by an $(F_R)_A^\infty$ curve from Eq. 3.68 and bounded below by an $(F_R)_E^\infty$ curve with $F_d = F'$ from Eq. 3.74. Each shaded region represents all possible values of $(F_R)_E^\infty$ from Eq. 3.72 as F_d varies from F' to 1. The remaining three curves in each of Figs. 10 through 15 represent $(F_R)_A$ curves for M = 0.5, M = 0.1, and M = 0.0.* The M = 0.0 curves are also $(F_R)_{1\text{-}D}$

---

* Footnote on next page.

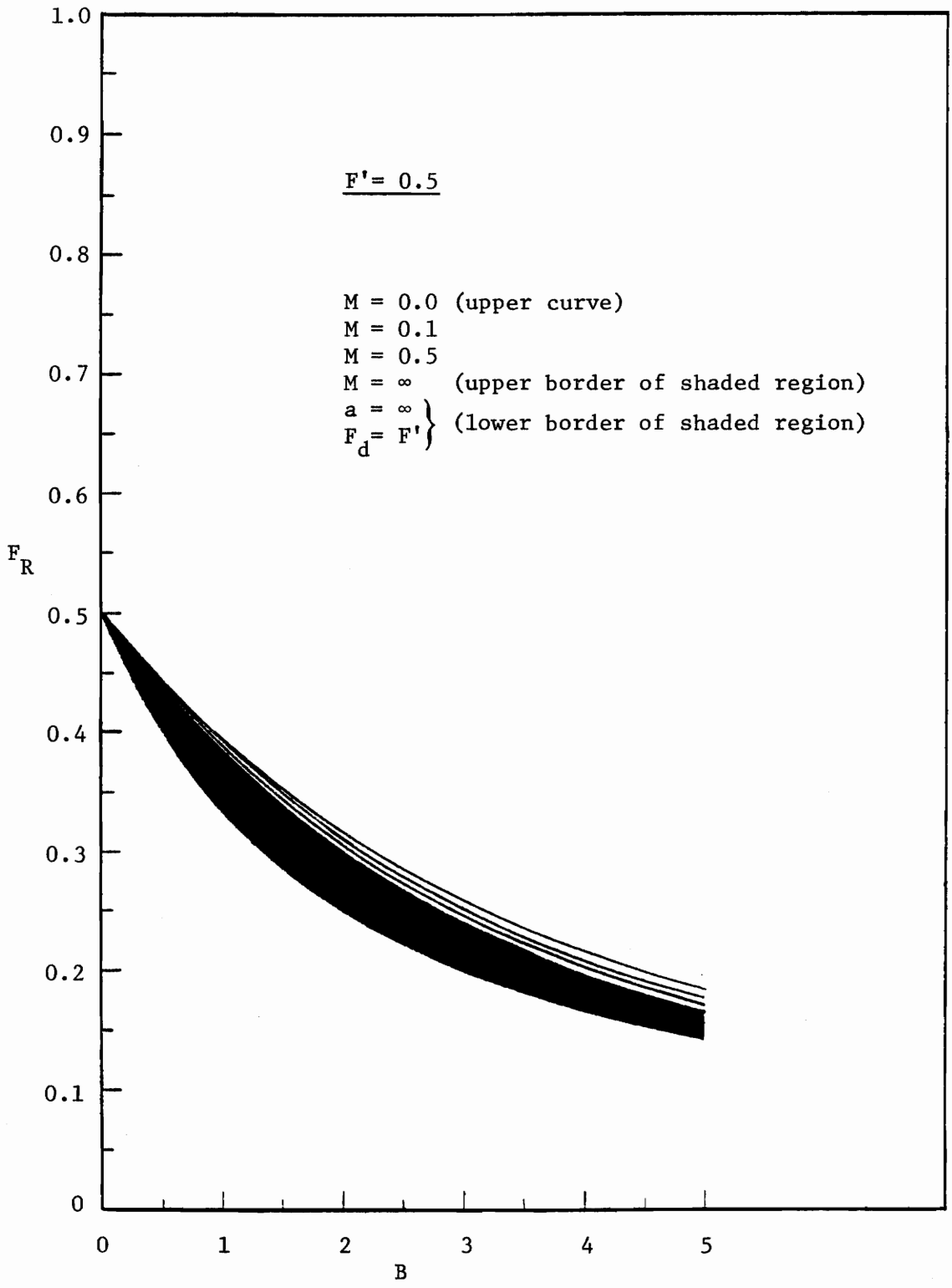

Figure 10. F_R vs B Curves -- F'= 0.5

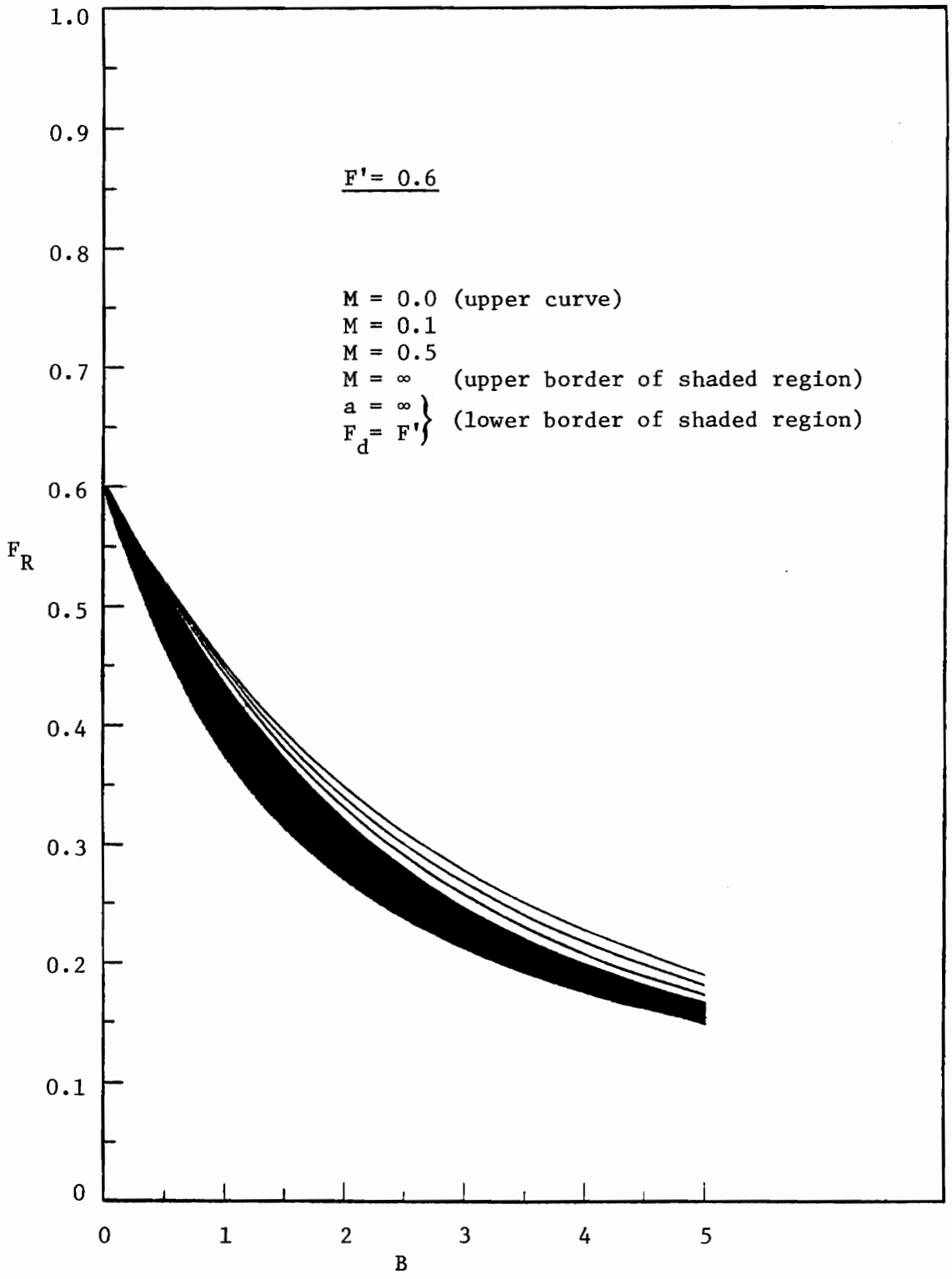

Figure 11. F_R vs B Curves -- F'= 0.6

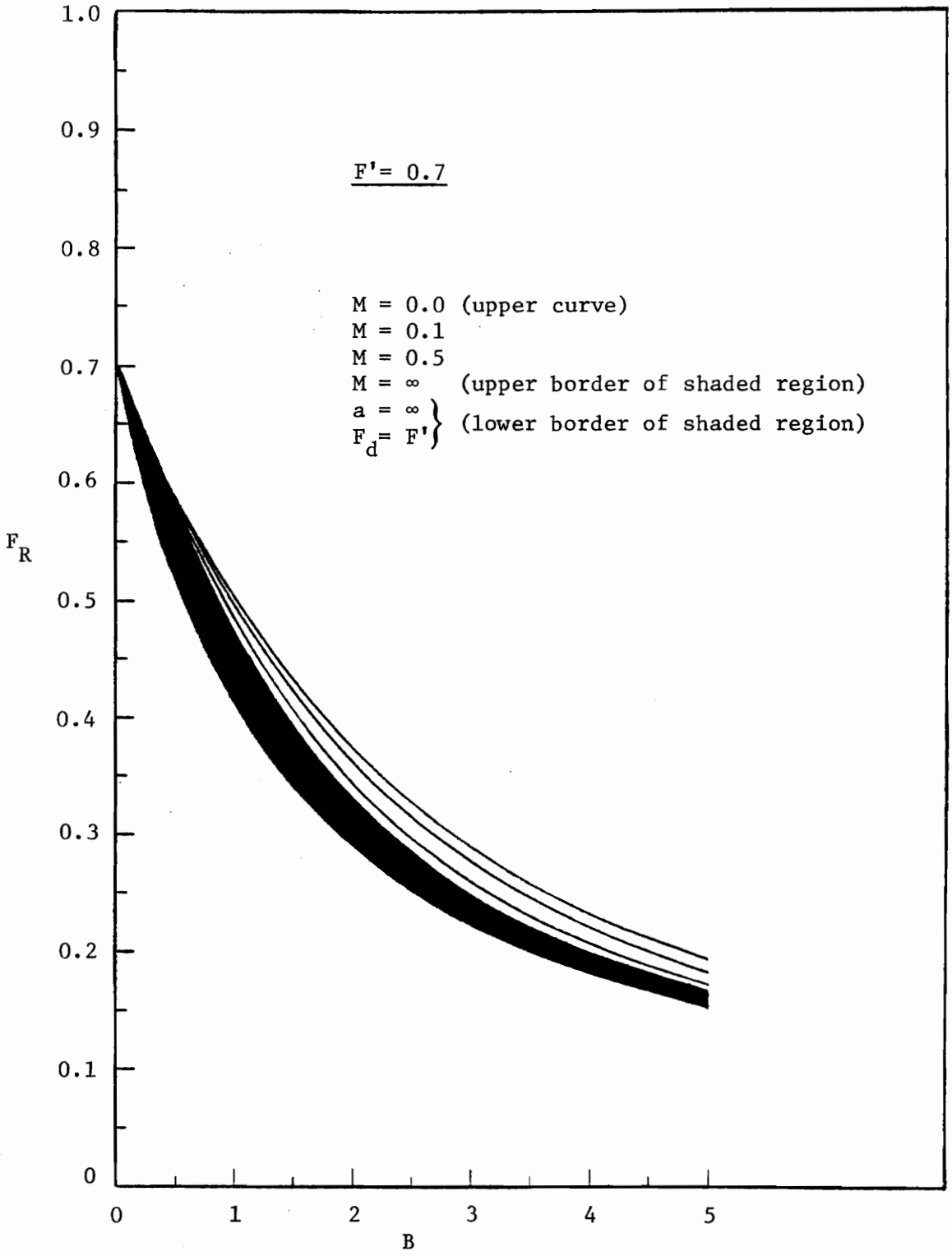

Figure 12. F_R vs B Curves -- F'= 0.7

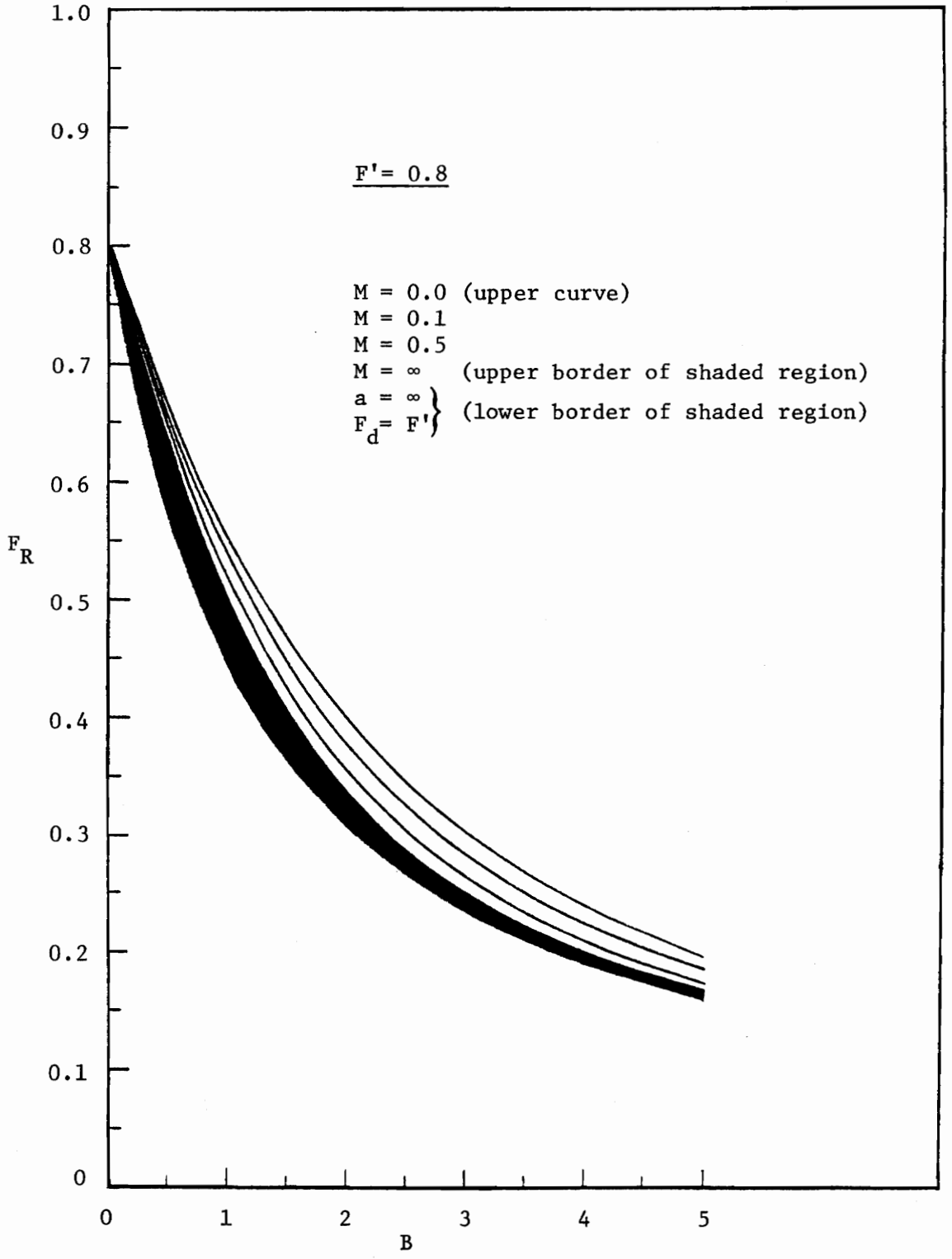

Figure 13. F_R vs B Curves -- F'= 0.8

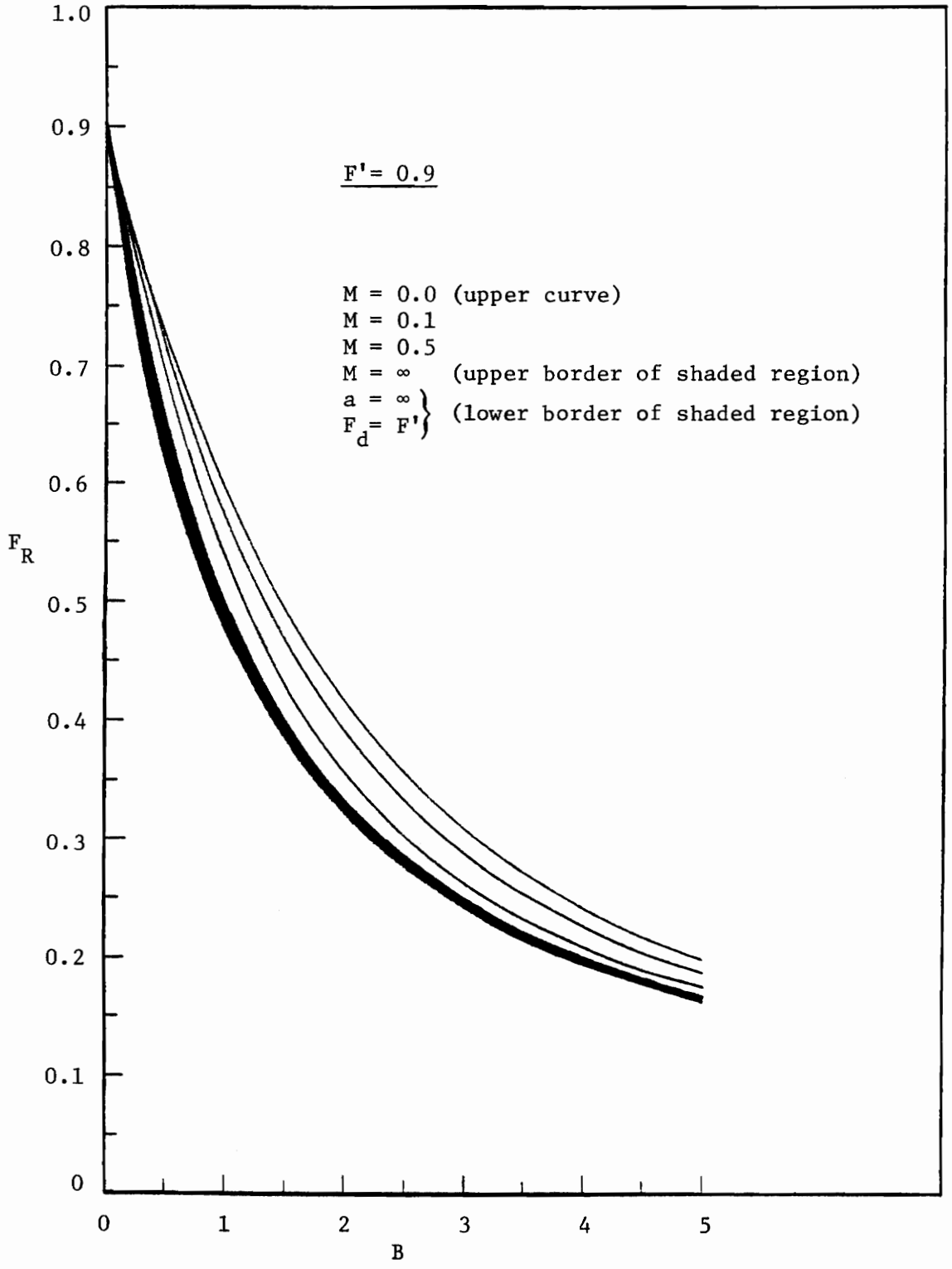

Figure 14. F_R vs B Curves -- F'= 0.9

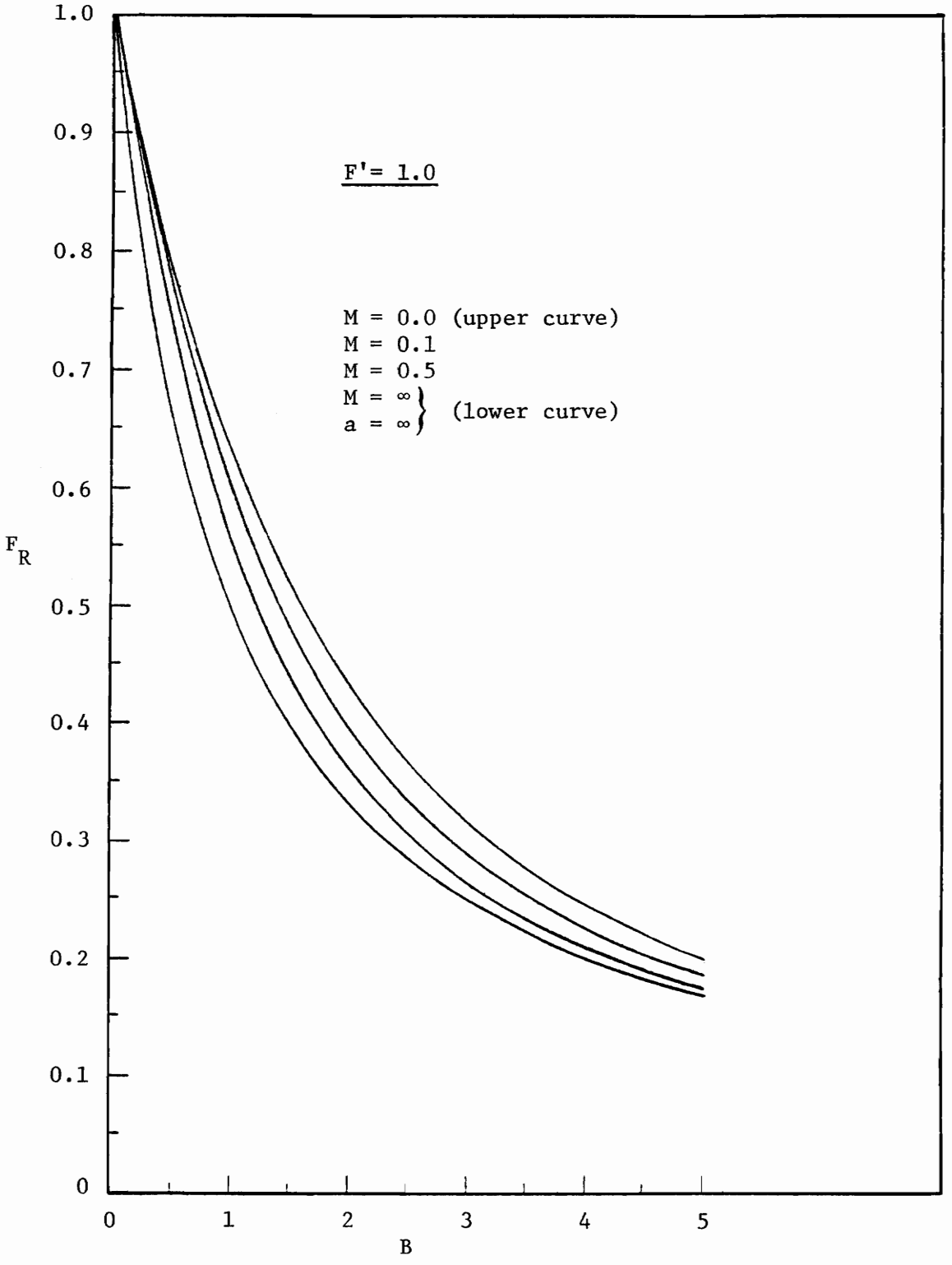

Figure 15. F_R vs B Curves -- F'= 1.0

curves, i.e., F_R curves from the one-dimensional fin method. Therefore the M = 0.0 curves provide a convenient reference point from which to evaluate the relative improvement in accuracy of the averaging and exact methods. Comparison of $(F_R)_{1-D}$ and $(F_R)_A$ values to $(F_R)_E$ values is shown only for the $(F_R)_E^{\infty}$ case. Exact method "shaded regions" for M = 0.1 and M = 0.5 cases proved impractical to obtain. A more convenient means of comparison between $(F_R)_E$ and $(F_R)_A$ for M = 0.1 and M = 0.5 cases is presented later in Chapter III.

However, at this point, the general trends of the exact method over the range of M and a-values will be noted. Since the exact method contains more dimensionless variables than the averaging method, a specific averaging set of B, M, and F' can be satisfied by an infinite number of exact method parameter sets. However, for all exact parameter sets which give the same B, M, and F' values, $(F_R)_E \leq (F_R)_A$. Since, in turn, $(F_R)_A \leq (F_R)_{1-D}$, the exact method consistently yields more conservative F_R values than either of the two existing methods. The second trend to be noted is the effect of a-values < ∞ on the width of "shaded regions" bordering each of the M-curves in Figs. 10 through 15. Ranges of a-values can be associated with each of the M-curves by considering Eq. 3.52, i.e., $M = a^2/c^2$. A practical

---

* Except for the shaded regions, Figs. 10 through 15 are replotted versions of graphs given by Phillips [2]. Phillips plotted $P_f(1)$ vs B for a similar range of M and F' values. The plots of F_R vs B in Figs. 10 through 15 are more convenient in that F_R and ψ_{pm} can be obtained directly and ψ_{fm}, given by F_R/F' can be easily calculated.

range of c-values is $0 \leq c < 4$. Table 3.1 gives a-ranges for various M-values when the values of c are restricted to $0 \leq c < 4$. Phillips notes that the $(F_R)_A^{\infty}$ curves are adequate for M-values greater than 10.* The corresponding $a = \infty$ shaded regions are adequate for a-values ≥ 30. For exact method parameter sets where $a < 30$ and $M > 10$, the shaded regions become narrower with decreasing a-values. The regions remain bounded above by the $(F_R)_A^{\infty}$ curves. As M decreases below 10, the associated exact "shaded regions" become narrower (as compared to the $a \geq 30$ shaded regions) with the maximum widths occurring at the maximum allowable a-values. At $M = 0$, the "shaded regions" collapse to the $(F_R)_{1-D}$ curves. A final trend to be noted is that the maximum widths of "shaded regions" bordering each of the M-curves occur only when two conditions are met. The first condition is the previously noted maximum allowable a-value. The second is the condition $F_d = F'$. When the a-value is the allowable maximum and $F_d = F'$, differences between $(F_R)_E$ and $(F_R)_A$ are at a maximum for given values of B, F', and M.

In conjunction with the general trends noted for the exact method over the range of M and a-values, Figs. 10 through 15 yield the following information:

1. As $B \to 0$, all three methods yield the same F_R values, i.e., $F_R \to F'$.
2. As $F' \to 1$, $(F_R)_E \to (F_R)_A$ for any value of M.

---

* The non-uniqueness of the M-curves for $M > 10$ accounts for the infinite a-range given in Table 3.1.

Table 3.1

The Range of a-values for Various M-values

M	a-range
0.0	0.0
0.1	$\leq$ 1.26
0.5	$\leq$ 2.83
10.0	$\leq$ 12.7
> 10.0	$\leq \infty$

3. As F' decreases, the differences between $(F_R)_A$ and $(F_R)_{1-D}$ values become smaller while the $(F_R)_E$ shaded regions become broader. The averaging method therefore unconditionally predicts decreasing axial conduction effects for smaller F' values. The exact results indicate that under the condition $F_d \simeq F'$, axial conduction effects will remain significant. For F' = 0.5, per cent differences between $(F_R)_E^{\infty}$ and $(F_R)_{1-D}$ values are as large as 26 per cent (at B = 2). The corresponding difference between $(F_R)_A^{\infty}$ and $(F_R)_{1-D}$ values at B = 2 is 3 per cent.

For values of F' < 0.5, the maximum per cent differences between $(F_R)_E^{\infty}$ and $(F_R)_A^{\infty}$ increase slightly and then fall off to zero as $F' \to 0$. However, cases where F' < 0.5 are of small significance for flat-plate collector application because of the low values of F_R.

When a < 30, the number of parameters required to evaluate $(F_R)_E$ for Type I geometry increases from three to five. Also, the heat removal factor must be evaluated by solving a truncated set of simultaneous linear equations. For Type I geometry, the coefficient matrix $\underline{\underline{A}}$ is a function of a, c, f, d_r', and u_r. The added complexity of the solution does not, however, prevent "shaded regions" from being obtained. "Shaded regions" for M-curves less than 10 are not shown because the "regions" overlap significantly for the lower range of F' values. Also, more specific information can be obtained by an alternate presentation. Since all conventional designs have a-values much

less than 30, more detailed parameter information is desirable for cases where a < 30.

The general trends discussed earlier in Chapter III indicate that maximum differences between $(F_R)_A$ and $(F_R)_E$ value are obtained for given B, F', and M values when the a-value is the maximum allowable and $F_d = F'$. A further trend to be noted is that the $F_d = F'$ case alone yields maximum differences between $(F_R)_A$ and $(F_R)_E$ values for each set of the remaining variables. From Eq. 3.63, the $F_d = F'$ case is met when $F_{ud} = 0$. The variable F_{ud} is equal to zero when either or both of the variables d_r' and $u_r \to \infty$. However, if $d_r' \to \infty$, then $F_d \to 1$ and $F' \to 1$. A full range of F' values is possible for the $F_{ud} = 0$ case only when $u_r \to \infty$. By restricting the u_r-variable to large values, a set of curves can be generated which give the maximum differences between $(F_R)_A$ and $(F_R)_E$ for a practical range of the remaining variables a, c, f, and d_r'. The four variables can be conveniently represented by the set* of B, M, F', and c.

Figures 16 and 17 show the per cent differences between $(F_R)_A$ and $(F_R)_E$ values vs B for families of F' and c-curves. The value of M is held constant for each figure at the values 0.1 and 0.5, respectively. A practical maximum u_r value of 3000 was used for both figures. The lower limits on c for each F' value in Figs. 16 and 17

---

* Note from Eq. 3.51 that $B = f \cdot F_{ud}$. When $F_{ud} \to 0$ by means of $u_r \to \infty$, the variable B remains finite because the variable f contains a cancelling R variable. The R variable is the physical variable responsible for large u_r values.

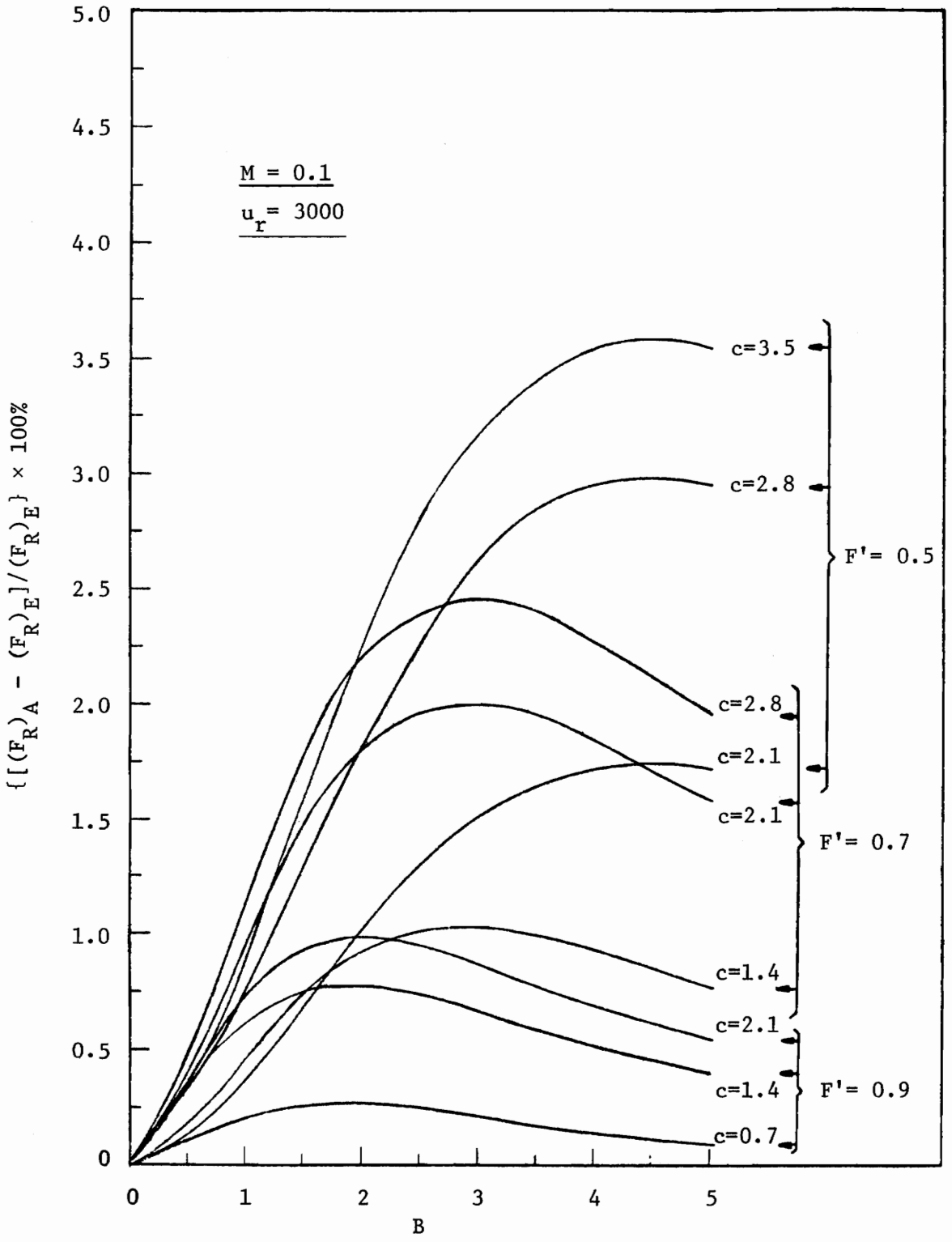

Figure 16. Per Cent Differences Between $(F_R)_A$ and $(F_R)_E$ -- M = 0.1

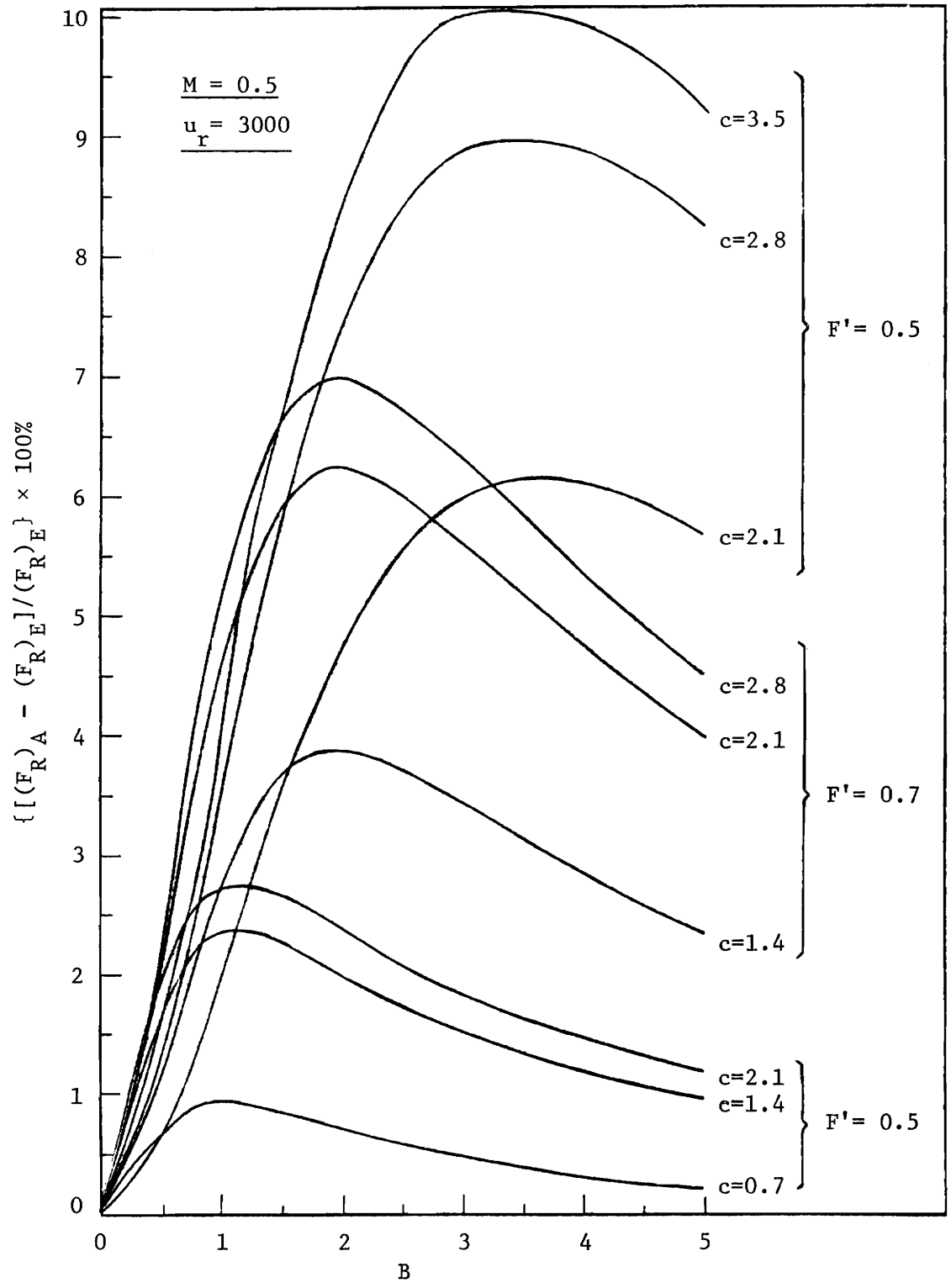

Figure 17. Per Cent Differences Between $(F_R)_A$ and $(F_R)_E$ -- M = 0.5

were chosen on the following basis. Since $F_{ud} \approx 0$ when $u_r = 3000$, F' is given by $F' \approx F_d$, i.e.,

$$F' \approx \frac{F + d_r'}{1 + d_r'} \tag{3.75}$$

Solving for d_r' in Eq. 3.75 gives

$$d_r' \approx \frac{F' - F}{1 - F'} \tag{3.76}$$

Since $d_r' > 0$, $F < F'$. Using the equality $F = (\tanh c)/c$, the inequality $F < F'$ sets a lower limit on the possible range of c-values. Table 3.2 shows values of F corresponding to various c-values. The lowest c-values for each F'-value were chosen sufficiently above the minimums indicated by Eq. 3.76 to avoid small d_r' values. Since d_r' is related to F_{ud} by the equation

$$F_{ud} = (1 + d_r')/u_r d_r' \tag{3.77}$$

small d_r' values would make $F_{ud} \not\approx 0$ and violate the $F_d \approx F'$ criterion. The upper limits on the c-values for each F'-value were chosen to prevent d_r' from exceeding reasonable values.

The curves in Figs. 16 and 17 are not limited to the $u_r = 3000$ case. The curves are approximately valid for any u_r-value where the term $F_{ud} \ll 1/F_d$, i.e., where $F' \approx F_d$. From Eq. 3.77, the minimum u_r-values for which $F_{ud} \ll 1/F_d$ are determined by the size of d_r'. In turn, the variable d_r' is related to the c-curves by Eq. 3.76 (when $F_{ud} \approx 0$). The larger valued c-curves of each c-family have larger d_r' values. Therefore the larger valued c-curves in each

Table 3.2

Values of F vs c

F	c
1.0	0.00
0.9	0.58
0.8	0.89
0.7	1.18
0.6	1.51
0.5	1.91

c-family of Figs. 16 and 17 are valid for a larger range of u_r values. Table 3.3 gives the range of c-curves in Figs. 16 and 17 which are valid for $u_r \geq 300$. The table was generated from an alternate form of Eq. 3.76, i.e.,

$$F \simeq F' - d_r'(1 - F') \tag{3.78}$$

where $d_r' \geq 0.2$. When $d_r' \geq 0.2$ and $u_r \geq 300$, $F_{ud} \leq 0.02$. The smaller c-curves in each c-family in Figs. 16 and 17 are valid for $u_r \geq 600$ under the $F_{ud} \leq 0.02$ criterion.

The approximate validity of Figs. 16 and 17 for cases where $F_{ud} \simeq 0$ indicates that beyond a certain value of u_r the value of $(F_R)_E$ changes only slightly for given values of B, M, F', and c. The c-curves in Figs. 16 and 17 show another asymptotic trend. For constant values of M, F', and u_r, the relative maximums of the c-curves do not increase monotonically with increasing c-values but rather increase more slowly between successive c-increases. For a given value of M, larger c-values imply larger a-values. Therefore the c-curve trend indicates that beyond a certain a-value the value of $(F_R)_E$ remains approximately constant for given values B, M, and F', u_r. This result is consistent with the trend noted earlier in this section that when $a \geq 30$, $(F_R)_E \simeq (F_R)_E^{\infty}$. When both u_r and a-values are beyond a specific value, the value of $(F_R)_E$ reaches the minimum value for given values of B, M, and F'.

Figures 16 and 17 show the maximum practical F_R errors incurred by the averaging method for M = 0.1 and M = 0.5. In conventional

Table 3.3

Ranges of c-curves in Figs. 16 and 17

Valid for $u_r \geq 300$

($F_{ud} \leq 0.02$)

F'	c-range
0.5	> 2.46
0.7	> 1.66
0.9	> 1.12

designs, the value of M is seldom above 0.5. Therefore, Figs. 16 and 17 give conservative estimates of the F_R error range involved in using the averaging method for the analysis of conventional flat-plate collector designs. The two figures can alternately be used in conjunction with Figs. 10 through 15 to visualize "shaded regions" for the M = 0.1 and M = 0.5 curves. From such a visualization, conservative estimates of the F_R error range involved in using the 1-D fin method can be made.

The per cent errors in ψ_{pm} and ψ_{fm} values between the averaging and the exact method are given exactly by F_R per cent differences. The application to ψ_{pm} errors is seen through the general equivalence of ψ_{pm} and F_R. Application to ψ_{fm} values results from the cancellation of the F' factor in the ψ_{fm} per cent difference equation. Per cent error values for ψ_{pm} and ψ_{fm} do not, however, translate directly into per cent error values for T_{pm} and T_{fm}. The per cent difference for actual temperatures is given by

$$\frac{(T_{pm})_A - (T_{pm})_E}{(T_{pm})_E} \cdot 100\% = \frac{(T_{pm})_E - T_a - S/U_L}{(T_{pm})_E} \cdot (\psi_{pm} \text{ \% error}) \tag{3.79}$$

for T_{pm} with a similar equation for T_{fm}. For typical operating conditions, i.e., S = 700 W/m^2, U_L = 5 $W/m^2°C$, T_a = 10°C, and $(T_{pm})_E$ = 60°C, Eq. 3.79 becomes

$$T_{pm} \text{ \% error} = \frac{-90}{60 + 273} \cdot (\psi_{pm} \text{ \% error})$$

i.e.,

$$T_{pm}\ \%\ \text{error} = -\ 0.27 \cdot (\psi_{pm}\ \%\ \text{error}) \tag{3.80}$$

Therefore T_{pm} and T_{fm} per cent differences may be significantly smaller than F_R per cent differences. Note also that since the ψ_{pm} (i.e., F_R) per cent differences are always positive, Eq. 3.80 yields $(T_{pm})_A$ values which are smaller than $(T_{pm})_E$. The same is true for $(T_{fm})_A$ and $(T_{fm})_E$.

The error ranges for F_R values in Figs. 16 and 17 were calculated assuming the same values of U_L and c_p for both the exact and averaging methods. As noted in Chapter I, the overall analysis for a specific collector requires an iterative evaluation of U_L and c_p through the dependence on T_{pm} and T_{fm}. The translation of ψ_{pm} and ψ_{fm} per cent differences into T_{pm} and T_{fm} differences also involves iterated values for U_L and $(\tau\alpha)_e$. Both U_L and $(\tau\alpha)_e$ are dependent on T_{pm}. Since different values of T_{pm} and T_{fm} are obtained for each method used, the error ranges for the final iterated values of F_R will be different from the values shown in Figs. 10 through 17. The iterative effect is of a secondary nature, however, since the error ranges of the initial T_{pm} and T_{fm} values are not as large as the initial F_R differences. The net effect is that the iterative F_R differences between the exact and the averaging methods will be slightly greater than the values shown in Figs. 10 through 17. The iterative effect on differences between $(F_R)_A$ and $(F_R)_{1\text{-}D}$ will be more significant, in general, since the magnitude of the initial T_{pm} and T_{fm} differences are usually larger than those between the averaging and the exact methods.

In summary, Figs. 16 and 17 provide useful information about the applicability of the averaging method for conventional design parameter ranges. Figs. 10 through 15 show a broader range of parameter effects and provide a convenient means of evaluating and comparing F_R, ψ_{pm}, and ψ_{fm} values. When used together, Figs. 10 through 17 allow solar-collector designers to evaluate the possible errors resulting from the use of approximate thermal analyses.

The Range of Analysis Errors for Conventional Flat-Plate Collectors

The majority of flat-plate solar collectors are within the parameter ranges $M \leq 0.1$, $c \leq 1.4$, $u_r < 3000$, and $F' \geq 0.7$. Figure 17 indicates that for such collectors the averaging method yields non-iterated F_R values accurate to within 1 per cent. From Figs. 12 through 15, the corresponding $(F_R)_{1-D}$ values are accurate to within 10 per cent. The maximum $(F_R)_{1-D}$ error occurs when $B \simeq 2.5$, $M = 0.1$, and $F' = 1$. Note that the maximum $(F_R)_{1-D}$ error occurs when the $(F_R)_A$ error is zero. The preceding error ranges cover both thermosyphon operation (1.67×10^{-4} kg/sec $\leq \dot{m} \leq 2.08 \times 10^{-3}$ kg/sec) and the National Bureau of Standards recommended forced convective flow rate ($\dot{m} = 5 \times 10^{-3}$ kg/sec) [9]. By considering forced flow operation alone, the B-range is restricted to $B < 0.5$ For $B < 0.5$ the $(F_R)_A$ values are correct to within 0.50 per cent and the $(F_R)_{1-D}$ values are correct to within 5 per cent.

Analysis of the Fundamental Differences Between Models

The differences between F_R, ψ_{pm}, and ψ_{fm} values for each of the three methods lie fundamentally in the different formulations of the absorber-plate and fluid energy equations. However, the solution formulations given in Chapters II and III are difficult to compare directly because of the numerous differences in governing equations and boundary conditions.

It is therefore convenient to formulate the 1-D fin and exact methods in terms of $\bar{\theta}_p(\beta)$ -- the average transverse plate temperature used in the averaging method. Note that $\bar{\theta}_p(\beta)$ is defined as

$$\bar{\theta}_p(\beta) = \frac{W-D}{W} \int_0^1 \theta_p(\eta,\beta)\, d\eta + \frac{D}{W}\, \theta_b(\beta) \tag{3.81}$$

where $\theta_b(\beta)$ is given by $\theta_p(1,\beta)$ for the exact method. Evaluation of the 1-D fin equations in terms of $\bar{\theta}_p(\beta)$ is straightforward. For the exact method, the $\theta_p(\eta,\beta)$ variables in Eqs. 3.5, 3.6, and 3.10 are replaced by the separable form $\theta_p(\eta,\beta) = N(\eta)\, B(\beta)$. Equation 3.5 is integrated over η and weighted by (W-D)/W. Equation 3.10 is weighted by D/W. Addition of the resulting forms of Eqs. 3.5 and 3.10 yield an absorber-plate governing equation in terms of $\bar{\theta}_p(\beta)$. The comparative equations for the three methods are as follows:

1-D Fin Method --

$$\text{Plate:}\quad -WU_L\, \bar{\theta}_p(\beta) - WU_G[\bar{\theta}_p(\beta) - \theta_f(\beta)] = 0 \tag{3.82}$$

$$\text{Fluid:}\quad \frac{\dot{m}c_p}{L}\frac{d\Theta_f(\beta)}{d\beta} - WU_G[\bar{\Theta}_p(\beta) - \Theta_f(\beta)] = 0 \tag{3.83}$$

Averaging Method --

$$\text{Plate:}\quad Wk_p\delta_p\frac{d^2\bar{\Theta}_p(\beta)}{d\beta^2} - WU_L\bar{\Theta}_p(\beta) - WU_G[\bar{\Theta}_p(\beta) - \Theta_f(\beta)] = 0 \tag{3.84}$$

$$\text{Fluid:}\quad \frac{\dot{m}c_p}{L}\frac{d\Theta_f(\beta)}{d\beta} - WU_G[\bar{\Theta}_p(\beta) - \Theta_f(\beta)] = 0 \tag{3.85}$$

Exact Method --

$$\text{Plate:}\quad Wk_p\delta_p\frac{d^2\bar{\Theta}_p(\beta)}{d\beta^2} - WU_L\bar{\Theta}_p(\beta) - \frac{1}{R}[\Theta_b(\beta) - \Theta_f(\beta)] = 0 \tag{3.86}$$

$$\text{Fluid:}\quad \frac{\dot{m}c_p}{L}\frac{d\Theta_f(\beta)}{d\beta} - \frac{1}{R}[\Theta_b(\beta) - \Theta_f(\beta)] = 0 \tag{3.87}$$

Equations 3.86 and 3.87 are for Type I-II geometries while Eqs. 3.82 through 3.85 are applicable for all geometries for which U_G factors can be found. Only Type I-II geometry will be considered here.

Once the plate and fluid equations are cast in the same form, the specific differences between models become apparent. Comparison of Eqs. 3.82 and 3.83 with Eqs. 3.84 and 3.85 shows only one difference, i.e., the addition of an averaged axial conduction term in Eq. 3.84. Comparison of the averaging and exact-method equations yields two conclusions. First, Eqs. 3.84 and 3.86 both contain the same axial

conduction term. Therefore, the average axial-conduction term used in the averaging method is seen to introduce no approximation into the absorber-plate governing equation. Secondly, the only difference between the governing equations for the averaging and exact methods is in the expressions for the useful heat gain $q_u(\beta)$. For the averaging method, $q_u(\beta)$ is given by

$$q_u(\beta) = U_G W [\bar{\Theta}_p(\beta) - \Theta_f(\beta)] \tag{3.88}$$

The exact-method expression for $q_u(\beta)$ is

$$q_u(y) = \frac{1}{R} [\Theta_b(\beta) - \Theta_f(\beta)] \tag{3.89}$$

From Eqs. 3.88 and 3.89, it is seen that the averaging method assumes an additional relation between $\bar{\Theta}_p(\beta)$ and $\Theta_b(\beta)$. The assumed relation is given by

$$\Theta_b(\beta) = RWU_G \bar{\Theta}_p(\beta) + [1 - RWU_G] \Theta_f(\beta) \tag{3.91}$$

For cases where Eq. 3.91 does not hold, the local useful heat gain will be incorrectly calculated.

With regard to boundary conditions, the $\bar{\Theta}_p(\beta)$ formulation absorbs the η-direction boundary conditions. The fluid inlet condition $\Theta_f(0) = \Theta_{fi}$ is required for all three methods. For the 1-D fin method, no other boundary restraints can be imposed. The β-direction boundary conditions for the averaging method are

$$\left.\frac{d\bar{\theta}_p(\beta)}{d\beta}\right|_{\beta=0} = \left.\frac{d\bar{\theta}_p(\beta)}{d\beta}\right|_{\beta=1} = 0 \tag{3.92}$$

For the exact method, the β-direction boundary conditions are specified locally, i.e.,

$$\left.\frac{d\theta_p(\eta,\beta)}{d\beta}\right|_{\beta=0} = \left.\frac{d\theta_p(\eta,\beta)}{d\beta}\right|_{\beta=1} = 0 \tag{3.93}$$

A consequence of the constant U_G concept can be seen from Eq. 3.91. Differentiation of Eq. 3.91 with respect to β yields

$$\frac{d\theta_b(\beta)}{d\beta} = RWU_G \frac{d\bar{\theta}_p(\beta)}{d\beta} + [1 - RWU_G] \frac{d\theta_f(\beta)}{d\beta} \tag{3.94}$$

When Eq. 3.92 is substituted into Eq. 3.94, the result is

$$\left.\frac{d\theta_b(\beta)}{d\beta}\right|_{\substack{\beta=0\\ \beta=1}} = [1 - RWU_G] \left.\frac{d\theta_f(\beta)}{d\beta}\right|_{\substack{\beta=0\\ \beta=1}} \tag{3.95}$$

Thus, the U_G formulation does not, in general, restrain the axial base heat flow to zero at the boundaries.

It was noted in Chapter II that the averaging method is a good approximation when the plate conductance is large. For large values of plate conductance, the fin efficiency $F \to 1$. From the definition of U_G (Eq. 2.42), when $F \to 1$, the term WU_G reduces to $1/R$. From Eq. 3.91, $\theta_b(\beta) \to \bar{\theta}_p(\beta)$. Therefore Eqs. 3.88 and 3.89 become identical

and Eq. 3.95 reduces to an insulated boundary condition. This case was noted earlier in Chapter III as one situation where $F_d \to 1$ and $(F_R)_A \to (F_R)_E$. The variable F_d also approaches 1 when $D \to W$. When $D \to W$, the term WU_G again approaches the value $1/R$ and $\bar{\theta}_p(\beta) \to \theta_b(\beta)$.

Maximum differences between models occur when $a \to \infty$ and $F_{ud} \to 0$. When $a \to \infty$, the error due to non-restrained β-direction boundary conditions becomes large. When $F_{ud} \to 0$, the resistance R is small. When $R \to 0$, Eq. 3.95 reduces to

$$\left.\frac{d\theta_b}{d\beta}\right|_{\substack{\beta=0\\ \beta=1}} = \left.\frac{d\theta_f}{d\beta}\right|_{\substack{\beta=0\\ \beta=1}} \tag{3.96}$$

For small values of R, the derivative of the fluid temperature at the inlet is large. The insulated $\beta = 0$ boundary condition is therefore violated the most under the $F_{ud} \to 0$ condition. Minimum differences between models occur when $M \to 0$. In this situation, the insulated boundary conditions are satisfied by definition and the U_G concept becomes valid.

Absorber-Plate and Fluid Temperature Profile Comparisons Between Models

An analysis of absorber-plate and fluid temperature distributions provides insight into the local differences between models. The absorber-plate temperature distributions for the 1-D fin, averaging*,

* Note that temperature profiles in the η-direction cannot be evaluated in the averaging method.

and exact methods are given in terms of $\psi_p(\eta,\beta)$ by

$$\psi_p(\eta,\beta) = \frac{F'}{F_d}\frac{\cosh c\eta}{\cosh c} e^{-BF'\beta} \tag{3.97}$$

$$\bar{\psi}_p(\beta) = \frac{a_1 e^{r_1\beta} + a_2 e^{r_2\beta} + a_3 e^{r_3\beta}}{D(b_1 + b_2 + b_3)} \tag{3.98}$$

and

$$\psi_p(\eta,\beta) = \sum_{n=0}^{M_T} C_n \cosh \gamma_n\eta \cos \lambda_n{}^*\beta \tag{3.99}$$

respectively. Equations 3.97 and 3.99 can be integrated over η and dimensionally weighted (as in Eq. 3.81) to yield $\bar{\psi}_p(\beta)$ equations comparable to Eq. 3.98. The resulting equations are, respectively,

$$\bar{\psi}_p(\beta) = F'e^{-BF'\beta} \tag{3.100}$$

and

$$\bar{\psi}_p(\beta) = \sum_{n=0}^{M_T} C_n (F_d)_n \cosh \gamma_n \cos \lambda_n{}^*\beta \tag{3.101}$$

where

$$(F_d)_n = \frac{F_n + d_r'}{1 + d_r'} \quad \text{and} \quad F_n = \frac{\tanh \gamma_n}{\gamma_n}$$

The fluid temperature distributions for the 1-D fin, averaging, and exact methods are given in terms of $\psi_f(\beta)$ by

$$\psi_f(\beta) = e^{-BF'\beta} \tag{3.102}$$

$$\psi_f(\beta) = \frac{b_1 e^{r_1\beta} + b_2 e^{r_2\beta} + b_3 e^{r_3\beta}}{b_1 + b_2 + b_3} \tag{3.103}$$

and

$$\psi_f(\beta) = e^{-f\beta} + \sum_{n=0}^{M_T} \frac{C_n \cosh \gamma_n}{1 + (\lambda_n^*/f)^2} \left(\cos \lambda_n^*\beta + \frac{\lambda_n^*}{f} \sin \lambda_n^*\beta - e^{-f\beta}\right) \tag{3.104}$$

Figures 18 and 19 show various temperature profiles for each of the three methods for the parameter set M = 0.5, F' = 0.5, B = 3.5, c = 3.5, and u_r = 3000. The parameter set corresponds to the maximum point on the F' = 0.5, c = 3.5 curve in Fig. 17. As noted earlier in Chapter III, the curves are approximately valid for any u_r- value where $F_{ud} \simeq 0$. To convert "ψ" values to "T" values, typical operating conditions of T_{fi} = 50 C, T_a = 10 C, and S/U_L = 140 C were chosen. Figure 18 shows the absorber-plate temperature profiles in the transverse direction from the plate centerline (η = 0) to the tube base (η = 1) for inlet (β = 0) and outlet (β = 1) locations. The "*" locations in Fig. 18 represent $\bar{T}_p(\beta)$ values for the specific curves of each method. Note that the $\bar{T}_p(\beta)$ values for the averaging and exact models show reasonable agreement. In Fig. 19, both the average axial plate temperature, $\bar{T}_p(\beta)$, and the fluid temperature profiles, $T_f(\beta)$, are shown. Also, the $T_b(\beta)$ curve for the exact method is shown. The $T_b(\beta)$ curves for the averaging and exact methods are indistinguishable from the respective $T_f(\beta)$ curves. Note that the exact $T_b(\beta)$ curve has

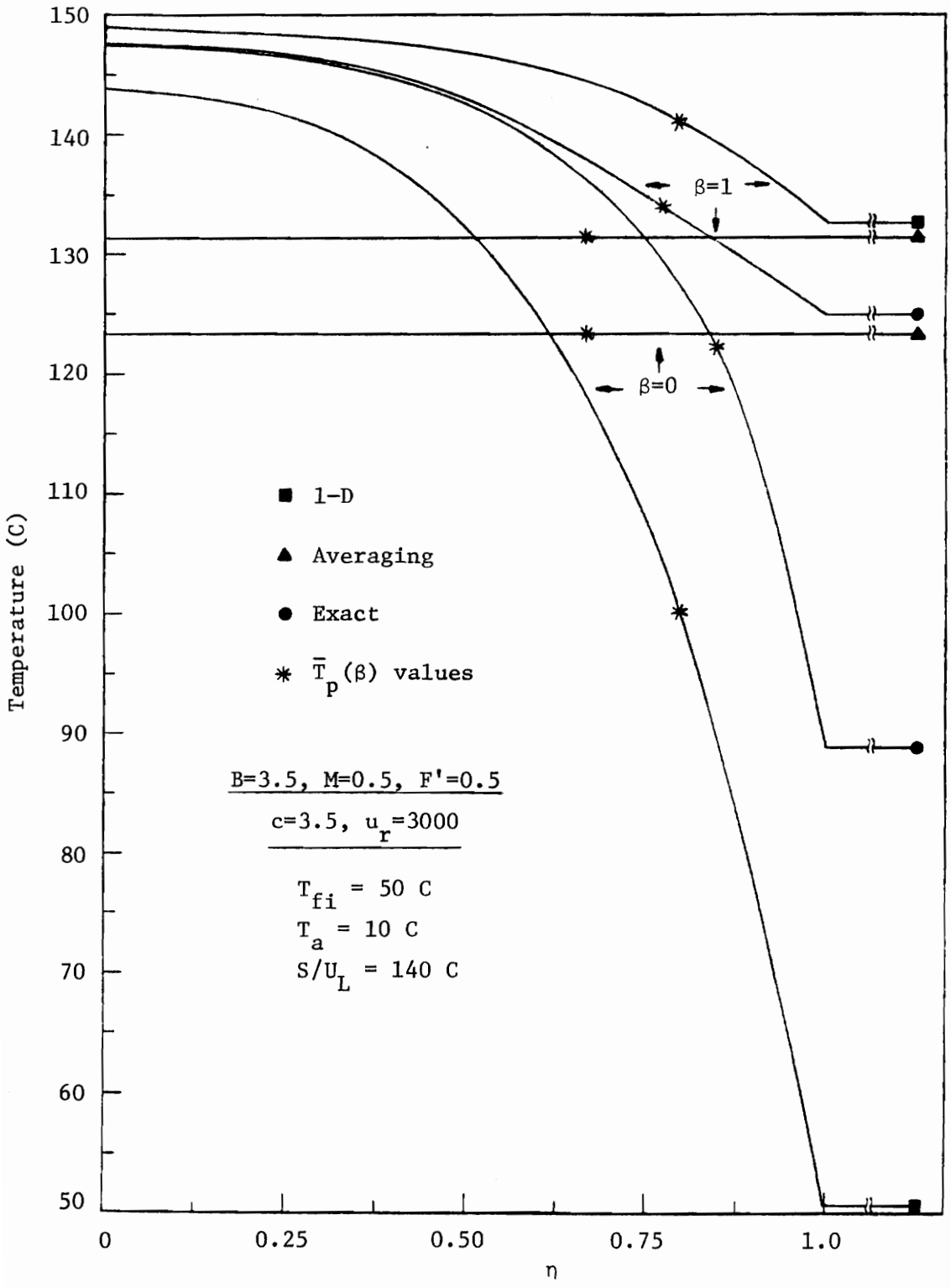

Figure 18. Transverse Plate Temperature Profiles -- $T_p(\eta,0)$ and $T_p(\eta,1)$

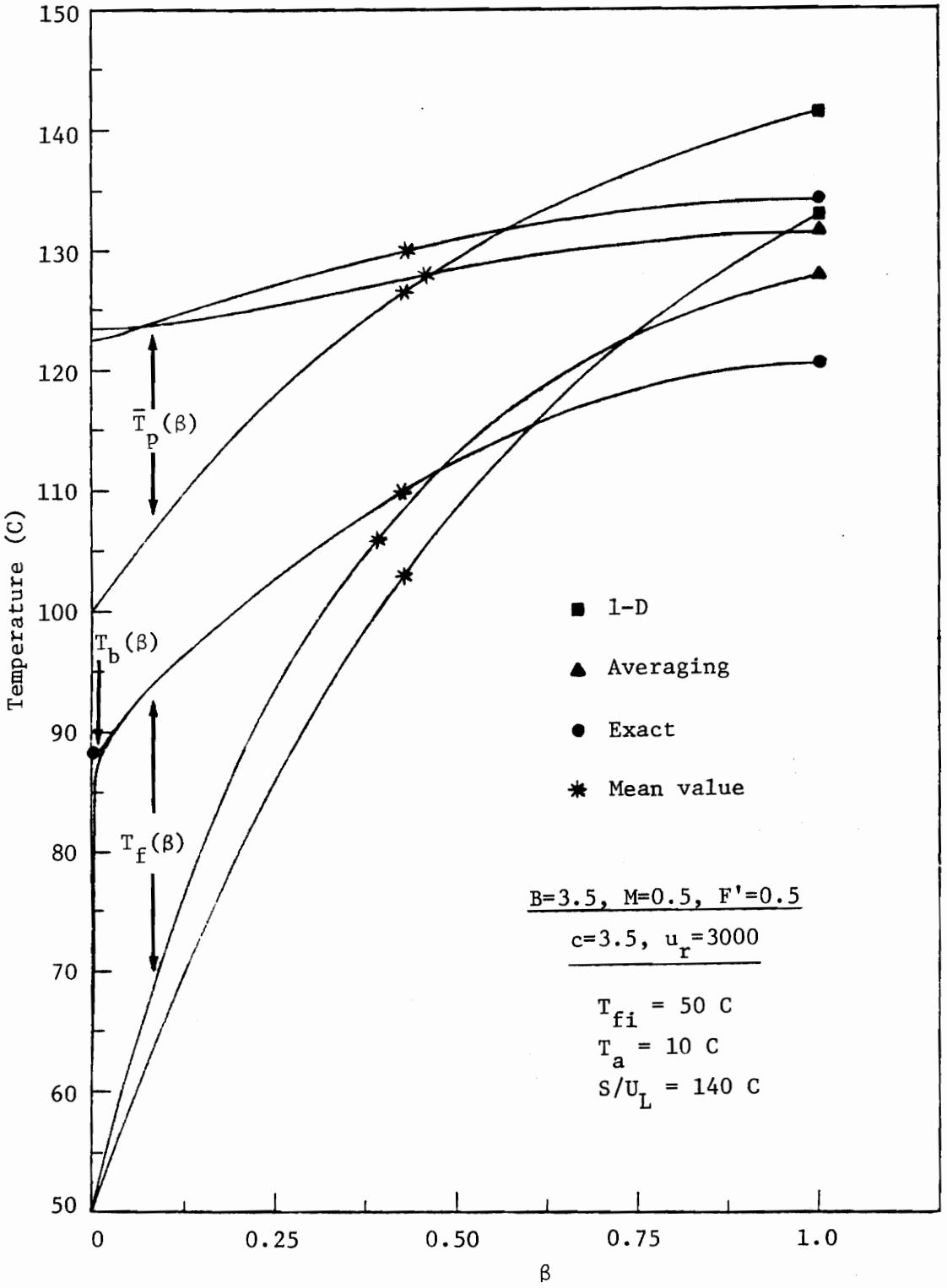

Figure 19. Axial Temperature Profiles -- $\bar{T}_p(\beta)$ and $T_f(\beta)$

the correct zero slope at $\beta = 0$ and $\beta = 1$ while the $T_b(\beta)$ curves for the 1-D fin and averaging methods do not. The "*" locations on each of the $\bar{T}_p(\beta)$ and $T_f(\beta)$ curves in Fig. 19 indicate the values of T_{pm} and T_{fm} for each of the three methods. The exact T_{pm} and T_{fm} values are underestimated by both of the existing methods with the averaging method giving the closest estimates. Note that $(T_{fm})_E > (T_{fm})_A$ even though $(T_{fo})_E < (T_{fo})_A$. The general relations*

$$\psi_{pm} = F_R \tag{3.65}$$

$$\psi_{fm} = \frac{F_R}{F'} \tag{3.66}$$

and

$$\psi_{pm} = F' \psi_{fm} \tag{3.67}$$

in conjunction with Fig. 19, provide insight into the physical reason why axial conduction reduces the F_R value. Axial conduction in the absorber plate results in additional heat gain by the fluid in the

---

* General equations for ψ_{bm}, Q_u, and η_c can also be written, as follows:

$$\psi_{pm} = F_d \psi_{bm}$$

$$Q_u = -A_p U_L F_R \Theta_{fi}$$

and

$$\eta_c = -\frac{U_L F_R \Theta_{fi}}{HR}$$

Eqs. 3.65, 3.66, and 3.67 can be used to obtain equations for Q_u and η_c in terms of Θ_{fm} or Θ_{pm}, also.

inlet region. The redistribution of heat flow causes the mean fluid temperature to increase above the 1-D fin value. From Eq. 3.67, when T_{fm} is increased, ψ_{fm} and ψ_{pm} are both decreased. Smaller ψ_{pm} values translate into larger T_{pm} values. The larger the value of T_{pm}, the more heat is lost to the ambient. Therefore, by conservation of energy, less useful energy gain is possible. Equation 3.65 shows that for larger T_{pm} values (i.e., smaller values of ψ_{pm}) the F_R value is reduced. A similar effect occurs between the averaging and exact methods because the averaging method underestimates the local values of $q_u(\beta)$ in the inlet region. The large differences in exact and averaging $T_f(\beta)$ values in the inlet region are the result of the $q_u(\beta)$ differences.

Summary

The analysis presented in Chapter III has both general and specific applications. By an extension of the separation of variables technique, an analytical solution is obtained for a coupled boundary condition problem. The solution technique presented is applicable to many types of conduction-convection problems. The specific application to parallel-flow flat-plate solar collectors allows an exact analytical treatment of the absorber-plate governing equation. The plate-fluid coupling is treated exactly except for the neglecting of axial conduction in the tubes for Type I and III geometries. The resulting solution yields more conservative estimates of flat-plate collector performance than existing models.

The exact analysis provides a means for parametrically evaluating the validity of the existing models. The exact analysis indicates that for the majority of conventional parallel-flow flat-plate collectors the averaging model yields good results. The comparable $(F_R)_{1-D}$ values have a possible error range of 10 per cent. The exact method becomes significantly more accurate than either of the existing methods when $M > 0.1$ and $F' \leq 0.7$. Figures 10 through 17 provide a convenient means for comparison between models and for evaluating conventional and new design situations.

IV. THEORETICAL ANALYSIS FOR A LOCALIZED EDGE LOSS

Introduction

The overall collector loss coefficient U_L has conventionally been treated as independent of position [1]. Consequently, the edge loss effect has been artificially distributed over the total absorber plate area. Also conventionally, the edge and bottom losses have been expressed in terms of one-dimensional heat flow equations. For further details, see Appendix I.

The purpose of the following analysis is two-fold. First, the new model provides a means for determining the applicability of conventional edge-loss assumptions. Secondly, the model has the inherent capability to better evaluate performance and design questions related to edge effects.

In departing from the standard analysis, the present analysis will consider two sectionally uniform loss coefficients -- U_{LI} for internal collector sections and U_{LE} for edge sections. For parallel-flow collectors, the use of sectional loss coefficients eliminates the conventional symmetry midway between the flow tubes. Instead, the temperature distribution in each tube-plate section is influenced by the neighboring sections. Consequently, a set of first-order coupled linear differential equations must be solved instead of one such equation which is the usual case for parallel flow collectors. For serpentine collectors, the equations for neighboring sections are coupled even when a single loss coefficient U_L is used [10]. Thus the

implementation of two loss coefficients for the serpentine case does not introduce additional complexities. In fact, much of the notation from the serpentine analysis given in reference 10 is used in the following development since the case of parallel flow with sectional loss coefficients is similar in form to the serpentine case. The following analysis is specifically for the parallel-flow case. The differences between the parallel and serpentine equations are noted.

The basic steps of the 1-D fin parallel-flow treatment are followed. First, expressions for the temperature distribution in each absorber plate must be found. From these, the useful energy gain for each tube can be found. Then, a first order differential equation is obtained for each flow channel from an energy balance on the fluid. The 1-D fin assumption of negligible axial conduction within the absorber plates is retained to allow localized edge effects to be considered independently of Chapter III results.

Absorber Plate Temperature Distributions

Figure 20 shows the model used for the localized edge loss analysis where U_{LI} and U_{LE} are defined as

$$U_{LI} = U_{TI} + U_{BI} + U_{EI} \tag{4.1}$$

for plate-cover regions $j = 1,2,\ldots,N_T-1$, and

$$U_{LE} = U_{TE} + U_{BE} + U_{EE} \tag{4.2}$$

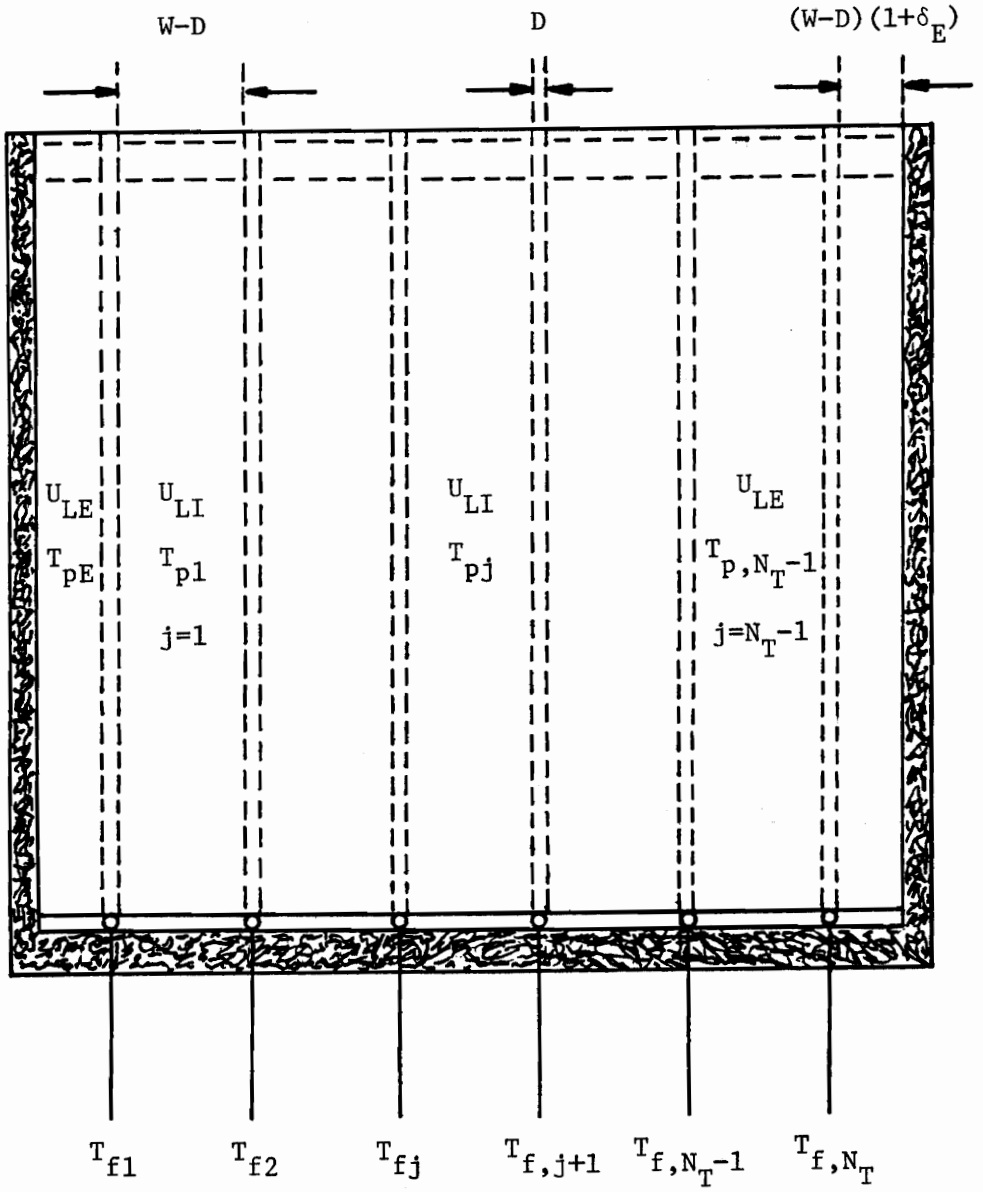

Figure 20. Localized Edge Loss Model

for plate-cover regions j = 0 and j = N_T. The evaluation of U_{LI} and U_{LE} is discussed in Appendix I.

For the internal absorber plates (j = 1,2,...,N_T-1), an energy balance yields the following governing equation.

$$k_p \delta_p \frac{d^2 T_{pj}}{dx^2} - U_{LI}(T_{pj} - T_a) + S = 0 \tag{4.3}$$

where the subscript p refers to the absorber plate. Letting

$\psi_{pj} = \dfrac{T_{pj} - T_a - S/U_{LI}}{T_{bj} - T_a - S/U_{LI}}$ and $m_I^2 = U_{LI}/k_p \delta_p$, Eq. 4.3 becomes

$$\frac{d^2 \psi_{pj}}{dx^2} - m_I^2 \psi_{pj} = 0 \tag{4.4}$$

For the edge absorber plates, the governing equation may be written as

$$\frac{d^2 \Theta_{pE}}{dx^2} - m_E^2 \Theta_{pE} = 0 \tag{4.5}$$

where $\Theta_{pE} = T_{pE} - T_a - S/U_{LE}$ and $m_E^2 = U_{LE}/k_p \delta_p$.

Next it is convenient to choose non-dimensional coordinate systems for both the edge and interior absorber plates.

For the interior plates (j = 1,2,...,N_T-1), let

$$\xi_j = \{x - [(j - 1) W + (W + D)/2]\}/(W - D) \tag{4.6}$$

The transformation makes the transverse coordinate 0 and 1 at the left and right base regions, respectively, of each interior absorber plate. In terms of ξ_j, Eq. 4.4 becomes

$$\frac{d^2\psi_{pj}}{d\xi_j^2} - n_I^2 \psi_{pj} = 0 \quad \text{where} \quad n_I^2 = \frac{U_{LI}(W - D)^2}{k_p \delta_p} \tag{4.7}$$

Equation 4.7 has the general solution

$$\psi_{pj}(\xi_j) = C_1 \sinh n_I \xi_j + C_2 \cosh n_I \xi_j \tag{4.8}$$

For the edge absorber plates, it will be assumed that both plates have the same dimensions and the same types of boundary conditions. Accordingly, only the left-side edge absorber plate needs to be considered. For this plate, choose

$$\xi_E = [x - (\frac{W - D}{2})(1 + \delta_E)]/[(\frac{W - D}{2})(1 + \delta_E)] \tag{4.9}$$

Conventionally, edge absorber plates are assumed to be half as wide as the interior plates. However, since many collector designs do not conform to this ideal situation, δ_E is included to account for the different designs. In terms of ξ_E, Eq. 4.5 becomes

$$\frac{d^2\Theta_{pE}}{d\xi_E} - n_E^2 \Theta_{pE} = 0 \quad \text{where} \quad n_E^2 = \frac{U_{LE}(\frac{W - D}{2})^2(1 + \delta_E)^2}{k_p \delta_p} \tag{4.10}$$

Equation 4.10 has the general solution

$$\Theta_{pE}(\xi_E) = C_1 \sinh n_E \xi_E + C_2 \cosh n_E \xi_E \tag{4.11}$$

To obtain particular solutions for Eqs. 4.8 and 4.11, the appropriate boundary conditions must be formulated and applied.

For internal absorber plates, there are two types of boundary conditions, as shown in Fig. 21, to be considered.

Type 1 - adjacent tube base regions are at different temperatures.

$$\psi_{pj}(0) = 1 \quad \text{and} \quad \psi_{pj}(1) = \frac{\Theta_{b,j+1}}{\Theta_{bj}}$$

$$\text{where} \quad \Theta_{bj} = T_{bj} - T_a - S/U_{LI}$$

Type 2 - adjacent tube base regions are at the same temperature.

$$\psi_{pj}(0) = 1 \quad \text{and} \quad \psi_{pj}(1) = 1 \qquad (j = N_T/2)$$

Type 1 is the usual case for interior absorber plates. Type 2 boundary conditions arise for the case of an N_T(even)-tube parallel-flow collector, for which x-direction symmetry will occur about the center of the $N_T/2$ absorber plate (mid-plate symmetry). For the case of an N_T(odd)-tube parallel-flow collector, the symmetry line splits the $(N_T + 1)/2$ tube (mid-tube symmetry) and Type 1 boundary conditions apply. For serpentine collectors, all interior absorber plates have Type 1 boundary conditions.

The following analysis will be written in a general fashion to allow calculations to be made for either the entire collector surface (full-plate) or half of the collector surface (mid-plate or mid-tube symmetry).

For Type 1 boundary conditions, the particular solution to Eq. 4.8 is

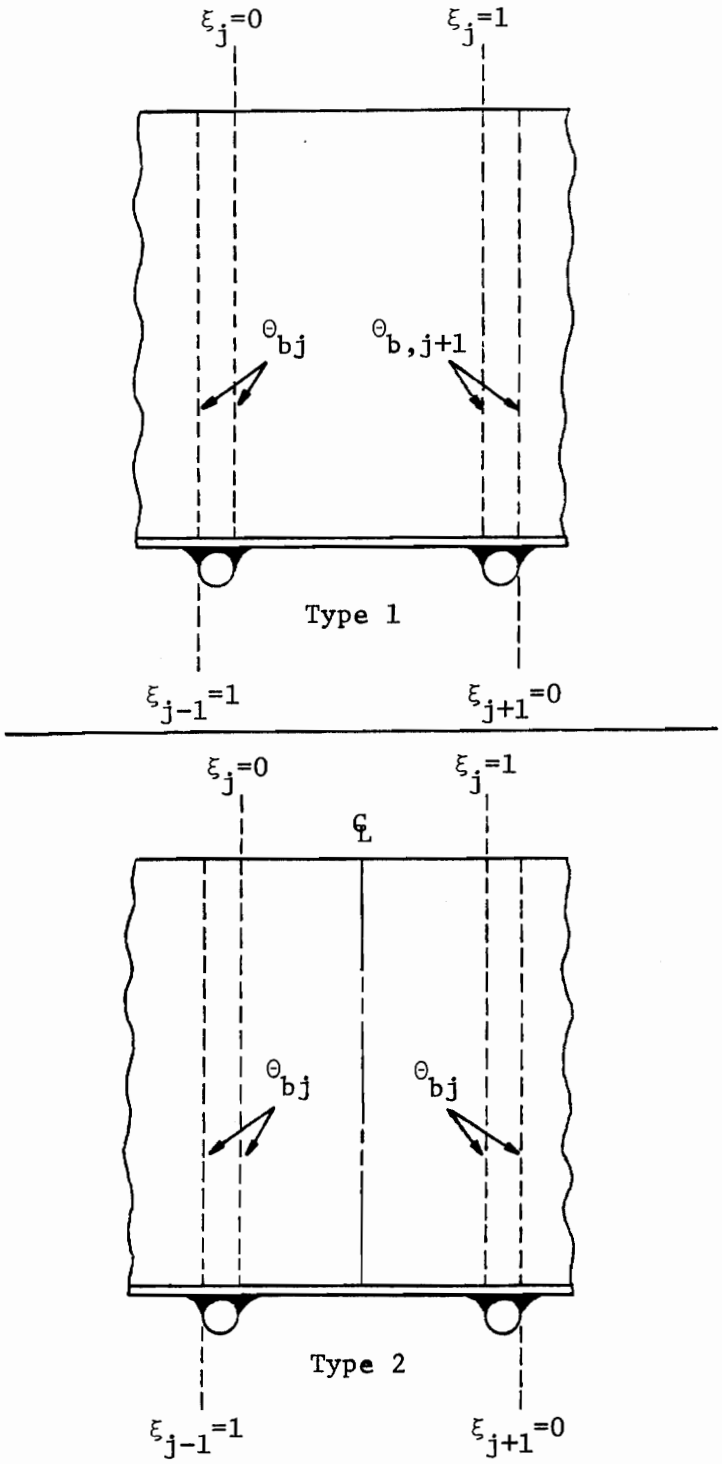

Figure 21. Type 1 and Type 2 Boundary Conditions -- Internal Absorber Plates

$$\psi_{pj}(\xi_j) = \frac{\frac{\Theta_{b,j+1}}{\Theta_{bj}} \sinh\ n_I\xi_j + \sinh\ n_I(1 - \xi_j)}{\sinh\ n_I} \qquad (4.12)$$

For Type 2 boundary conditions Eq. 4.11 becomes

$$\psi_{pj}(\xi_j) = \frac{\sinh\ n_I\xi_j + \sinh\ n_I\ (1 - \xi_j)}{\sinh\ n_I} \qquad (4.13)$$

For the edge absorber plates the boundary conditions are more involved. To include the possibility of conduction in the x-direction from the absorber plate to the edge structure of the collector, the conventional insulated boundary condition is replaced by a conduction heat loss condition, q_{EC}.

For the left-side edge absorber plate this condition is

$$q_{EC} = \frac{k_p\delta_p}{(\frac{W - D}{2})(1 + \delta_E)} \frac{dT_{PE}(0)}{d\xi_E} = k_{ins,E}S_e[T_{pE}(0) - T_a] \qquad (4.14)$$

where S_e is the edge structure shape factor. The evaluation of S_e is discussed in Appendix I. Letting

$$\alpha_E = \frac{k_{ins,E}S_e(\frac{W - D}{2})(1 + \delta_E)}{k_p\delta_p} \quad \text{and} \quad \Phi_{pE} = T_{pE} - T_a$$

Eq. 4.14 becomes

$$\frac{d\Phi_{pE}(0)}{d\xi_E} - \alpha_E\ \Phi_{pE}(0) = 0 \qquad (4.15)$$

The other boundary condition for the left-side edge absorber plate is

$$\Phi_{pE}(1) = \Phi_{b1} \quad \text{where} \quad \Phi_{b1} = T_{b1} - T_a \tag{4.16}$$

In terms of Φ_{pE}, Eq. 4.11 becomes

$$\Phi_{pE}(\xi_E) = \frac{S}{U_{LE}} + C_1 \sinh n_E\xi_E + C_2 \cosh n_E\xi_E \tag{4.17}$$

Applying Eqs. 4.15 and 4.16 to Eq. 4.17 gives

$$\Phi_{pE}(\xi_E) = \frac{S}{U_{LE}} + \Phi_{b1} f(\xi_E) - \frac{S}{U_{LE}} [f(\xi_E) + g(\xi_E)] \tag{4.18}$$

where

$$f(\xi_E) = \frac{\frac{\alpha_E}{n_E} \sinh n_E\xi_E + \cosh n_E\xi_E}{\frac{\alpha_E}{n_e} \sinh n_E + \cosh n_E} \tag{4.19}$$

and

$$g(\xi_E) = \frac{\frac{\alpha_E}{n_E} \sinh n_E(1 - \xi_E)}{\frac{\alpha_E}{n_E} \sinh n_E + \cosh n_E} \tag{4.20}$$

Rewriting Eq. 4.18 in terms of $\Theta_{b1} = \Phi_{b1} - S/U_{LI}$ and $\Theta_{pE} = \Phi_{pE} - S/U_{LE}$ gives

$$\Theta_{pE}(\xi_E) = f(\xi_E)(\Theta_{b1} + \frac{S}{U_{LI}} - \frac{S}{U_{LE}}) - g(\xi_E) \frac{S}{U_{LE}} \tag{4.21}$$

The equation for the right-side edge absorber plate is identical to Eq. 4.21 if the $\xi_E = 0$ location for the right-side plate is taken at the extreme edge of the plate and the $\xi_E = 1$ location is on the N_T'th tube base, i.e., the reverse coordinate system of that for the left-side plate.

Evaluation of the Useful Energy Gain

Let q_j^+ and q_j^- be the heat flow rates per differential length in the flow direction entering the left tube base of plate segment j in the positive and negative x-directions, respectively [10].

For interior plates

$$q_j^+ = \left. \frac{-k_p \delta_p \Theta_{b,j-1}}{W - D} \frac{d\psi_{p,j-1}}{d\xi_{j-1}} \right|_{\xi_{j-1} = 1}, \quad 2 \leq j \leq N_T \tag{4.22}$$

and

$$q_j^- = \left. \frac{k_p \delta_p \Theta_{pj}}{W - D} \frac{d\psi_{pj}}{d\xi_j} \right|_{\xi_j = 0}, \quad 1 \leq j \leq (N_T - 1) \tag{4.23}$$

From Eq. 4.12 for interior plates with Type 1 boundary conditions

$$\left. \frac{d\psi_{p,j-1}}{d\,\xi_{j-1}} \right|_{\xi_{j-1} = 1} = \frac{n_I \left[\frac{\Theta_{bj}}{\Theta_{b,j-1}} \cosh n_I - 1 \right]}{\sinh n_I} \tag{4.24}$$

and

$$\left.\frac{d\psi_{pj}}{d\xi_j}\right|_{\xi_j = 0} = \frac{n_I \left[\frac{\Theta_{b,j+1}}{\Theta_{bj}} - \cosh n_I\right]}{\sinh n_I} \qquad (4.25)$$

Using Eqs. 4.24 and 4.25 in Eqs. 4.22 and 4.23 gives

$$q_j^+ = K\,[\Theta_{b,j-1} - \Theta_{bj} \cosh n_I] \;,\; 2 \le j \le N_T \qquad (4.26)$$

and

$$q_j^- = K\,[\Theta_{b,j+1} - \Theta_{bj} \cosh n_I],\; 1 \le j \le (N_T - 1) \qquad (4.27)$$

where

$$K = \frac{k_p \delta_p n_I}{(W - D) \sinh n_I}$$

The range of j values given above holds for a full-plate calculation. If mid-plate symmetry is used (N_T even), N_T is replaced by $N_T/2$. For mid-tube symmetry (N_T odd), N_T is replaced by $(N_T + 1)/2$.

For mid-plate symmetry, for $j = N_T/2$, q_j^+ is given by Eq. 4.26. However, q_j^- is calculated from Eq. 4.23 with $j = N_T/2$ and ψ_{pj} taken from Eq. 4.13. The result is

$$q_j^- = K\,\Theta_{pj}\,[1 - \cosh n_I],\; j = N_T/2 \qquad (4.28)$$

For mid-tube symmetry, since $\Theta_{b,j+1} = \Theta_{b,j-1}$ for $j = (N_T + 1)/2$, Eqs. 4.26 and 4.27 yield

$$q_j^+ = q_j^- = K\,[\theta_{b,j-1} - \theta_{bj} \cosh n_I],\ j = (N_T + 1)/2 \tag{4.29}$$

The heat flow from the left-side edge absorber plate into the 1st tube, q_1^+, is given by

$$q_1^+ = \frac{-k_p \delta_p}{(\frac{W - D}{2})(1 + \delta_E)} \left.\frac{d\theta_{pE}}{d\xi_E}\right|_{\xi_E = 1} \tag{4.30}$$

From Eq. 4.21

$$\left.\frac{d\theta_{pE}}{d\xi_E}\right|_{\xi_E = 1} = \omega\gamma\left(\theta_{b1} + \frac{S}{U_{LI}} - \frac{S}{U_{LE}}\right) + \frac{\omega S}{U_{LE}} \tag{4.31}$$

where

$$\omega = \frac{\alpha_E}{\frac{\alpha_E}{n_E} \sinh n_E + \cosh n_E}$$

and

$$\gamma = \cosh n_E + \frac{n_E}{\alpha_E} \sinh n_E$$

Note that if $\alpha_E = 0$, $\omega = 0$ but $\omega\gamma \neq 0$. Using Eq. 4.31, Eq. 4.30 becomes

$$q_1^+ = K[-V\,\theta_{b1} \cosh n_I - SH] \tag{4.32}$$

where

$$V = \frac{\omega\gamma \tanh n_I}{(n_I/2)(1 + \delta_E)}$$

and

$$H = \cosh n_I \left[V\left(\frac{1}{U_{LI}} - \frac{1}{U_{LE}}\right) + \frac{\omega \tanh n_I}{U_{LE}(n_I/2)(1 + \delta_E)} \right]$$

The form of Eq. 4.32 was chosen for later convenience. Note that for a full plate calculation $q_{N_T}^{-} = q_1^{+}$.

Using Eqs. 4.26, 4.27, 4.28, 4.29, and 4.32, equations may be written for the total heat flow into the j^{th} tube base, q_j, by summing the individual plate heat flow.

$$q_j = q_j^{+} + q_j^{-} \tag{4.33}$$

For tubes bounded on both sides by plates with Type 1 boundary conditions, Eqs. 4.26 and 4.27 give

$$q_j = K \left[\Theta_{b,j-1} - 2\,\Theta_{bj} \cosh n_I + \Theta_{b,j+1}\right] \tag{4.34}$$

where j ranges from

$2 \leq j \leq (N_T - 1)$ (full-plate)

$2 \leq j \leq (N_T/2 - 1)$ (mid-plate symmetry)

$2 \leq j \leq [(N_T + 1)/2 + 1]$ (mid-tube symmetry)

For the case of mid-plate symmetry, Eqs. 4.26 and 4.28 give

$$q_j = K \left[\Theta_{b,j-1} - 2\,\Theta_{bj} \cosh n_I + \Theta_{bj}\right], \; j = N_T/2 \tag{4.35}$$

For mid-tube symmetry, Eq. 4.28 gives

$$q_j = K \left[2\,\Theta_{b,j-1} - 2\,\Theta_{bj} \cosh n_I\right], \; j = (N_T + 1)/2 \tag{4.36}$$

From Eqs. 4.27 and 4.32

$$q_1 = K\,[\Theta_{b2} - (1 + V)\Theta_{b1}\cosh n_I - SH] \tag{4.37}$$

Combining Eqs. 4.34 through 4.37, a general equation -- valid for all j -- can be written for q_j.

$$q_j = K\,\{\Theta_{b,j-1}[1 - \delta_{j1} + \delta_{jN}\Omega_1] - \Theta_{bj}\{[2 + (V - 1)\cdot (\delta_{j1} + \delta_{jN}\Omega_2)]\cosh n_I - \delta_{jN}\Omega_3\} + \Theta_{b,j+1}\cdot [1 - \delta_{jN}] - SH[\delta_{j1} + \delta_{jN}\Omega_2]\} \tag{4.38}$$

where δ_{jk} is the Kronecker delta function defined as

$$\delta_{jk} = 1 \text{ for } j = k$$

$$\delta_{jk} = 0 \text{ for } j \neq k$$

and where

$\Omega_1 = 1$ for mid-tube symmetry calculation

$= 0$ for no mid-tube symmetry calculation

$\Omega_2 = 1$ for full-plate calculation

$= 0$ for no full-plate calculation

$\Omega_3 = 1$ for mid-plate symmetry calculation

$= 0$ for no mid-plate symmetry calculation

The total useful energy gained by the fluid in tube segment j per unit length in the flow direction, q_{uj}, is equal to the sum of the net heat flow from the absorber plates plus the net energy collected in unit time per unit length on the surface of tube j. The assumption is made that all the tubes have the same loss coefficient as that for interior absorber plates, i.e., U_{LI}. Therefore, the loss coefficient U_{LE} applies only to the edge absorber-plate regions and not to the adjacent tube regions. At this point, the analysis depends, as in the preceding chapters, on the type of tube and sheet assembly chosen, i.e., Type I, II, or III as shown in Fig. 3. For the reason given in Chapter II, Type I geometry is again chosen for the analysis, which in the limiting case includes Type II. After the Type I analysis details have been shown, the Type III case will be outlined for completeness.

For the Type I case, summing all the plate and tube energy gains gives

$$q_{uj} = q_j + D[S - U_{LI}(T_{bj} - T_a)] \tag{4.39}$$

Rewriting in terms of Θ_{bj}

$$q_{uj} = q_j - DU_{LI}\Theta_{bj} \tag{4.40}$$

The useful energy gain, q_{uj}, is transferred to the fluid through the resistance R defined previously. Thus

$$q_{uj} = (T_{bj} - T_{fj})/R \tag{4.41}$$

This equation assumes that T_{bj} is uniform over the j^{th} tube

cross-section. Equation 4.41 can be written as

$$q_{uj} = (\Theta_{bj} - \Theta_{fj})/R \tag{4.42}$$

where

$$\Theta_{fj} = T_{fj} - T_a - S/U_{LI}$$

Equations 4.38, 4.40, and 4.42 can be used to solve for q_u in terms of Θ_f. Solving Eq. 4.42 for Θ_{bj} gives

$$\Theta_{bj} = \Theta_{fj} + R\, q_{uj} \tag{4.43}$$

The right side of Eq. 4.40 is a temperature function of Θ_b alone. Substitution of Eq. 4.43 in Eq. 4.40, through the use of Eq. 4.38, gives the following equation in q_u and Θ_f.

$$\begin{aligned} & q_{uj}\{1 - KR[\nu - (V - 1)(\delta_{j1} + \delta_{jN}\Omega_2)\cosh n_I + \delta_{jN}\Omega_3]\} \\ & \quad - q_{u,j-1}KR[1 - \delta_{j1} + \delta_{jN}\Omega_1] - q_{u,j+1}KR[1 - \delta_{jN}] \\ & \quad = K\{\Theta_{fj}[\nu - (V - 1)(\delta_{j1} + \delta_{jN}\Omega_2)\cosh n_I + \delta_{jN}\Omega_3] \\ & \quad + \Theta_{f,j-1}[1 - \delta_{j1} + \delta_{jN}\Omega_1] + \Theta_{f,j+1}[1 - \delta_{jN}] \\ & \quad - SH[\delta_{j1} + \delta_{jN}\Omega_2]\} \end{aligned} \tag{4.44}$$

where

$$\nu = -2\cosh n_I - DU_{LI}/K \tag{4.45}$$

Equation 4.44 can be written in matrix form as

$$[\underline{\underline{I}} - KR\,\underline{\underline{\Gamma}}]\,\underline{q}_u = K\,[\underline{\underline{\Gamma}}\,\underline{\Theta}_f + \underline{C}] \tag{4.46}$$

where single underlines denote an N x 1 matrix, double underlines denote an N x N matrix, $\underline{\underline{I}}$ is the identity matrix,

$$\underline{q}_u = \begin{bmatrix} q_{u1} \\ \cdot \\ \cdot \\ \cdot \\ q_{uN} \end{bmatrix}, \quad \underline{\Theta}_f = \begin{bmatrix} \Theta_{f1} \\ \cdot \\ \cdot \\ \cdot \\ \Theta_{fN} \end{bmatrix}, \quad \underline{C} = \begin{bmatrix} -SH \\ 0 \\ \cdot \\ \cdot \\ 0 \\ -SH\Omega_2 \end{bmatrix},$$

and $\underline{\underline{\Gamma}}$ has the elements

$$\underline{\underline{\Gamma}}_{jk} = [\nu - (V - 1)(\delta_{j1} + \delta_{jN}\Omega_2)\cosh n_I + \delta_{jN}\Omega_3]\delta_{jk}$$

$$+ \delta_{j,k-1} + \delta_{j,k+1}[1 + \delta_{jN}\Omega_1]$$

Solving for $\underline{q}_u$ in Eq. 4.46,

$$\underline{q}_u = K\,[\underline{\underline{I}} - KR\,\underline{\underline{\Gamma}}]^{-1}[\underline{\underline{\Gamma}}\,\underline{\Theta}_f + \underline{C}] \tag{4.47}$$

For the Type III design, the net energy collected on the j^{th} tube surface is based on the tube temperature, T_{tj}, instead of T_{bj}, as is the case for the Type I design. The Type III complement of Eq. 4.40 is

$$q_{uj} = q_j - DU_{LI}\Theta_{tj} \tag{4.48}$$

However, Θ_{bj} and Θ_{tj} are related by the additional energy balance

$$q_j = C_B(\Theta_{bj} - \Theta_{tj}) \tag{4.49}$$

Equation 4.41 has the Type III complement of

$$q_{uj} = (\Theta_{tj} - \Theta_{fj})/R_2 \tag{4.50}$$

where $R_2 = 1/(h_f \pi D_i)$. By solving Eq. 4.49 for Θ_{bj} and using the result to eliminate Θ_{bj}, $\Theta_{b,j-1}$, and $\Theta_{b,j+1}$ from Eq. 4.38, a matrix equation in $\underline{q}$ and $\underline{\Theta}_t$ results. Solving the matrix equation for $\underline{q}$ and substituting into the matrix form of Eq. 4.48 gives an equation in $\underline{q}_u$ and $\underline{\Theta}_t$. Using Eq. 4.50 to eliminate $\underline{\Theta}_t$ gives finally an equation in $\underline{q}_u$ and $\underline{\Theta}_f$ similar to Eq. 4.47. The result for the Type III case is

$$\underline{q}_u = K\,[\underline{\underline{I}} - KR_2[\underline{\underline{I}} - \frac{K}{C_B}\,\underline{\underline{\Gamma}}^*]^{-1}\,[\underline{\underline{I}} - \frac{K}{C_B}\,\underline{\underline{\Gamma}}^*]^{-1}\,[\underline{\underline{\Gamma}}^*\,\underline{\Theta}_f + \underline{C}] \tag{4.51}$$

where

$$\Gamma^*_{jk} = [-2 - (V-1)(\delta_{j1} + \delta_{jN}\Omega_2)\cosh n_I + \delta_{jN}\Omega_3]\delta_{jk}$$

$$+ \delta_{j,k-1} + \delta_{j,k+1}[1 + \delta_{jN}\Omega_1]$$

and the other symbols are as previously defined.

In the remaining development the only difference between the Type I-II and the Type III cases is in the expressions for $\underline{q}_u$ given by Eqs. 4.47 or 4.51, respectively. The preceding analysis has been for parallel flow collectors. The changes required for the serpentine analysis are noted at the end of the next section.

Development and Solution of Fluid Temperature Equations

From an energy balance on a differential fluid element in the j^{th} tube, the following differential equation is obtained.

$$\dot{m}c_p \frac{d\Theta_{fj}}{dy} - q_{uj} = 0 \tag{4.52}$$

In matrix form, Eq. 4.52 becomes

$$\dot{m}c_p \frac{d\underline{\Theta}_f}{dy} - \underline{q}_u = 0 \tag{4.53}$$

Substitution of Eq. 4.47 into Eq. 4.53 and non-dimensionalizing the variables gives

$$\frac{d\underline{\phi}_f}{d\beta} - \frac{KL}{\dot{m}c_p} [\underline{\underline{I}} - KR\ \underline{\underline{\Gamma}}]^{-1} \underline{\underline{\Gamma}}\ \underline{\phi}_f = \frac{KL}{\dot{m}c_p \Theta_{fi}} [\underline{\underline{I}} - KR\ \underline{\underline{\Gamma}}]^{-1} \underline{C} \tag{4.54}$$

where

$\phi_{fj} = \frac{\Theta_{fj}}{\Theta_{fi}}$, $\beta = \frac{y}{L}$, L = useful collector length, and

$\Theta_{fi} = T_{fi} - T_a - S/U_{LI}$.

Equation 4.54 is a set of first-order coupled inhomogeneous linear ordinary differential equations. Note that if $U_{LI} = U_{LE}$ and $\alpha_E = 0$, the equations become homogeneous, the solution of which gives the same results as the one-dimensional fin method.

Assuming a uniform inlet fluid temperature, Θ_{fi}, the boundary conditions for Eq. 4.54 may be written as

$$\phi_{fj}(0) = 1, \; j = 1,2,\ldots,N \tag{4.55}$$

where N is given by N_T, $N_T/2$, or $(N_T + 1)/2$ depending on whether a full-plate, mid-plate symmetry or mid-tube symmetry calculation is made, respectively.

Equation 4.54 is of the form

$$\frac{d\underline{\phi}_f}{d\beta} - \underline{\underline{A}}\,\underline{\phi}_f = \underline{B} \tag{4.56}$$

To solve this set of equations, first $\underline{B}$ is set to zero and the homogeneous system is solved. The homogeneous system is the classical eigenvalue problem:

$$[\lambda_j \underline{\underline{I}} - \underline{\underline{A}}]\,\underline{c}^j = 0, \; j = 1,2,\ldots,N \tag{4.57}$$

where λ_j is an eigenvalue of $\underline{\underline{A}}$ and $\underline{c}^j$ is the eigenvector associated with the j^{th} eigenvalue. Equation 4.57 may be obtained from

$$\frac{d\,\underline{\phi}_f}{d\beta} - \underline{\underline{A}}\,\underline{\phi}_f = 0 \tag{4.58}$$

by looking for general solutions of the form

$$\underline{\phi}_f = \underline{c}^j\, e^{\lambda_j \beta} \tag{4.59}$$

Substituting Eq. 4.59 into Eq. 4.58 yields Eq. 4.57.

Once the eigenvalues and eigenvectors have been found, the inhomogeneous system can be solved. The method of solution depends upon the symmetry of the matrix $\underline{\underline{A}}$.

For full-plate (N_T even or odd) and mid-plate symmetry (N_T even) cases, $\underline{\underline{A}}$ is a real symmetric matrix and is therefore Hermetian. For such a matrix the eigenvalues and eigenvectors are real. More importantly, for a Hermetian $\underline{\underline{A}}$, a set of N mutually orthogonal (thus linearly independent) unit eigenvectors $\underline{u}^1$, $\underline{u}^2$, . . . , $\underline{u}^N$ exists such that there is a diagonalization transformation $\underline{\underline{U}}^T \underline{\underline{A}} \underline{\underline{U}} = \underline{\underline{\Lambda}}$ where $\underline{\underline{\Lambda}}$ is a diagonal matrix with diagonal entries equal to the eigenvalues of the $\underline{\underline{A}}$ matrix [11]. The eigenvalues occur in the same columns as the associated eigenvectors $\underline{u}^j$ occur within $\underline{\underline{U}}$. The importance of the diagonalization transformation is that it can be used to uncouple any set of differential equations in the form of Eq. 4.56 (which includes Eq. 4.54).

For the case of mid-tube symmetry (N_T odd), $\underline{\underline{A}}$ is a non-symmetric real matrix. If all of the eigenvalues of $\underline{\underline{A}}$ are distinct, then there exists the diagonalization transformation $\underline{\underline{E}}^{-1} \underline{\underline{A}} \underline{\underline{E}} = \underline{\underline{\Lambda}}$ where $\underline{\underline{E}}$ is the matrix whose columns are the N linearly independent eigenvectors of $\underline{\underline{A}}$ and $\underline{\underline{\Lambda}}$ is the previously defined diagonal matrix of eigenvalues [11]. If the eigenvalues are not all distinct, the Jordan-Canonical form must be used to solve the equations. However, rather than use the Jordan-Canonical form, the method adopted here is to calculate the full-plate (symmetric $\underline{\underline{A}}$) case if the mid-tube case fails to yield distinct eigenvalues.

To uncouple Eq. 4.56, the substitution $\underline{\phi}_f = \underline{\underline{U}} \underline{\psi}_f$ or $\underline{\phi}_f = \underline{\underline{E}} \underline{\psi}_f$, depending upon whether or not $\underline{\underline{A}}$ is symmetric, is made. The following procedure will be shown for the case where $\underline{\underline{A}}$ is non-symmetric with

distinct eigenvalues. The symmetric case is identical when $\underline{\underline{E}}^{-1}$ and $\underline{\underline{E}}$ are replaced by $\underline{\underline{U}}^{T}$ and $\underline{\underline{U}}$ respectively and N is assigned the appropriate value. Substituting $\underline{\phi}_f = \underline{\underline{E}}\ \underline{\psi}_f$ in Eq. 4.56 gives

$$\underline{\underline{E}}\ \frac{d\underline{\psi}_f}{d\beta} - \underline{\underline{A}}\ \underline{\underline{E}}\ \underline{\psi}_f = \underline{B} \tag{4.60}$$

Premultiplying Eq. 4.60 by $\underline{\underline{E}}^{-1}$ gives

$$\frac{d\underline{\psi}_f}{d\beta} - \underline{\underline{E}}^{-1}\ \underline{\underline{A}}\ \underline{\underline{E}}\ \underline{\psi}_f = \underline{\underline{E}}^{-1}\ \underline{B} \tag{4.61}$$

Replacing $\underline{\underline{E}}^{-1}\ \underline{\underline{A}}\ \underline{\underline{E}}$ by $\underline{\underline{\Lambda}}$,

$$\frac{d\underline{\psi}_f}{d\beta} - \underline{\underline{\Lambda}}\ \underline{\psi}_f = \underline{\underline{E}}^{-1}\ \underline{B} \tag{4.62}$$

The boundary conditions on $\underline{\psi}_f$ are obtained from Eq. 4.55 and the substitution formula $\underline{\phi}_f(0) = \underline{\underline{E}}\ \underline{\psi}_f(0)$. Thus

$$\underline{\psi}_f(0) = \underline{\underline{E}}^{-1}\underline{\phi}_f(0) \tag{4.63}$$

Equation 4.62 is no longer a coupled set of equations, i.e., the j^{th} equation within Eq. 4.62 is now a function of only ψ_{fj} rather than a function of all the ϕ_{fj}'s, as was the case in Eq. 4.56. Accordingly, Eq. 4.62 may be written as

$$\begin{aligned} \frac{d\psi_{f1}}{d\beta} - \lambda_1\ \psi_{f1} &= D_1 \\ &\vdots \\ \frac{d\psi_{fN}}{d\beta} - \lambda_N\ \psi_{fN} &= D_N \end{aligned} \tag{4.64}$$

where

$$D_j = (\underline{\underline{E}}^{-1}\underline{B})_j$$

The general solution for $\underline{\psi}$ is

$$\psi_{fj} = e^{\lambda_j \beta}\left[\psi_{fj}(0) + \frac{D_j}{\lambda_j}\right] - \frac{D_j}{\lambda_j} \tag{4.65}$$

The final solution is obtained by solving for the original dependent variable $\underline{\phi}_f$, i.e.,

$$\underline{\phi}_f = E\ \underline{\psi}_f \tag{4.66}$$

where $\underline{\psi}_f$ is given by Eq. 4.65.

The changes required for the serpentine analysis are as follows [10]. The governing equation for the fluid (comparable to Eq. 4.54) is given by

$$\frac{d\underline{\phi}_f}{d\beta} - \frac{KL}{\dot{m}c_p}\underline{\underline{\Delta}}[\underline{\underline{I}} - KR\underline{\underline{\Gamma}}]^{-1}\ \underline{\underline{\Gamma}}\ \underline{\phi}_f = \frac{KL}{\dot{m}c_p\ \Theta_{fi}}[\underline{\underline{I}} - KR\underline{\underline{\Gamma}}]^{-1}\underline{C} \tag{4.67}$$

where $\Delta_{jk} = (-1)^j\delta_{jk}$. The boundary conditions for Eq. 4.67 are:

$$\begin{aligned}
&\phi_{f1}(0) = 1 \\
&\phi_{f,j+1}(0) = \P\phi_{fj}(0) \quad (j = \text{even}) \\
&\phi_{f,j+1}(1) = \P\phi_{fj}(1) \quad (j = \text{odd})
\end{aligned} \tag{4.68}$$

where

$$\P = \exp[-DU_{LI}W/\dot{m}c_p(1 + RDU_{LI})]$$

The inclusion of the $\underline{\underline{\Delta}}$ matrix in Eq. 4.67 results in a coefficient matrix $\underline{\underline{A}}$ which is non-symmetric regardless of the type of calculation (i.e., full-plate, mid-plate, or mid-tube). Under the assumption that all of the eigenvalues of the $\underline{\underline{A}}$ matrix are distinct, the general solution for $\underline{\psi}_f$ given by Eq. 4.65 applies. The values of $\psi_f(0)$ are obtained from application of the boundary conditions given by Eq. 4.68 and the use of the transformation $\underline{\phi}_f = \underline{\underline{E}}\ \underline{\psi}_f$. The values of $\underline{\psi}_f(0)$ are given by the equation

$$\underline{\psi}_f(0) = [\underline{\underline{W}}]^{-1}\ [\underline{Y} - \underline{\underline{V}}\underline{Z}] \tag{4.69}$$

where

$$W_{jk} = E_{jk} \qquad (j = 1)$$
$$W_{jk} = \P E_{j-1,k} - E_{jk} \qquad (j = \text{odd},\ j \neq 1)$$
$$W_{jk} = [\P E_{j-1,k} - E_{jk}]e^{\lambda_k} \qquad (j = \text{even})$$

$$Y_j = 1 \qquad (j = 1)$$
$$Y_j = 0 \qquad (j \neq 0)$$

$$V_{jk} = 0 \qquad (j = \text{odd})$$
$$V_{jk} = [\P E_{j-1,k} - E_{jk}][e^{\lambda_k} - 1] \qquad (j = \text{even})$$

and

$$Z_j = D_j/\lambda_j$$

Evaluation of Mean Temperatures

As noted in Chapter I, the absorber plate thermal analysis is only one part of the overall iterative scheme required to evaluate

the instantaneous collector efficiency η_c. For the conventional edge loss treatment, values of T_{pm} and T_{fm} are required for the Q_L and Q_u iterations. Upon convergence, the value of T_{fo} is required to evaluate η_c. For the localized edge loss model, additional mean temperature values are required to couple the absorber-plate thermal analysis to the Q_L iteration. The use of two different loss coefficients U_{LI} and U_{LE} requires that values be obtained for T_{pm_I} and T_{pm_E}, i.e., the internal and edge absorber-plate mean temperatures, respectively. The overall mean plate temperature T_{pm} is also required to evaluate the value of $(\tau\alpha)_e$ since no provisions are made for sectional $(\tau\alpha)_e$ values.* The values of c_p and R -- dependent on T_f -- are assumed adequately evaluated from the overall mean fluid temperature T_{fm}. For parallel flow, the average fluid outlet temperature $\bar{T}_{fo}$ is needed to evaluate η_c. In summary, the temperature quantities required for the localized edge loss model with parallel flow are T_{pm_I}, T_{pm_E}, T_{pm}, T_{fm}, and $\bar{T}_{fo}$. For the serpentine configuration, $\bar{T}_{fo}$ is replaced by T_{fo} of the exit tube.

Values for $\bar{T}_{fo}$ and T_{fm} are obtained from arithmetic averages of individual-channel outlet and mean fluid temperatures, respectively. Thus in terms of Θ_f

$$\bar{\Theta}_{fo} = [\sum_{j=1}^{N_T} \Theta_{fj}(1)]/N_T \tag{4.70}$$

*Sectional $(\tau\alpha)_e$ values could have been included by using S_I and S_E values rather than a uniform S value. However, for practical purposes the difference is minimal since $(\tau\alpha)_e$ variations with temperature are an order of magnitude less than U_L variations.

and

$$\Theta_{fm} = [\sum_{j=1}^{N_T} \Theta_{fmj}]/N_T \tag{4.71}$$

The term Θ_{fmj} in Eq. 4.71 is the mean j^{th}-tube fluid temperature given, from integration of Eq. 4.66 over β, by

$$\underline{\Theta}_{fm} = \Theta_{fi} \underline{E} \underline{\psi}_{fm} \tag{4.72}$$

where

$$\psi_{fmj} = [e^{\lambda_j} - 1][\psi_{fj}(0) + D_j/\lambda_j]/\lambda_j - D_j/\lambda_j$$

from Eq. 4.65.

The evaluation of the mean plate temperatures requires knowledge of the mean j^{th} base and fluid temperatures -- Θ_{bmj} and Θ_{fmj}, respectively. Integration of Eq. 4.43 over β gives the equation

$$\underline{\Theta}_{bm} = \underline{\Theta}_{fm} + R\, \underline{q}_{um} \tag{4.73}$$

where

$$\underline{q}_{um} = K[\underline{\underline{I}} - KR\underline{\underline{\Gamma}}]^{-1}[\underline{\underline{\Gamma}}\underline{\Theta}_{fm} + \underline{C}]$$

from Eq. 4.47. Equation 4.73 may be rewritten as

$$\underline{\Theta}_{bm} = [\underline{\underline{I}} + KR[\underline{\underline{I}} - KR\underline{\underline{\Gamma}}]^{-1}\underline{\underline{\Gamma}}]\underline{\Theta}_{fm} + KR[\underline{\underline{I}} - KR\underline{\underline{\Gamma}}]^{-1}\underline{C} \tag{4.74}$$

From knowledge of $\underline{\Theta}_{bm}$, the mean j^{th} plate temperature Θ_{pmj} can be evaluated. Integration of Eqs. 4.12 and 4.13 over β and ξ_j gives

for internal plates:

(1) with Type 1 boundary conditions

$$\Theta_{pmj} = \frac{F_I}{2} (\Theta_{bmj} + \Theta_{bm,j+1}) \tag{4.75}$$

(2) with Type 2 boundary conditions

$$\Theta_{pmj} = F_I \Theta_{bmj} \tag{4.76}$$

where F_I is the conventional fin efficiency factor with U_L replaced by U_{LI}, i.e.,

$$F_I = \frac{\tanh(n_I/2)}{n_I/2}$$

For the edge absorber plates, integration of Eq. 4.21 over β and ξ_E gives

$$\Theta_{pm_E} = \bar{f}(\Theta_{bm1} + S/U_{LI} - S/U_{LE}) - \bar{g}\ S/U_{LE} \tag{4.77}$$

where

$$\bar{f} = \frac{\alpha_E(\cosh n_E - 1)/n_E + \sinh n_E}{\alpha_E \sinh n_E + n_E \cosh n_E}$$

and

$$\bar{g} = \frac{\alpha_E(\cosh n_E - 1)/n_E}{\alpha_E \sinh n_E + n_E \cosh n_E}$$

The value of T_{pm_E} is obtained directly from Eq. 4.77, i.e.,

$$T_{pm_E} = \Theta_{pm_E} + T_a + S/U_{LE} \tag{4.78}$$

The value of T_{pm_I} is obtained by an arithmetic average of the interior plate temperatures and the plate base temperatures, weighted according to dimensions:

(1) Full-plate, $N = N_T$

$$\Theta_{pm_I} = [(\Theta_{pm1} + \ldots + \Theta_{pm,N-1})(W-D) + (\Theta_{bm1} + \ldots + \Theta_{bmN})D]/[W(N-1)+ D] \quad (4.79)$$

(2) Mid-plate symmetry, $N = N_T/2$

$$\Theta_{pm_I} = 2[(\Theta_{pm1} + \ldots + \Theta_{pm,N-1})(W-D) + \Theta_{pmN}(W-D)/2 + (\Theta_{bm1} + \ldots + \Theta_{bmN})D]/[W(N-1)+ D] \quad (4.80)$$

(3) Mid-tube symmetry, $N = (N_T + 1)/2$

$$\Theta_{pm_I} = 2[(\Theta_{pm1} + \ldots + \Theta_{pm,N-1})(W-D) + (\Theta_{bm1} + \ldots + \Theta_{bm,N-1})D + \Theta_{bmN}D/2]/[W(N-1)+D] \quad (4.81)$$

The conversion from Θ_{pm_I} to T_{pm_I} is given by

$$T_{pm_I} = \Theta_{pm_I} + T_a + S/U_{LI} \quad (4.82)$$

The overall mean plate temperature T_{pm} is obtained from the relation

$$\Theta_{pm} = \{\Theta^{I}_{pm_E}(W-D)(1 + \delta_E) + \Theta_{pm_I}[W(N_T-1)+D]\}/W_p \quad (4.83)$$

where W_p is the total width of the collector receiving area, i.e.,

$$W_p = WN_T + \delta_E(W-D) \tag{4.84}$$

and

$$\Theta^I_{pm_E} = \Theta_{pm_E} + S/U_{LE} - S/U_{LI} \tag{4.85}$$

The use of $\Theta^I_{pm_E}$ in Eq. 4.83 rather than Θ_{pm_E} is necessary so that all the Θ terms in Eq. 4.83 are referenced to U_{LI}. The conversion from Θ_{pm} to T_{pm} is given by*

$$T_{pm} = \Theta_{pm} + T_a + S/U_{LI} \tag{4.86}$$

Results from the Localized Edge Loss Model and Comparisons with Conventional Edge Loss Treatment

Both the sectional and uniform loss coefficient models are incorporated into an existing computer program [12] capable of handling the Q_u and Q_L iterations required to evaluate U_{TI}, U_{TE}, and U_T. The assumption of one-dimensional heat loss through the top, bottom, and sides of the collector is made for both models. This assumption is adequate for the purpose of evaluating the relative improvement derived from the use of sectional loss coefficients. Results are obtained from the localized edge loss model for a specific collector

*Note that the temperature variable Θ used in Chapter IV (with the exception of Θ values subscripted with an E) are referenced to U_{LI} while in Chapters II and III the variable Θ is referenced to U_L.

under typical operating conditions. The results are compared to the predictions of conventional edge loss treatment.

The collector chosen for analysis is the PPG Baseline collector. The PPG collector has a roll-bond, aluminum absorber plate with a flat-black coating and 13 parallel-flow channels. The external dimensions of the collector are 0.868 m x 1.935 m. The absorber-plate receiving surface is 0.841 m x 1.908 m with a tube-to-tube spacing W of 6.35 cm. The edge absorber plate has a δ_E value of 0.3051. An x-z cross-section of the edge assembly and cover system is shown in Fig. 22. The edge assembly extends around the entire periphery of the collector. Further details of the collector dimensions and collector property values can be found in references 12 and 13.

The PPG collector was chosen for analysis because the ratio of the PPG peripheral heat losses to top and bottom losses is large compared to most collectors with comparable absorber-plate surface area.* For a parallel-flow collector with large peripheral heat losses, the mean edge-absorber-plate temperature will be significantly smaller than the overall mean plate temperature. The applicability of a uniform loss coefficient treatment is uncertain in this situation. The PPG collector was also convenient for analysis because the edge assembly structure is such that both the S_e and δ_E factors can be used.

The evaluation of the bottom and edge loss coefficients for the

*Collectors with less absorber-plate surface area may have a larger ratio of peripheral to top and bottom losses since the respective area ratios are larger. However, most collectors presently marketed are comparable in size to the PPG collector.

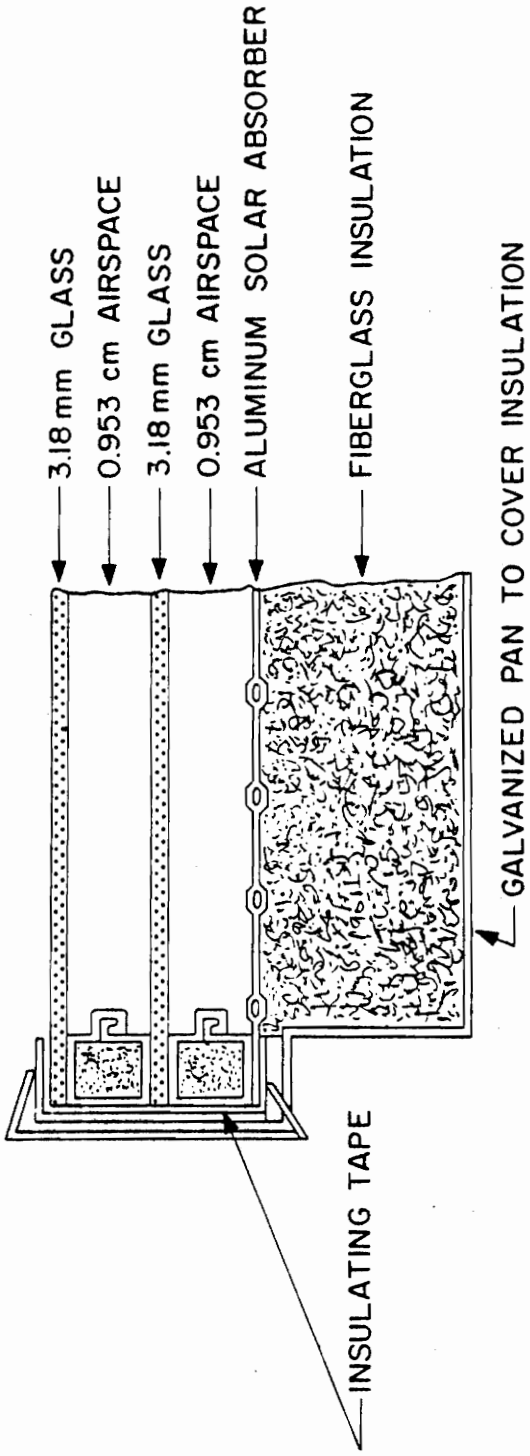

Figure 22. X-Z Cross Section of the PPG Collector

PPG collector are complicated by the geometry of the collector housing. The expressions for U_{EE}, U_{BE}, U_{EI}, U_{BI}, U_E, and U_B given in Appendix I must be modified by appropriate area ratios. The details of the calculations are omitted since they are not germane to the model comparisons. The main requirement for valid model comparisons is that the calculations be consistent between models. Table 4.1 gives the calculated values of the bottom and edge loss coefficients for each method. A wind speed of 3 m/s was assumed for the calculations. The evaluation of the top loss coefficients U_{TE}, U_{TI}, and U_T follows the procedure given in Appendix I.

Figure 23 shows the resulting absorber-plate temperature profiles in the transverse direction from the collector edge to the collector centerline. Transverse profiles are given for both models at axial locations $\beta = 0$ and $\beta = 1$. The acronyms LEL and CEL denote the localized edge loss model and the conventional edge loss model, respectively. Note that the tube regions for the CEL profiles are displaced slightly from the LEL tube locations. To account for the δ_E factor in the CEL model, the tube-to-tube spacing W is replaced by an effective spacing W_{eff} given by

$$W_{eff} = W + \delta_E(W-D)/N_T \tag{4.87}$$

For the PPG collector, W_{eff} is 6.47 cm. The assumed operating conditions for Fig. 23 are T_{fi} = 50 C, T_a = 0 C, V_w = 3 m/s, G = 0.02 kg/s-m^2, HR = 1000 w/m^2, and a collector slope of 45°. The coolant fluid was assumed to be water containing no antifreeze.

Table 4.1

Calculated Values for the Bottom and Edge Loss Coefficients for the PPG Collector

(V_w = 3 m/s)

Localized Edge Loss Model

U_{EI} = 0.50 w/m^2-C U_{BI} = 1.50 w/m^2-C

U_{EE} = 1.96 w/m^2-C U_{BE} = 20.0 w/m^2-C

S_e = 9.63

Conventional Edge Loss Model

U_E = 1.64 w/m^2-C U_B = 2.96 w/m^2-C

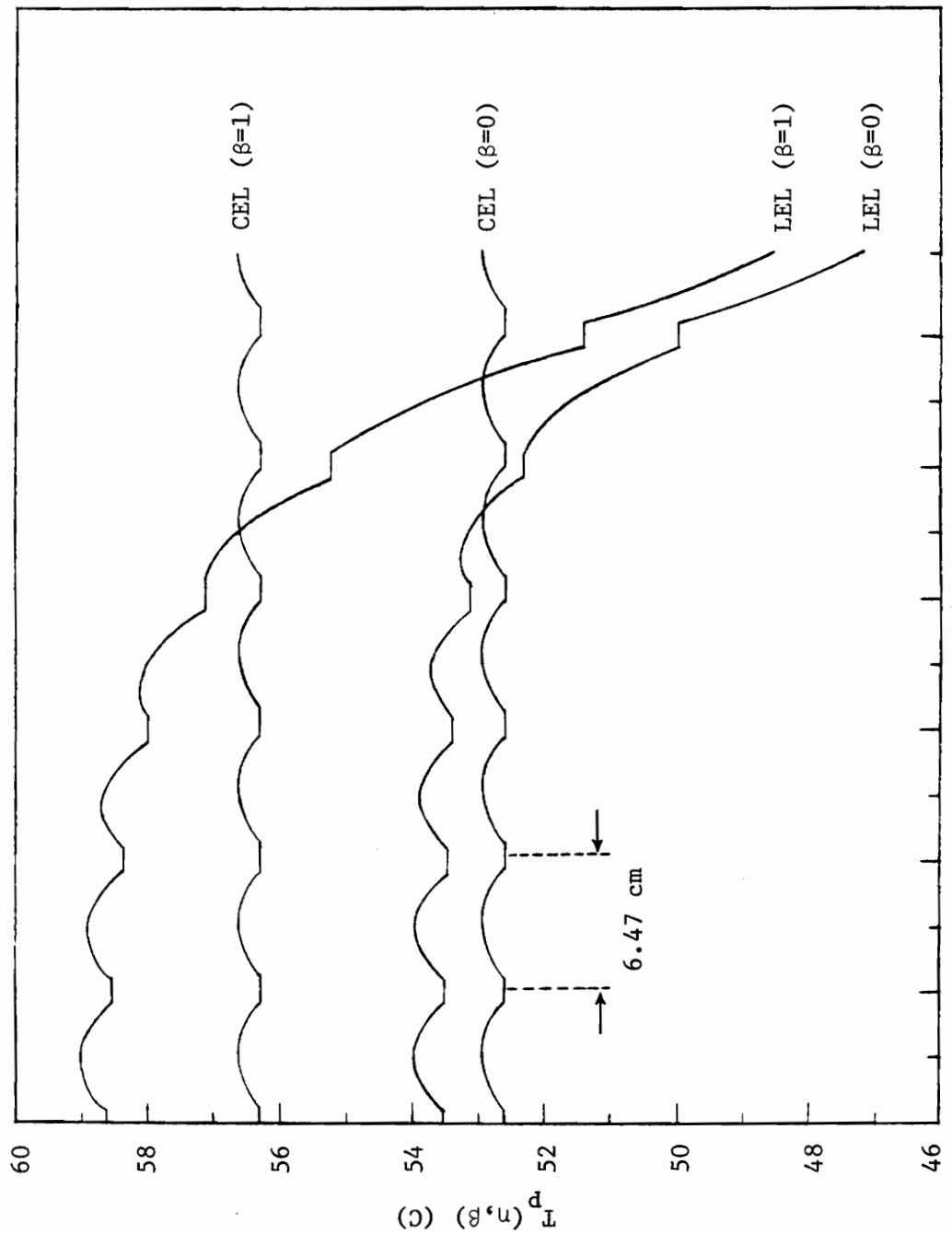

Figure 23. PPG Absorber-Plate Transverse Temperature Profiles -- LEL and CEL Models

Table 4.2 gives the corresponding values obtained for η_c, F_R, $(\tau\alpha)_e$, T_{pm}, T_{pm_I}, T_{pm_E}, T_{fm}, T_{fo}, Q_u, U_L, U_{LI}, and U_{LE} for each model.* From Table 4.2 and Fig. 23, it is noted that even though the temperature profiles vary significantly between models, the absolute difference in η_c values is only 1.53 per cent. For a given collector, the magnitude of the η_c differences between models depends on the operating conditions T_{fi}, T_a, V_w, G, and HR. Table 4.3 gives η_c values obtained for the LEL and CEL models over a range of operating conditions. Each operating condition is varied while the remaining conditions are held at the standard condition of T_{fi} = 50 C, T_a = 0 C, V_w = 3 m/s, G = 0.02 kg/s-m^2, and HR = 1000 w/m^2. The range of each variable is ordered from left to right in the particular manner which gives increasing η_c differences between models. Note that the absolute differences in efficiency increase for operating conditions which decrease collector efficiency. Therefore, maximum differences between the LEL and CEL models occur for operating conditions which yield low collector efficiencies. In all cases, the value of η_c is

*An equivalent value of U_L for the LEL model is obtained from Eq. 2.32, i.e.,

$$U_{L,equiv} = \frac{S - G(T_{fo} - T_{fi})}{T_{pm} - T_a}$$

The heat removal factor F_R is given for the LEL model by

$$F_R = \frac{G(T_{fo} - T_{fi})}{S - U_{L,equiv}(T_{fi} - T_a)}$$

Table 4.2

Comparison of Output Values from the Collector Efficiency Program for the CEL and LEL Models

(Standard Operating Conditions)

	CEL	LEL
η_c	33.00	34.53
F_R	0.897	0.904
$(\tau\alpha)_e$	0.773	0.773
T_{pm}	54.66 C	54.71 C
T_{pm_I}	54.66 C	55.19 C
T_{pm_E}	54.66 C	49.10 C
T_{fm}	52.00 C	52.09 C
T_{fo}	53.94 C	54.13 C
Q_u	529.4 w	554.1 w
U_L	8.107 w/m^2-C	7.819 w/m^2-C
U_{LI}	8.107 w/m^2-C	5.515 w/m^2-C
U_{LE}	8.107 w/m^2-C	25.34 w/m^2-C

Table 4.3

Comparison of η_c Values for the CEL and LEL Models for a Range of Operating Conditions

	T_{fi}			
	25 C	50 C	75 C	
CEL	51.26	33.00	12.66	} η_c
LEL	52.09	34.53	14.90	
	T_a			
	10 C	0 C	-10 C	
CEL	39.74	33.00	25.68	} η_c
LEL	41.04	34.53	27.50	
	V_w			
	1 m/s	3 m/s	5 m/s	
CEL	42.03	33.00	25.16	} η_c
LEL	42.59	34.53	28.04	
	G			
	.03 kg/s-m^2	.02 kg/s-m^2	.01 kg/s-m^2	
CEL	33.65	33.00	31.32	} η_c
LEL	35.09	34.53	33.05	
	HR			
	1100 w/m^2	1000 w/m^2	900 w/m^2	
CEL	36.24	33.00	29.03	} η_c
LEL	37.65	34.53	30.72	

underestimated by the conventional edge loss treatment. For the cases shown in Table 4.3, the absolute differences in η_c values are less than 3 per cent. The relative differences in η_c values are as large as 15 per cent. However, the large relative differences always occur for low values of η_c.

The error incurred by distributing the heat loss from the transverse perimeter area over the internal and edge absorber plates is small for parallel-flow collectors. The transverse perimeter area is typically at least half of the longitudinal perimeter area. Also, the opposing transverse areas are adjacent to the highest and lowest temperature regions of the collector -- the outlet and inlet regions, respectively. The use of distributed edge losses results in an overestimation of the inlet-region edge losses and an underestimation of the outlet-region losses. For typical parallel-flow collectors with forced-flow operation, the useful heat gain per unit length, $q_u(y)$, is approximately the same at the inlet and outlet of the collector. Consequently, the errors in heat loss calculations at both ends of the collector tend to balance out.

The results presented are a worst case analysis for the PPG collector. The effects of a mounting assembly and specific housing assembly details are not included. Therefore, the results given in Table 4.3 represent the maximum error attributable to the conventional edge loss treatment for typical parallel-flow collectors under a range of operating conditions.

In both parallel and serpentine flow configurations, the largest

collector dimension is typically in the flow direction. Therefore the LEL model localizes the edge losses for the largest peripheral areas in both flow configurations. The temperature distributions on the peripheral area of the serpentine collector are such that, for forced-flow operation ($\dot{m} \approx 5 \times 10^{-3}$ kg/s), the error incurred by the CEL treatment is smaller than that for the parallel-flow case. The opposing longitudinal areas of the serpentine collector are subject to the minimum and maximum collector temperatures. This is in contrast to the parallel-flow case where the minimum and maximum temperatures occur at the opposing transverse perimeter areas. For forced flow operation, the useful heat gain per unit length is approximately the same at the inlet and outlet tube sections in the serpentine collector. Thus the CEL errors in heat loss calculations for both longitudinal perimeter areas approximately cancel. For smaller mass flow rates, some error will result from the distribution of the longitudinal edge losses in the CEL treatment since $q_u(y)$ at the serpentine inlet section will be larger than at the outlet section. The inlet section will be more effective than the outlet section and the use of the mean plate temperature for edge loss calculations will underestimate the performance of the collector. In such cases, the LEL model is a convenient improvement since only minor changes are required to incorporate the LEL model into the serpentine analysis. The edge losses from the transverse perimeter areas of the serpentine collector are adequately treated by the CEL model for thermosyphon and forced-flow operation. The CEL treatment is adequate for transverse edge loss calculations because the

mean transverse plate temperature remains approximately constant across the longitudinal direction. Consequently, even in worst case analyses, errors resulting from the CEL treatment of serpentine collectors will remain within the error bounds obtained for comparably sized and designed parallel-flow collectors.

A listing of the FORTRAN program for the localized edge loss model is given in Appendix IV. The program is written in subprogram form for convenient insertion into an overall iterative program. The program given is for Type I and II geometries and parallel-flow. The modifications required for the serpentine configuration and Type III geometry can be made without causing major changes in the program.

Summary

The localized edge loss model presented in Chapter IV provides the capability to better analyze edge effects in flat-plate collectors. With proper modification, the analysis is applicable for both serpentine and parallel-flow configurations and for Type I, II, and III geometries.

The model was used in Chapter IV to determine the applicability of conventional edge loss treatment in which the edge losses are distrib- over the entire collector receiving area. The parallel-flow PPG collector was analyzed as a worst case situation for standard size collectors. The results indicate that the conventional edge loss treatment yields η_c values accurate to within 3 per cent absolute and 15 per cent relative for typical ranges of operating conditions. The maximum errors occur for low values of η_c. For serpentine collectors, the conventional

edge loss treatment is qualitatively shown to give η_c values within the error bounds of comparable parallel-flow situations.

The localized edge loss model has other potential applications. The model gives more realistic predictions of the temperature distributions in flat-plate collectors. This improvement could be used to more accurately determine the maximum collector temperature under stagnation (no-flow) conditions. The model has the capabilities of variable edge-plate width and non-insulated longitudinal perimeter boundary conditions. These capabilities could be used to determine the most efficient width for the edge plate for a given collector housing and mounting assembly. The effects of shading in parallel-flow collectors could be investigated by setting the incident solar radiation HR equal to zero for the edge plate region. Also, the generality of the model with respect to flow configuration allows the use of one basic program for both situations. Comparison of serpentine and parallel-flow collector performance would be facilitated by the need to program only one model.

V. FINAL DISCUSSION, CONCLUSIONS, AND RECOMMENDATIONS

Each of the two new models developed in Chapters III and IV provide one improvement over existing analytical absorber-plate thermal analyses. In the first new model, the need for an approximate treatment of axial conduction effects is eliminated for parallel-flow collectors. In the second new model, provisions are made for a more accurate analysis of the longitudinal edge losses in both parallel-flow and serpentine configurations. The 1-D fin method with conventional edge loss treatment is the common basis for comparison with the new models. The first new model is also compared to the analytical method given by Phillips.

The improvements are introduced separately for two reasons. First, the separate treatment allows the error range of each assumption to be evaluated. Secondly, the solution of the equations necessary to include both improvements in a single model would require considerable computational time. The dual solution would be warranted if both of the assumptions were strongly coupled. However, the localized edge loss treatment does not significantly affect the ratio of axial to transverse heat flow. Consequently, the errors in F_R values inherent in the 1-D fin method can be accounted for by an independent axial analysis.

For parallel-flow collectors, Figs. 10 through 17 can be used to correct for the axial effects. Noting that F_R and η_c are related by the equation

$$\eta_c = F_R[S - U_L(T_{fi} - T_a)]/HR \tag{5.1}$$

the net effect of improved axial and edge-loss treatments on the predicted values of η_c can be obtained. The net absolute per cent differences in η_c values are given by the equation

$$\eta_c \text{ net abs \% diff} = \{(\Delta F_R)_{LEL}[S - (U_L)_{LEL}(T_{fi} - T_a)]/HR + (\eta_c)_{CEL} - (\eta_c)_{LEL}\} \times 100\% \tag{5.2}$$

where $\Delta F_R = (F_R)_{1-D} - (F_R)_E$. Net relative per cent differences in η_c values are obtained by dividing Eq. 5.2 by the term $[(F_R)_E]_{LEL} \times [S - (U_L)_{LEL}(T_{fi} - T_a)]/HR$. The subscript LEL on F_R terms denotes that the F_R terms are to be evaluated from values of B, M, F', c, and u_r obtained from the LEL results. For the PPG collector under the range of operating conditions given in Table 4.3, $B < 0.2$, $M < 0.02$, $F' \approx 0.94$, $c \approx 0.12$, and $100 < u_r < 300$. From Figs. 14 and 15, the value of $(\Delta F_R)_{LEL}$ is insignificant for these parameter values. Therefore, the LEL values of η_c given in Table 4.3 need no correction for the axial effect. For parallel-flow situations in which $(\Delta F_R)_{LEL}$ is significant, Figs. 10 through 17 are used in conjunction with Eq. 5.2. For serpentine collectors, the effects of axial conduction should not be significant because of the balancing effect of the cross-flow of heat between tubes.

The net effect of the improved axial and edge-loss treatments depends strongly on the type of collector and the specific operating conditions. In general, the differences in η_c values between the 1-D

fin method with CEL treatment and the exact method with LEL treatment can be either positive, negative, or zero. However, since the individual error ranges noted in Chapters III and IV are opposite in sign, the net differences can be no larger than either of the individual error ranges. The maximum error values in either direction are possible only when the effect of one improvement is negligible. When conventional edge loss treatment is adequate, the F_R error ranges given in Chapter II for the axial effect can be translated directly into η_c error ranges (assuming the iterative effect is negligible). When axial effects are negligible, the error ranges given in Chapter IV apply.

Approximate axial and edge-loss treatments have been cited [14] as possible explanations for discrepancies which exist between experimental and theoretical results. The results from Chapters III and IV indicate that, for typical collectors and operating conditions, the approximate axial and edge-loss treatments are not the primary cause of the cited discrepancies. Consequently, other possible sources of error need to be examined to determine whether the primary source of error is in the theoretical assumptions or in the experimental procedures.

Possible remaining sources of error in the conventional theoretical analysis include: (1) the uncertainty in the optical properties of the absorber plate and covers; (2) the effect of diffuse solar radiation; (3) the evaluation of the flow properties at the mean fluid temperature; (4) the uncertainty in heat transfer properties of the collectors in relation to methods of assembly and design configurations; (5) the linearization of the top loss coefficient; (6) the

assumption of one-dimensional heat loss through the top, bottom, and sides of the collector; (7) the effect of flow headers; and (8) the assumption of steady-state behavior. Further research is needed to determine whether the remaining approximations cause significant error for typical collectors and operating conditions.

With regard to the experimental procedures, one possible source of error is the use of metal connectors for the inlet and outlet piping connections. The large thermal conductivities of such connectors may allow significant heat flow into the connecting pipes. The use of plastic connectors between the collector and the piping system would eliminate any question regarding this effect.

While the two new methods do not indicate the primary source of error between experimental and theoretical results for typical collectors, the new methods do provide more accurate performance evaluation over a wide range of collector types. Figures 10 through 17 in Chapter III provide a convenient means of comparison between the 1-D fin, averaging, and exact methods. The graphs indicate that the exact method becomes significantly more accurate than either of the existing methods when $M > 0.1$ and $F' < 0.7$. The second new method has the inherent capability to better evaluate performance and design questions related to edge effects. The generality of the second new model with respect to flow configuration allows the use of one basic program for both situations.

The solution technique presented in the first new method has potential application to a number of conduction-convection problems.

To the author's knowledge, an analytical solution to such a coupled conduction-convection boundary condition problem has not been previously presented. However, the technique has been previously applied to conduction problems with interface boundary conditions [15] and to potential flow problems [16].

In Chapters II and III, convenient relations between the mean plate and fluid temperatures and the heat removal factor F_R were obtained (Eqs. 3.65 and 3.66). Equation 3.65 is applicable for any flat-plate collector for which an equivalent overall loss coefficient can be obtained. Equation 3.66 requires the assumptions of parallel-flow, constant tube spacing W (or W_{eff}) with edge spacing W/2 (or $W_{eff}/2$), and a uniform loss coefficient U_L. Therefore, Eq. 3.65 is valid for LEL and CEL treatments of parallel-flow and serpentine collectors. Equation 3.66 (and Eq. 3.77) is limited to CEL parallel-flow analysis.

REFERENCES

1. Duffie, J, A., and W. A. Beckman, Solar Energy Thermal Processes, John Wiley and Sons, New York, 1974, pp. 74-83, 120-168.

2. Phillips, W. F., "Axial Conduction in a Flat-Plate Solar Collector," AIChE paper, AIChE-57, 1976.

3. Hottel, H. C., and B. B. Woertz, "The Performance of Flat-Plate Solar-Heat Collectors," ASME Transactions, Vol. 64, 1942, pp. 91-104.

4. Whillier, A., "Design Factors Influencing Solar Collector Performance," Low Temperature Engineering Applications of Solar Energy, ASHRAE, New York, 1967, pp. 27-33.

5. Bliss, R. W., Jr., "The Derivation of Several 'Plate-Efficiency Factors' Useful in the Design of Flat-Plate Solar-Heat Collectors," Solar Energy, Vol. 3, 1959, pp. 55-64.

6. Tabor, H., "Radiation, Convection, and Conduction Coefficients in Solar Collectors," Bulletin of the Research Council of Israel, Vol. 6C, 1958, pp. 155-176.

7. Klein, S. A., "The Effects of Thermal Capacitance Upon the Performance of Flat-Plate Solar Collectors," MS thesis, University of Wisconsin, 1973, pp. 21.

8. Arpaci, V. S., Conduction Heat Transfer, Addison-Wesley Publishing Company, Reading, Mass., 1966, pp. 193-194.

9. Kirchhoff, R. H., and M. Billups, "A Two-Dimensional Heat Transfer Model of a Flat-Plate Collector," ASME paper, 76-WA/Sol-2,1976.

10. Abdel-Khalik, S. I., "Heat Removal Factor for a Flat-Plate Solar Collector with a Serpentine Tube," Solar Energy, Vol. 18, pp. 59-64.

11. Franklin, J. N., Matrix Theory, Prentice-Hall Inc., Englewood Cliffs, N. J., 1968, pp. 71-79, 98-102.

12. Thomas, W. C., and A. G. Dawson, "Analysis of Data and Results for the Roundrobin Flat-Plate Collector Test Program, VPI&SU Report No. ENG 77-23, 1977.

13. "Baseline Solar Collector," Glass Division, PPG Industries, Inc., One Gateway Center, Pittsburgh, Pa. 15222, 1974.

14. Dennison, T. M., "Experimental Evaluation of the Overall Loss Coefficient and Effective Transmittance-Absorptance Product for Flat-Plate Solar Collectors," MS thesis, VPI&SU, 1976, pp. 46-49, 52-61.

15. Coppari, L. A., "A Theoretical Analysis of the Temperature Response in a Bimetallic, Composite Geometry, Nuclear Reactor Pressure Vessel Undergoing a Loss-of-Coolant Accident," PhD thesis, VPI&SU, 1977.

16. Yeh, H. C., "Method of Solving the Potential Field in Complicated Geometries and the Potential Flow in the Lower Plenum of a Pressurized Water Reactor," Nuclear Engineering and Design, Vol. 32, 1975, pp. 85-104.

APPENDICES

APPENDIX I. EVALUATION OF THE OVERALL LOSS COEFFICIENT U_L

Conventional Analysis

The conventional analysis of U_L given here is a summary of the overall-loss-coefficient treatment given by Duffie and Beckman [1]. Several simplifying assumptions were given in Chapter II relating to the absorber-plate thermal analysis. The simplifying assumptions relating to the evaluation of U_L are as follows:

1. Absorption of solar energy by the covers can be treated separately from the collector heat loss calculation.
2. There is one-dimensional heat flow through the covers.
3. There is negligible temperature drop through each cover.
4. The sky can be considered as a blackbody for long-wavelength radiation at an equivalent sky temperature.
5. Cover properties are independent of temperature.
6. Losses through the front, back, and sides of the collector are to the same ambient temperature.
7. Heat loss through the sides and bottom of the collector is one-dimensional.
8. Heat loss through the sides of the collector may be uniformly distributed over the entire collector surface.
9. The overall loss coefficient U_L may be treated as independent of position.

Under the simplifying assumptions, the collector losses can be evaluated by means of a one-dimensional thermal network. Figure 24.a shows a one-dimensional network for a three cover system. The resistances R_3, R_4, R_5, and R_6 are each composed of convection and linearized-radiation terms, i.e.,

$$R_i = \frac{1}{h_{ci} + h_{ri}}, \quad i = 3,4,5,6 \tag{I.1}$$

For radiation heat transfer between parallel plates (i = 3,4,5), h_{ri} is given by

$$h_{ri} = \frac{\sigma(T_1 + T_2)(T_1^2 + T_2^2)}{1/\varepsilon_1 + 1/\varepsilon_2 - 1}, \quad i = 3,4,5 \tag{I.2}$$

where σ is the Stefan-Boltzmann constant and ε_1 and ε_2 are the emissivities of adjacent parallel plates 1 and 2. The radiation heat transfer coefficient h_{r6} is given by

$$h_{r6} = \sigma\varepsilon_{cover,3}(T_{cover,3} + T_{sky})(T_{cover,3}^2 + T_{sky}^2)\frac{(T_{cover,3} - T_{sky})}{(T_{cover,3} - T_a)} \tag{I.3}$$

where

$$T_{sky} = 0.0552\ [T_a/°K]^{1.5}\ °K \tag{I.4}$$

The convective heat transfer coefficient h_{ci} is given by natural convection relations [1] for cover-to-cover and cover-to-plate regions (i = 3,4,5). The convective heat transfer coefficient h_{c6} is given in w/m^2-C by

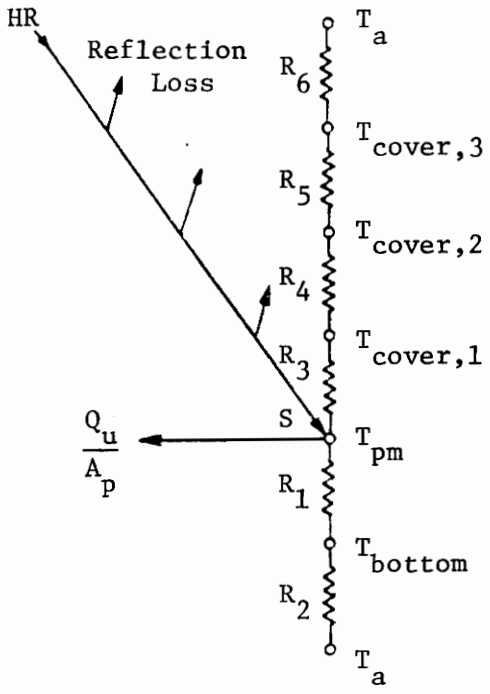

(a) Thermal Network for a Flat-Plate Solar Collector

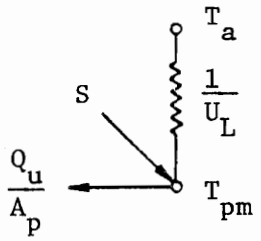

(b) Equivalent Thermal Network

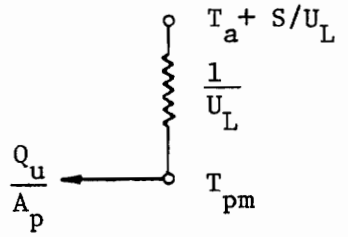

(c) Alternate Representation

Figure 24. Basic Thermal Networks for a Flat-Plate Solar Collector

$$h_{c6} = 5.7 + 3.8V_w \tag{I.5}$$

where V_w is the wind velocity in m/s. The top loss coefficient U_T is given by

$$U_T = \frac{1}{R_3 + R_4 + R_5 + R_6} \tag{I.6}$$

The natural convection and linearized-radiation heat transfer coefficients contained within U_T are non-linear temperature functions. Therefore the top loss coefficient must be iteratively evaluated from an assumed value of T_{pm}. The bottom loss coefficient U_B is given by

$$U_B = \frac{1}{R_1 + R_2} \tag{I.7}$$

where R_1 is the resistance to heat flow through the back insulation and R_2 is the sum of the convection and radiation resistances to heat flow to the environment. For most practical situations, R_2 is much smaller than R_1 and can be neglected. Therefore, for one-dimensional heat flow, U_B is given by

$$U_B = \frac{1}{R_1} = \frac{k_{ins,B}}{t_B} \tag{I.8}$$

where $k_{ins,B}$ is thermal conductivity of the back insulation and t_B is the back insulation thickness. For the evaluation of U_E, the edge losses are first evaluated by assuming one-dimensional sideways heat flow around the perimeter of the collector structure, i.e.,

$$Q_E = U_E' P_c d_c (T_{pm} - T_a) \tag{I.9}$$

where d_c is the collector depth, P_c is the collector perimeter, and U_E' is the local edge loss coefficient given by

$$U_E' = \frac{1}{\frac{k_{ins,E}}{t_E} + R_2} \tag{I.10}$$

where t_E and $k_{ins,E}$ refer, respectively, to the thickness and thermal conductivity of the edge structure. Since U_L is based on collector receiving area A_p, an equivalent edge loss coefficient based on A_p is needed. The equivalent edge loss coefficient U_E is given by

$$U_E = U_E' P_c d_c / A_p \tag{I.11}$$

The overall loss coefficient U_L is the sum of U_T, U_B, and U_E. Figure 24.b shows the equivalent thermal network in terms of U_L. Figure 24.b is a thermal network representation of the equation

$$S - U_L(T_{pm} - T_a) = Q_u/A_p \tag{I.12}$$

Equation I.12 can be rewritten as

$$U_L(S/U_L + T_a - T_{pm}) = Q_u/A_p \tag{I.13}$$

Using Eq. I.13, Fig. 24.b can be given alternately by Fig. 24.c. Figure 24.c is the representation used in Chapter II.

Localized Edge Loss Treatment

For collectors in which the local edge loss coefficient U_E' is significant, the mean plate temperature of the edge plates may be

significantly less than the value of the overall mean plate temperature. For such cases, Eq. I.9 overestimates the edge heat loss. The top and bottom losses for the edge plates are similarly overestimated. An improvement in the evaluation of the collector heat losses can be made by considering two distinct loss coefficients U_{LI} and U_{LE}. The subscripts I and E refer to internal and edge plate sections, respectively. The loss coefficients U_{LI} and U_{LE} are composed of top, bottom, and edge loss coefficients, i.e.,

$$U_{LI} = U_{TI} + U_{BI} + U_{EI} \tag{I.14}$$

and

$$U_{LE} = U_{TE} + U_{BE} + U_{EE} \tag{I.15}$$

The top loss coefficients U_{TI} and U_{TE} are given by the conventional equations with T_{pm} values replaced by T_{pm_I} and T_{pm_E} values, respectively. The bottom loss coefficients U_{BI} and U_{BE} have the conventional form. The edge loss coefficients U_{EI} and U_{EE} represent the heat losses through the respective perimeter area perpendicular to the flow direction. The heat losses through the remainder of the perimeter area are accounted for by the shape factor S_e. The loss coefficients U_{EI} and U_{EE} are given, in general, by the equations

$$U_{EI} = \frac{2\, U_E' d_c}{L} \tag{I.16}$$

and

$$U_{EE} = \frac{U_E' d_c (W_c - W_I)/2}{L(\frac{W - D}{2})(1 + \delta_E)} \tag{I.17}$$

where $W_I = WN_T - (W - D)$ and W_c is the collector external width. Equations I.16 and I.17 are valid for box-type collector assemblies. For collector assemblies other than box-type, modifications of the area ratios may be necessary.

The shape factor S_e introduced in Chapter IV provides a means for including transverse conduction heat loss from the edge absorber plates through the collector edge assembly. The shape factor approach is applicable only when the edge absorber plate is in contact with the edge structure. A first-order approximation to the value of S_e can be made by assuming that the edge structure adjacent to the edge plate has the temperature $T_{pE}(0)$. Under this assumption, S_e is given by

$$S_e = U_E' d_c / k_{ins,E} \tag{I.18}$$

More accurate analysis of S_e requires a two-dimensional analysis of the edge structure. However, Eq. I.18 is adequate for the purposes of Chapter IV. When the edge absorber plate is not in contact with the edge structure, transverse conduction heat loss through the edge plate is small. In this situation, the shape factor S_e is set equal to zero and the edge loss through the perimeter area parallel to the flow direction is calculated by the conventional method. Equation I.17 for U_{EE} is replaced by the equation

$$U_{EE} = \frac{U_E' d_c [L_c + (W_c - W_I)/2]}{L(\frac{W - D}{2})(1 + \delta_E)} \qquad \text{(I.19)}$$

where L_c is the collector external length. Equation I.16 remains valid for the calculation of U_{EI}.

APPENDIX II. CONSTANTS AND LIMITING CASES FOR THE AVERAGING METHOD

For the averaging method, the plate and fluid temperature distributions are given [2] by

$$\bar{P}_p(\beta) = 1 - \frac{a_1 e^{r_1\beta} + a_2 e^{r_2\beta} + a_3 e^{r_3\beta}}{d(b_1 + b_2 + b_3)} \tag{II.1}$$

and

$$P_f(\beta) = 1 - \frac{b_1 e^{r_1\beta} + b_2 e^{r_2\beta} + b_3 e^{r_3\beta}}{b_1 + b_2 + b_3} \tag{II.2}$$

where

$$P_s = \frac{T_s - T_{fi}}{S + T_a - T_{fi}}$$

The constants used in Eqs. II.1 and II.2 are defined as follows:

$$a_1 = r_2 r_3 (e^{r_2} - e^{r_3}) \quad , \quad b_1 = a_1/(r_1 + d)$$

$$a_2 = r_3 r_1 (e^{r_3} - e^{r_1}) \quad , \quad b_2 = a_2/(r_2 + d)$$

$$a_3 = r_1 r_2 (e^{r_1} - e^{r_2}) \quad , \quad b_3 = a_3/(r_3 + d)$$

$$r_1 = 2\alpha^{1/2} \cos(\psi/3) - d/3$$

$$r_2 = -2\alpha^{1/2} \cos[(\psi + \pi)/3] - d/3$$

$$r_3 = -2\alpha^{1/2} \cos[(\psi - \pi)/3] - d/3$$

$$\psi = \cos^{-1}(\mu/\alpha^{3/2})$$

$$\alpha = [1/M(1 - F') + d^2/3]/3$$

$$\mu = d[(2 - 3F')/M(1 - F') - 2\,d^2/9]/6$$

$$d = F'B/(1 - F')$$

The limiting solution for F_R when $F' = 1$ is given by

$$F_R = 1 - \frac{(1 + M_1/M_2)e^{-M_1}}{1 + M_1MB + (M_1/M_2 - M_1MB)e^{-(M_1 + M_2)}} \Big/ B \qquad \text{(II.3)}$$

where

$$M_{1,2} = \frac{(4MB^2 + 1)^{\frac{1}{2}} \mp 1}{2MB}$$

and the minus sign applies to M_1. Phillips [2] notes that Eq. II.3 is adequate for $F' > .95$.

APPENDIX III. COMPUTER PROGRAM FOR THE EXACT METHOD

The form of the exact solution as presented in Chapter III (Eq. 3.46) presents some difficulty for large values of M_T or a. When the terms $n\pi a$ in Eqs. 3.44 and 3.45 become $\gtrsim 170$, the cosh γ_n and sinh γ_n terms exceed the computer exponent overflow limit. The problem can be avoided by solving for $C_n \cosh \gamma_n$ rather than C_n. Equations 3.44 and 3.45 are replaced by

$$\sum_{n=2,4,..}^{\infty} C_n^* D_n^* - \frac{F_c}{E_c} \sum_{n=1,3,..}^{\infty} C_n^* D_n^* + C_o^* A_c^* / E_c = 1 \qquad \text{(III.1)}$$

and

$$\sum_{n=i,i+2,..}^{\infty} C_n^* D_n^* (1 - 2E_{mn}/B_m) + \sum_{\substack{n=j,j+2,.. \\ n \neq m}}^{\infty} C_n^* D_n^* + C_m^* A_m^* / B_m + C_o^* = 1 \qquad \text{(III.2)}$$

where

$$C_n^* = C_n \cosh \gamma_n$$

$$A_c^* = BF_d + E_c$$

$$A_m^* = \frac{f\gamma_m}{2g} + \frac{f}{2g}(h + g + r_m) - D_m^*(f - 2B_m)/2$$

$$D_n^* = \frac{1}{1 + (\lambda_n^*/f)}$$

The FORTRAN program which follows is based on Eqs. III.1 and III.2. The Scientific Subroutine Package (SSP) subroutines ARRAY and SIMQ are used in conjunction with the subroutine TWODAX (Two-Dimensional Axial).

The total computational time required for an $M_T = 30$ case is 4 seconds on an IBM 370 computer.

```
      SUBROUTINE TWODAX (MT,LDIST,TFM,TPM,TFO,FR,FE,FP,MV,B)                A    1
C                                                                           A    2
C                                                                           A    3
C     SUBROUTINE TWODAX CALCULATES THE MEAN PLATE AND FLUID TEMPS,          A    4
C                       THE OUTLET FLUID TEMP, THE HEAT REMOVAL             A    5
C                       FACTOR FR, AND THE TEMP DISTR IN A                  A    6
C                       PARALLEL-FLOW FLAT-PLATE SOLAR COLLECTOR.           A    7
C                                                                           A    8
C                                                                           A    9
C     OPTIONS -- MT,LDIST                                                   A   10
C                                                                           A   11
C               MT =      NO. OF EXPANSION COEFFICIENTS TO BE               A   12
C                         CALCULATED (1-99)                                 A   13
C                                                                           A   14
C               LDIST = 0   OMIT TEMP DISTR CALCULATION                     A   15
C               LDIST = 1   CALCULATE TEMP DISTR                            A   16
C                                                                           A   17
C                                                                           A   18
C     SSP SUBROUTINES USED -- SIMQ, ARRAY                                   A   19
C                                                                           A   20
C                                                                           A   21
C     FUNCTION SUBROUTINES USED -- XXP                                      A   22
C                                                                           A   23
C                                                                           A   24
C     COMMON BLOCK INPUT --                                                 A   25
C                                                                           A   26
C                          A1 = A    (NON-DIM)                            A   27
C                          A2 = C    (NON-DIM)                            A   28
C                          A3 = F    (NON-DIM)                            A   29
C                          A4 = DRP  (NON-DIM)                            A   30
C                          A5 = UR   (NON-DIM)                            A   31
C                          A6 = TA   (DEG C)                              A   32
```

```
C                              A7 = TFI (DEG C)                                  A  33
C                              A8 = S   (W/SQ M)                                 A  34
C                              A9 = UL  (W/SQ M-C)                               A  35
C                                                                                A  36
C                                                                                A  37
      COMMON A1,A2,A3,A4,A5,A6,A7,A8,A9                                          A  38
      REAL T(99,99),AM(99),BM(99),CM(99),DM(99),EMN(99,99),TPD(5,13),TF(         A  39
     113),INP(9801),LMDST,MV                                                     A  40
      A=A1                                                                       A  41
      C=A2                                                                       A  42
      F=A3                                                                       A  43
      DRP=A4                                                                     A  44
      UR=A5                                                                      A  45
      TA=A6                                                                      A  46
      TFI=A7                                                                     A  47
      S=A8                                                                       A  48
      UL=A9                                                                      A  49
      N=MT-1                                                                     A  50
      NN=MT                                                                      A  51
      NDS=9801                                                                   A  52
C     ------------------------------------------                                 A  53
C     CALCULATE CONSTANTS AND BASIC COEFFICIENTS                                 A  54
C     ------------------------------------------                                 A  55
      FE=TANH(C)/C                                                               A  56
      FD=(FE+DRP)/(1+DRP)                                                        A  57
      FUD=(1+DRP)/UR/DRP                                                         A  58
      MV=(A/C)**2                                                                A  59
      B=F*FUD                                                                    A  60
      FP=1/(1/FD+FUD)                                                            A  61
      PI=4.*ATAN(1.)                                                             A  62
      H=DRP*C**2                                                                 A  63
      G=H*UR                                                                     A  64
```

```
      GH=(G+H)/G                                                        A  65
      EF=XXP(-F)                                                        A  66
      EC=1.-EF                                                          A  67
      FC=1.+EF                                                          A  68
      AC=B*FO+EC                                                        A  69
      IF (N.EQ.0) GO TO 17                                              A  70
      DO 3 M=1,N                                                        A  71
      LMDST=PI*M                                                        A  72
      C2=1.+(LMDST/F)**2                                                A  73
      GM=SQRT(C**2+(LMDST*A)**2)                                        A  74
      C3=1.-(-1.)**M*EF                                                 A  75
      C4=(G+H+A**2*DRP*LMDST**2)*F/G                                    A  76
      BM(M)=C3/C2                                                       A  77
      IF (GM.LT.160.) GO TO 1                                           A  78
      TANH1=1.0                                                         A  79
      GO TO 2                                                           A  80
1     CONTINUE                                                          A  81
      TANH1=TANH(GM)                                                    A  82
2     CONTINUE                                                          A  83
      AM(M)=(F*GM*TANH1/G+C4-(F-2.0*BM(M))/C2)/2.                       A  84
      DM(M)=1.0/C2                                                      A  85
3     CONTINUE                                                          A  86
      DO 4 I=1,N,2                                                      A  87
      DO 4 J=2,N,2                                                      A  88
      P=I                                                               A  89
      Q=J                                                               A  90
4     EMN(I,J)=1./(1.-(P/Q)**2)                                         A  91
      DO 5 I=2,N,2                                                      A  92
      DO 5 J=1,N,2                                                      A  93
      P=I                                                               A  94
      Q=J                                                               A  95
5     EMN(I,J)=1./(1.-(P/Q)**2)                                         A  96
```

```
C     ------------------------------------                              A  97
C     CALCULATE VALUES FOR THE COEFFICIENT                              A  98
C     MATRIX -- COLUMNS 2 - MT, ROWS 2 - MT                             A  99
C     ------------------------------------                              A 100
      I=0                                                               A 101
      KK=1                                                              A 102
6     CONTINUE                                                          A 103
      I=I+1                                                             A 104
      DO 7 J=1,N,2                                                      A 105
      IF (J+KK.GT.N) GO TO 7                                            A 106
      T(I,J+KK)=DM(J+KK)*(1.-2.*EMN(I,J+KK)/BM(I))                      A 107
7     CONTINUE                                                          A 108
      T(I,I)=AM(I)/BM(I)                                                A 109
      IF (I.GE.N) GO TO 9                                               A 110
      IF (KK.EQ.0) GO TO 8                                              A 111
      KK=0                                                              A 112
      GO TO 6                                                           A 113
8     CONTINUE                                                          A 114
      KK=1                                                              A 115
      GO TO 6                                                           A 116
9     CONTINUE                                                          A 117
      I=0                                                               A 118
      K=0                                                               A 119
10    CONTINUE                                                          A 120
      I=I+1                                                             A 121
      IF (I.GT.N) GO TO 14                                              A 122
      IF (K.EQ.0) GO TO 12                                              A 123
      DO 11 J=2,N,2                                                     A 124
      IF (J.EQ.I) GO TO 11                                              A 125
      T(I,J)=DM(J)                                                      A 126
11    CONTINUE                                                          A 127
      K=0                                                               A 128
```

```
      GO TO 10                                                          A 129
12    CONTINUE                                                          A 130
      DO 13 J=1,N,2                                                     A 131
      IF (J.EQ.I) GO TO 13                                              A 132
      T(I,J)=DM(J)                                                      A 133
13    CONTINUE                                                          A 134
      K=1                                                               A 135
      GO TO 10                                                          A 136
14    CONTINUE                                                          A 137
C     ------------------------------------                              A 138
C     MOVE MATRIX ELEMENTS OVER & DOWN ONE                              A 139
C     TO MAKE ROOM FOR 1ST ROW AND COLUMN                               A 140
C     ------------------------------------                              A 141
      DO 15 I=1,N                                                       A 142
      DO 15 J=1,N                                                       A 143
15    EMN(I+1,J+1)=T(I,J)                                               A 144
      DO 16 I=2,NN                                                      A 145
      DO 16 J=2,NN                                                      A 146
16    T(I,J)=EMN(I,J)                                                   A 147
C     ------------------------------------------------                  A 148
C     CALCULATE 1ST ROW AND COLUMN OF COEFFICIENT MATRIX                A 149
C     ------------------------------------------------                  A 150
17    CONTINUE                                                          A 151
      T(1,1)=AC/EC                                                      A 152
      IF (NN.LE.1) GO TO 22                                             A 153
      DO 18 J=2,NN,2                                                    A 154
18    T(1,J)=-FC*DM(J-1)/EC                                             A 155
      IF (NN.LE.2) GO TO 20                                             A 156
      DO 19 J=3,NN,2                                                    A 157
19    T(1,J)=DM(J-1)                                                    A 158
20    CONTINUE                                                          A 159
      DO 21 I=2,NN                                                      A 160
```

```
21    T(I,1)=1.0                                                    A 161
22    CONTINUE                                                      A 162
C     ------------------------------                                A 163
C     CALCULATE EXPANSION COEFFICIENTS                              A 164
C     ------------------------------                                A 165
      DO 23 I=1,NN                                                  A 166
23    CM(I)=1.0                                                     A 167
      IF (N.GE.1) GO TO 24                                          A 168
      CM(1)=CM(1)/T(1,1)                                            A 169
      GO TO 25                                                      A 170
24    CONTINUE                                                      A 171
      CALL ARRAY (2,NN,NN,NDS,99,99,INP,T)                          A 172
      CALL SIMQ (NDS,INP,CM,NN,KS)                                  A 173
      PRINT , KS                                                    A 174
25    CONTINUE                                                      A 175
C     ----------------------------                                  A 176
C     CALCULATE FR, TPM, TFM, AND TFO                               A 177
C     ----------------------------                                  A 178
      FR=FD*CM(1)                                                   A 179
      PSIFM=FR/FP                                                   A 180
      PSIPM=FR                                                      A 181
      PSIFO=1.-B*FP                                                 A 182
      THTAFI=TFI-TA-S/UL                                            A 183
      TFO=PSIFO*THTAFI+TA+S/UL                                      A 184
      TFM=PSIFM*THTAFI+TA+S/UL                                      A 185
      TPM=PSIPM*THTAFI+TA+S/UL                                      A 186
C     ------------------------------                                A 187
C     CALCULATE PLATE TEMP DISTRIBUTION                             A 188
C     ------------------------------                                A 189
      IF (LDIST.EQ.0) GO TO 37                                      A 190
      DO 29 J=1,13                                                  A 191
      XJ=J-1                                                        A 192
```

```
      BETA=1.0*XJ/12.0                                                    A 193
      DO 28 K=1,5                                                         A 194
      ETA=1.0*(K-1)/4.0                                                   A 195
      SUM=0.0                                                             A 196
      DO 27 I=1,NN                                                        A 197
      M=I-1                                                               A 198
      GM=SQRT(C**2+(PI*M*A)**2)                                           A 199
      IF (ETA.GT.0.99) GO TO 26                                           A 200
      IF (GM.GT.160) GO TO 27                                             A 201
      SUM=SUM+CM(I)*COSH(GM*ETA)/COSH(GM)*COS(PI*M*BETA)                  A 202
      GO TO 27                                                            A 203
26    CONTINUE                                                            A 204
      SUM=SUM+CM(I)*COS(PI*M*BETA)                                        A 205
27    CONTINUE                                                            A 206
      TPD(K,J)=SUM                                                        A 207
28    CONTINUE                                                            A 208
29    CONTINUE                                                            A 209
C     ------------------                                                  A 210
C     CALCULATE FLUID DIST                                                A 211
C     ------------------                                                  A 212
      DO 32 J=1,13                                                        A 213
      XJ=J-1                                                              A 214
      BETA=1.0*XJ/12.0                                                    A 215
      EFB=XXP(-F*BETA)                                                    A 216
      SUM=0.0                                                             A 217
      IF (NN.EQ.1) GO TO 31                                               A 218
      DO 30 I=2,NN                                                        A 219
      M=I-1                                                               A 220
      X=PI*M                                                              A 221
      GM=SQRT(C**2+(X*A)**2)                                              A 222
30    SUM=SUM+CM(I)*(COS(X*BETA)+X/F*SIN(X*BETA)-EFB)/(1.0+(X/F)**2)      A 223
31    CONTINUE                                                            A 224
```

```
      TF(J)=SUM+EFB+(1.0-EFB)*CM(1)                                    A 225
32    CONTINUE                                                         A 226
C     ---------------------                                            A 227
C     CONVERT FROM PSI TO T                                            A 228
C     ---------------------                                            A 229
      DO 33 J=1,13                                                     A 230
      TF(J)=TF(J)*THTAFI+TA+S/UL                                       A 231
33    CONTINUE                                                         A 232
      DO 34 J=1,13                                                     A 233
      DO 34 K=1,5                                                      A 234
      TPD(K,J)=TPD(K,J)*THTAFI+TA+S/UL                                 A 235
34    CONTINUE                                                         A 236
      WRITE (1,38)                                                     A 237
      DO 35 J=1,13                                                     A 238
      WRITE (1,41) J                                                   A 239
      WRITE (1,42) (TPD(K,J),K=1,5)                                    A 240
35    CONTINUE                                                         A 241
      WRITE (1,40)                                                     A 242
      DO 36 J=1,13                                                     A 243
      WRITE (1,39) J,TF(J)                                             A 244
36    CONTINUE                                                         A 245
37    CONTINUE                                                         A 246
      RETURN                                                           A 247
C                                                                      A 248
38    FORMAT (/,40X,23HPLATE TEMP DISTRIBUTION,/)                      A 249
39    FORMAT (/,2X,12HY LOCATION  ,I2,2X,E16.6,/)                      A 250
40    FORMAT (/////,6X,23HFLUID TEMP DISTRIBUTION,/)                   A 251
41    FORMAT (//,12H Y LOCATION ,I2)                                   A 252
42    FORMAT (/,5E18.6)                                                A 253
      END                                                              A 254
      REAL FUNCTION XXP*4(ZZ)                                          B   1
      IF (ZZ.GE.-150.0) GO TO 1                                        B   2
```

```
      XXP=0.0                                                    B    3
      GO TO 2                                                    B    4
1     CONTINUE                                                   B    5
      XXP=EXP(ZZ)                                                B    6
2     CONTINUE                                                   B    7
      RETURN                                                     B    8
      END                                                        B    9
```

APPENDIX IV. COMPUTER PROGRAM FOR THE LEL MODEL

The FORTRAN program which follows is for the parallel-flow case. The program can be modified for the serpentine configuration from the information given in Chapter IV. Total computational time for the PPG collector (N_T = 13) with the mid-tube symmetry option is approximately 4.5 seconds. The full-plate option requires 8.5 seconds of computational time on an IBM 370 system.

```
      SUBROUTINE LEL (NT,NNT,LDIST,TFO,TFM,TBM,TPMA,TPME,TPMI)                A    1
C                                                                             A    2
C                                                                             A    3
C     SUBROUTINE LEL CALCULATES THE TRANSVERSE PLATE TEMP DISTR,              A    4
C                    FLUID MEAN OUTLET TEMP, MEAN FLUID TEMP,                 A    5
C                    MEAN BASE TEMP, AND MEAN PLATE TEMP (DEG C)              A    6
C                    FOR A FLAT PLATE SOLAR COLLECTOR WITH                    A    7
C                    LOCALIZED EDGE LOSSES.                                   A    8
C                                                                             A    9
C     OPTIONS: NT,NNT,LDIST                                                   A   10
C                                                                             A   11
C              NT=  ----- NO OF TUBES IN COLLECTOR (1 TO 15)                  A   12
C                                                                             A   13
C              NNT= ----- OPTION FOR TYPE OF CALCULATION                      A   14
C                                                                             A   15
C              NNT=1 ---- N=NT (FULL PLATE)                                   A   16
C              NNT=2 ---- N=NT/2 (HALF-PLATE WITH NT EVEN)                    A   17
C              NNT=3 ---- N=(NT+1)/2 (HALF-PLATE WITH NT ODD)                 A   18
C                                                                             A   19
C              LDIST ---- OPTION FOR CALC TRANSVERSE PLATE DISTR              A   20
C                                                                             A   21
C              LDIST=0 -- OMIT TRANSVERSE CALC                                A   22
C              LDIST=1 -- CALC TRANSVERSE PL. DISTR.                          A   23
C                                                                             A   24
C     SSP SUBROUTINES USED: GMPRD,MINV,ATEIG,HSBG,ARRAY,EIGEN                 A   25
C                                                                             A   26
C     OTHER SUBROUTINES:  AVE                                                 A   27
C                                                                             A   28
C     FUNCTION SUBPROGRAMS USED: KD                                           A   29
C                                                                             A   30
C                                                                             A   31
C     COMMON BLOCK INPUT:                                                     A   32
```

```
C                                                                       A  33
C                                                                       A  34
C     A1=Y=PL LENGTH-M                  A10=CP=SP HEAT-KJ/KG-C          A  35
C     A2=D=TUBE OD-M                    A11=W=TUBE SPAC-M               A  36
C     A3=DI=TUBE ID-M                   A12=TI=INL TEMP-C               A  37
C     A4=DLT=PL THK-M                   A13=TA=AMB TEMP-C               A  38
C     A5=XKP=COND PL-W/M-C              A14=HT=INSULATION-W/SQ-M        A  39
C     A6=UL=INT LOSS COEF-W/M-C         A15=TAE=TRANS-ABS PROD          A  40
C     A7=CB=BOND COND-W/M-C             A16=SE1=EDGE SHP FACTOR         A  41
C     A8=HFI=HT TR COEF-W/SQ-M-C        A17=ULE=LOSS COEF FOR EDGE ABS PL A  42
C     A9=XMDOT=MASS FL RT-KG/SEC        A18=XKI=EDGE INSL COND-W/M-C    A  43
C     A19=DLTE=NON-DIM EDGE WIDTH                                       A  44
C                                                                       A  45
C                                                                       A  46
      IMPLICIT REAL*8 (B-H,K,M,O-Z)                                     A  47
      COMMON A1,A2,A3,A4,A5,A6,A7,A8,A9,A10,A11,A12,A13,A14,A15,A16,A17,  A  48
     1A18,A19                                                           A  49
      REAL*8 AE,ALPHA,ADJ,NP,NE,LL,IANA,INF,INH1,INHF,NORM,NGSH         A  50
      DIMENSION DEL(15,15), GM(15,15), KGM(15,15), DELS(15,15), TPD(15,1  A  51
     15), LL(225), EIVAL(225), EIVEC(15,15), MAT1(15,15), TEIVEC(15,15),  A  52
     2 CEIVAL(15,15), INH(225), INH1(225), MM(225), CDTFD(225), INHF(225  A  53
     3), PHI(225), PSI(225), F1(225), D1(225), GD(15,15), GF(225), EXPO(  A  54
     4225), M1(225), M2(225), M3(225), M4(225), MAT(15,15), RI(225), IAN  A  55
     5A(225), ADJ(225), BM(225), NORM(225), SMAT(225), TP(225), TL(15)   A  56
      DIMENSION TR(15), FACF(15), FACG(15), DIV(15)                     A  57
      REAL*4 SNGL,TFO,TFM,TBM,TPMA,TPMI,TPME                            A  58
      ND=15                                                             A  59
      NDS=ND*ND                                                         A  60
C     **********                                                        A  61
C     SET MATRIX DIMENSION N                                            A  62
C     **********                                                        A  63
      IF (NNT.EQ.1) GO TO 1                                             A  64
```

```
      IF (NNT.EQ.2) GO TO 2                                          A  65
      IF (NNT.EQ.3) GO TO 3                                          A  66
1     N=NT                                                           A  67
      LOP1=0                                                         A  68
      LOP2=1                                                         A  69
      GO TO 4                                                        A  70
2     N=NT/2                                                         A  71
      LOP1=0                                                         A  72
      LOP2=0                                                         A  73
      GO TO 4                                                        A  74
3     N=(NT+1)/2                                                     A  75
      LOP1=1                                                         A  76
      LOP2=0                                                         A  77
4     CONTINUE                                                       A  78
      NST=N*N                                                        A  79
      IX=N-1                                                         A  80
C     **********                                                     A  81
C     BASIC COLLECTOR PARAMETERS                                     A  82
C     **********                                                     A  83
      Y=DBLE(A1)                                                     A  84
      D=DBLE(A2)                                                     A  85
      DI=DBLE(A3)                                                    A  86
      DLT=DBLE(A4)                                                   A  87
      XKP=DBLE(A5)                                                   A  88
      UL=DBLE(A6)                                                    A  89
      CB=DBLE(A7)                                                    A  90
      HFI=DBLE(A8)                                                   A  91
      XMDOT=DBLE(A9)                                                 A  92
      CP=DBLE(A10)                                                   A  93
      W=DBLE(A11)                                                    A  94
      TI=DBLE(A12)                                                   A  95
      TA=DBLE(A13)                                                   A  96
```

```
      HT=DBLE(A14)                                                          A  97
      TAE=DBLE(A15)                                                         A  98
      SS=HT*TAE                                                             A  99
      SE1=DBLE(A16)                                                         A 100
      ULE=DBLE(A17)                                                         A 101
      XKI=DBLE(A18)                                                         A 102
      DLTE=DBLE(A19)                                                        A 103
      WT=W*NT+(W-D)*DLTE                                                    A 104
C     **********                                                            A 105
C     CALCULATE LUMPED PARAMETERS                                           A 106
C     **********                                                            A 107
      R=1.0D+00/CB+1.0D+00/4.0D+00/DATAN(1.0D+00)/DI/HFI                     A 108
      NP=DSQRT(UL*(W-D)**2/XKP/DLT)                                         A 109
      K=XKP*DLT*NP/(W-D)/DSINH(NP)                                          A 110
      GAM=-2.0D+00*DCOSH(NP)-D*UL/K                                         A 111
      AE=XKI*SE1*((W-D)/2.0D+0)*(1.0D+0+DLTE)/XKP/DLT                       A 112
      NE=NP*(1.0D+0+DLTE)*DSQRT(ULE/UL)/2.0D+0                              A 113
      OM=AE/(AE*DSINH(NE)/NE+DCOSH(NE))                                     A 114
      OMV=(AE*DCOSH(NE)+NE*DSINH(NE))/(AE*DSINH(NE)/NE+DCOSH(NE))           A 115
      CAPL=OMV*DTANH(NP)*2.0D+0/NP/(1.0D+0+DLTE)                            A 116
      NGSH=-SS*DCOSH(NP)*(OM*DTANH(NP)*2.0D+0/NP/ULE/(1.0D+0+DLTE)+CAPL*    A 117
     1(1.0D+0/UL-1.0D+0/ULE))                                               A 118
      LOP3=1-LOP1-LOP2                                                      A 119
C                                                                           A 120
C                                                                           A 121
C     ---------- PROCEDURE ----------                                       A 122
C                                                                           A 123
C                                                                           A 124
C                        SET UP AND SOLVE                                   A 125
C                                                                           A 126
C      THE SET OF FIRST ORDER INHOMOG. LINEAR DIFF. EQS. IN PHI             A 127
C                                                                           A 128
```

```
C                              OF THE FORM                                      A 129
C                                                                               A 130
C     D(PHI)/DB - EPS*(INV(DEL+KGM))*GM*PHI = EPS/PHI*(INV(DEL+KGM))*INH        A 131
C                                                                               A 132
C                          ---------------                                      A 133
C                                                                               A 134
C     FIRST SOLVE THE HOMOGENOUS SYSTEM, I.E. THE EIGENVALUE PROBLEM:           A 135
C                                                                               A 136
C                 |EIVAL*DEL - EPS*(INVERSE(DEL+KGM))*GM|=0                    A 137
C                                                                               A 138
C                       WHICH IS OF THE USUAL FORM                              A 139
C                                                                               A 140
C                 |LAMBDA*IDENTITY MATRIX - COEFFICIENT MATRIX|=0              A 141
C                                                                               A 142
C                          ---------------                                      A 143
C                                                                               A 144
C     THEN SEPARATE THE EQUATIONS BY THE SUBSTITUTION: PHI = C * PSI            A 145
C                                                                               A 146
C          (WHERE C IS THE NXN MATRIX OF EIGENVECTORS)                          A 147
C                                                                               A 148
C             AND SOLVE FOR THE INHOMOGENOUS TERMS.                             A 149
C                                                                               A 150
C                          ---------------                                      A 151
C                                                                               A 152
C                                                                               A 153
C     **********************                                                    A 154
C     SET UP DEL MATRIX                                                         A 155
C     **********************                                                    A 156
      DO 5 I=1,N                                                                A 157
      DO 5 J=1,N                                                                A 158
      DEL(I,J)=0.0D+00                                                          A 159
      IF (I.NE.J) GO TO 5                                                       A 160
```

```
      DEL(I,J)=1.0D+00                                                    A 161
5     CONTINUE                                                            A 162
C     ********************                                                A 163
C     SET UP GM AND KGM MATRICES                                          A 164
C     ********************                                                A 165
      DO 6 I=1,N                                                          A 166
      DO 6 J=1,N                                                          A 167
      GM(I,J)=(GAM-(CAPL-1.0D+0)*(KD(I,1)+KD(I,N)*LOP2)*DCOSH(NP)+KD(I,N  A 168
     1)*LOP3)*KD(I,J)+KD(I,J-1)+KD(I,J+1)*(1.0D+0+KD(I,N)*LOP1)           A 169
      KGM(I,J)=-GM(I,J)*K*R                                               A 170
6     CONTINUE                                                            A 171
C     ********************                                                A 172
C     CALCULATE INVERSE OF (DEL+KGM)                                      A 173
C     ********************                                                A 174
      DO 7 I=1,N                                                          A 175
      DO 7 J=1,N                                                          A 176
7     DELS(I,J)=DEL(I,J)+KGM(I,J)                                         A 177
      CALL ARRAY (2,N,N,NDS,ND,ND,M1,DELS)                                A 178
      CALL MINV (M1,N,E,LL,MM,NST)                                        A 179
C     ********************                                                A 180
C     CALCULATE EPS*INVERSE(DEL+KGM)                                      A 181
C     ********************                                                A 182
      DO 8 I=1,NST                                                        A 183
8     M1(I)=K*Y/XMDOT/CP/1.0D+03*M1(I)                                    A 184
      CALL ARRAY (1,N,N,NDS,ND,ND,M1,DEL)                                 A 185
C     ********************                                                A 186
C     CALCULATE EPS*(INVERSE(DEL+KGM))*GM                                 A 187
C     ********************                                                A 188
      CALL ARRAY (2,N,N,NDS,ND,ND,M2,GM)                                  A 189
      CALL GMPRD (NST,M1,M2,M3,N,N,N)                                     A 190
      CALL ARRAY (1,N,N,NDS,ND,ND,M3,GM)                                  A 191
C     ********************                                                A 192
```

```
C       SAVE COEFFICIENT MATRIX                                          A 193
C       ***********************                                          A 194
        DO 9 I=1,N                                                       A 195
        DO 9 J=1,N                                                       A 196
        MAT(I,J)=GM(I,J)                                                 A 197
9       CONTINUE                                                         A 198
C       ***********************                                          A 199
C       CHECK SYMMETRY OF COEF MATRIX                                    A 200
C       (IF SYMM USE EIGEN)                                              A 201
C       (IF NON-SYMM USE HSBG AND ATEIG)                                 A 202
C       ***********************                                          A 203
        DO 10 I=1,N                                                      A 204
        DO 10 J=1,N                                                      A 205
        IF (I.EQ.J) GO TO 10                                             A 206
        DIFF=DABS((MAT(I,J)-MAT(J,I))/MAT(I,J))                          A 207
        IF (DIFF.LT.1.0D-06) GO TO 10                                    A 208
        WRITE (1,67)                                                     A 209
        GO TO 20                                                         A 210
10      CONTINUE                                                         A 211
C       ***********************                                          A 212
C       CALCULATE EIGENVALUES AND EIGENVECTORS FOR SYMMETRIC MATRIX      A 213
C       ***********************                                          A 214
        NM=N*(N+1)/2                                                     A 215
        JJ=1                                                             A 216
        DO 11 J=1,N                                                      A 217
        DO 11 I=1,N                                                      A 218
        IF (I.GT.J) GO TO 11                                             A 219
        SMAT(JJ)=MAT(I,J)                                                A 220
        JJ=JJ+1                                                          A 221
11      CONTINUE                                                         A 222
        CALL EIGEN (SMAT,M4,N,0,NM,NST)                                  A 223
        JJ=1                                                             A 224
```

```
      DO 13 J=1,N                                                       A 225
      DO 13 I=1,N                                                       A 226
      IF (I.GT.J) GO TO 12                                              A 227
      MAT(I,J)=SMAT(JJ)                                                 A 228
      JJ=JJ+1                                                           A 229
      GO TO 13                                                          A 230
12    CONTINUE                                                          A 231
      MAT(I,J)=0.0D+0                                                   A 232
13    CONTINUE                                                          A 233
      WRITE (1,68)                                                      A 234
      DO 14 I=1,N                                                       A 235
14    EIVAL(I)=MAT(I,I)                                                 A 236
      CALL ARRAY (1,N,N,NDS,ND,ND,M4,EIVEC)                             A 237
C     ********************                                            A 238
C     NORMALIZE THE EIGENVECTORS                                        A 239
C     ********************                                            A 240
      DO 15 J=1,N                                                       A 241
15    NORM(J)=0.0D+00                                                   A 242
      DO 17 J=1,N                                                       A 243
      DO 16 I=1,N                                                       A 244
16    NORM(J)=NORM(J)+EIVEC(I,J)**2                                     A 245
      NORM(J)=DSQRT(NORM(J))                                            A 246
17    CONTINUE                                                          A 247
      DO 18 I=1,N                                                       A 248
      DO 18 J=1,N                                                       A 249
18    EIVEC(I,J)=EIVEC(I,J)/NORM(J)                                     A 250
C     ********************                                            A 251
C     TAKE THE TRANSPOSE OF EIVEC                                       A 252
C     ********************                                            A 253
      DO 19 I=1,N                                                       A 254
      DO 19 J=1,N                                                       A 255
19    TEIVEC(I,J)=EIVEC(J,I)                                            A 256
```

```
      CALL ARRAY (2,N,N,NDS,ND,ND,M1,TEIVEC)                            A 257
      GO TO 30                                                          A 258
C     ********************                                              A 259
C     CALCULATE EIGENVALUES AND EIGENVECTORS FOR NON-SYMMETRIC MATRIX   A 260
C     ********************                                              A 261
20    CONTINUE                                                          A 262
      CALL ARRAY (2,N,N,NDS,ND,ND,M2,MAT)                               A 263
      CALL HSBG (N,M2,N,NST)                                            A 264
      CALL ATEIG (N,M2,EIVAL,BI,IANA,N,NST)                             A 265
C                                                                       A 266
C                                                                       A 267
C     CALCULATE EIGENVECTORS BY NORMALIZING THE N'TH COMPONENT OF THE   A 268
C     I'TH EIGENVECTOR TO 1.0 AND SOLVING THE REDUCED (N-1)*(N-1) SYSTEM A 269
C     (A-LAMBDA*I)*X=B FOR THE REMAINING COMPONENTS.                    A 270
C                                                                       A 271
C                                                                       A 272
      NSM=(N-1)*(N-1)                                                   A 273
      IM=1                                                              A 274
      DO 21 I=1,IX                                                      A 275
      BM(I)=-GM(I,N)                                                    A 276
21    CONTINUE                                                          A 277
      DO 22 I=1,IX                                                      A 278
      DO 22 J=1,IX                                                      A 279
22    MAT(I,J)=GM(I,J)                                                  A 280
23    CONTINUE                                                          A 281
      DO 24 I=1,IX                                                      A 282
      DO 24 J=1,IX                                                      A 283
      DELS(I,J)=0.00+00                                                 A 284
      IF (I.NE.J) GO TO 24                                              A 285
      DELS(I,J)=-EIVAL(IM)                                              A 286
24    CONTINUE                                                          A 287
      DO 25 I=1,IX                                                      A 288
```

```
      DO 25 J=1,IX                                                    A 289
25    MAT1(I,J)=DELS(I,J)+MAT(I,J)                                    A 290
      CALL ARRAY (2,IX,IX,NDS,ND,ND,M1,MAT1)                          A 291
      CALL MINV (M1,IX,E,LL,MM,NSM)                                   A 292
      CALL GMPRD (NSM,M1,BM,ADJ,IX,IX,1)                              A 293
C     ********************                                            A 294
C     CHECK FOR POSSIBILITY OF ZERO M'TH COMPONENT                    A 295
C     ********************                                            A 296
      DO 26 J=1,IX                                                    A 297
26    M2(J)=GM(N,J)                                                   A 298
      CALL GMPRD (NSM,M2,ADJ,LL,1,IX,1)                               A 299
      DIFF=DABS((LL(1)+GM(N,N)-EIVAL(IM))/LL(1))                      A 300
      IF (DIFF.LT.1.0D-06) GO TO 27                                   A 301
      WRITE (1,69)                                                    A 302
      GO TO 66                                                        A 303
27    CONTINUE                                                        A 304
      ADJ(N)=1.0D+00                                                  A 305
      DO 28 I=1,N                                                     A 306
28    EIVEC(I,IM)=ADJ(I)/ADJ(1)                                       A 307
      IF (IM.EQ.N) GO TO 29                                           A 308
      IM=IM+1                                                         A 309
      GO TO 23                                                        A 310
29    CONTINUE                                                        A 311
      CALL ARRAY (2,N,N,NDS,ND,ND,M1,EIVEC)                           A 312
      CALL MINV (M1,N,E,LL,MM,NST)                                    A 313
      CALL ARRAY (2,N,N,NDS,ND,ND,M4,EIVEC)                           A 314
30    CONTINUE                                                        A 315
C                                                                     A 316
C                                                                     A 317
C     USE EIGENVECTOR MATRIX TO SOLVE INHOMOGENOUS SYSTEM             A 318
C                                                                     A 319
C                                                                     A 320
```

```
C     ********************                                          A 321
C     CHECK EIGENVALUES AND EIGENVECTORS                           A 322
C     ********************                                          A 323
      CALL GMPRD (NST,M3,M4,M2,N,N,N)                              A 324
      CALL GMPRD (NST,M1,M2,M3,N,N,N)                              A 325
      CALL ARRAY (1,N,N,NDS,ND,ND,M3,CEIVAL)                       A 326
      DO 31 I=1,N                                                  A 327
      DIFF=DABS((EIVAL(I)-CEIVAL(I,I))/EIVAL(I))                   A 328
      IF (DIFF.LT.1.0D-06) GO TO 31                                A 329
      WRITE (1,70)                                                 A 330
      GO TO 66                                                     A 331
31    CONTINUE                                                     A 332
C     ********************                                          A 333
C     CALCULATE EPS*(INVERSE(DEL+KGM))/PHI(0)                      A 334
C     ********************                                          A 335
      DTHI=T1-TA-SS/UL                                             A 336
      DO 32 I=1,N                                                  A 337
      DO 32 J=1,N                                                  A 338
32    DEL(I,J)=DEL(I,J)/DTHI                                       A 339
      CALL ARRAY (2,N,N,NDS,ND,ND,M2,DEL)                          A 340
C     ********************                                          A 341
C     SET UP INHOMOGENOUS MATRIX INHF                              A 342
C     ********************                                          A 343
      DO 33 I=1,N                                                  A 344
33    INH(I)=0.0D+0                                                A 345
      INH(1)=NGSH                                                  A 346
      INH(N)=NGSH*LOP2                                             A 347
      CALL GMPRD (NST,M2,INH,INH1,N,N,1)                           A 348
      CALL GMPRD (NST,M1,INH1,INHF,N,N,1)                          A 349
C     ********************                                          A 350
C     SET UP PSI(0)= TEIVEC * PHI(0)                               A 351
C     ********************                                          A 352
```

```
      DO 34 I=1,N                                                        A 353
34    PHI(I)=1.0D+0                                                      A 354
      CALL GMPRD (NST,M1,PHI,PSI,N,N,1)                                  A 355
C     ********************                                               A 356
C     EVALUATE CONSTANTS IN INHOM. SEPARATED SOLUTIONS PSI(B)            A 357
C     ********************                                               A 358
      DO 35 I=1,N                                                        A 359
      F1(I)=-INHF(I)/EIVAL(I)                                            A 360
35    D1(I)=PSI(I)-F1(I)                                                 A 361
C     ********************                                               A 362
C     SOLVE FOR PHI(B)= EIVEC*PSI(B) = GD*EXPO + GF                      A 363
C     ********************                                               A 364
      DO 36 I=1,N                                                        A 365
      DO 36 J=1,N                                                        A 366
36    GD(I,J)=EIVEC(I,J)*D1(J)                                           A 367
      CALL ARRAY (2,N,N,NDS,ND,ND,M1,GD)                                 A 368
      CALL GMPRD (NST,M4,F1,GF,N,N,1)                                    A 369
      DO 37 I=1,N                                                        A 370
37    EXPO(I)=DEXP(EIVAL(I))                                             A 371
      CALL GMPRD (NST,M1,EXPO,CDTFO,N,N,1)                               A 372
      WRITE (1,71)                                                       A 373
      DO 38 I=1,N                                                        A 374
      CDTFO(I)=CDTFO(I)+GF(I)                                            A 375
      CDTFO(I)=CDTFO(I)*DTHI+TA+SS/UL                                    A 376
38    WRITE (1,72) I,CDTFO(I)                                            A 377
C     ********************                                               A 378
C     FIND DTFO AVE.                                                     A 379
C     ********************                                               A 380
      CALL AVE (N,CDTFO,DTFO,NNT,IX)                                     A 381
      TFO=SNGL(DTFO)                                                     A 382
C     ********************                                               A 383
C     FIND DTFI MEAN VALUES                                              A 384
```

```
C       **********                                                      A 385
        DO 39 I=1,N                                                     A 386
39      EXPO(I)=(EXPO(I)-1.0D+0)/EIVAL(I)                               A 387
        CALL GMPRD (NST,M1,EXPO,CDTFO,N,N,1)                            A 388
        DO 40 I=1,N                                                     A 389
40      CDTFO(I)=CDTFO(I)+GF(I)                                         A 390
C       **********                                                      A 391
C       FIND DTFM                                                       A 392
C       **********                                                      A 393
        CALL AVE (N,CDTFO,DTFM,NNT,IX)                                  A 394
        DTFM=DTFM*DTHI+TA+SS/UL                                         A 395
        TFM=SNGL(DTFM)                                                  A 396
C       **********                                                      A 397
C       FIND DTBI MEAN VALUES                                           A 398
C       **********                                                      A 399
        CONV=**XMDOT*CP*1.0D+03/Y                                       A 400
        DO 41 I=1,N                                                     A 401
        DO 41 J=1,N                                                     A 402
41      GM(I,J)=CONV*GM(I,J)                                            A 403
        DO 42 I=1,N                                                     A 404
42      INH1(I)=CONV*INH1(I)                                            A 405
        DO 43 I=1,N                                                     A 406
43      GM(I,I)=GM(I,I)+1.0D+0                                          A 407
        CALL ARRAY (2,N,M,NDS,ND,ND,M2,GM)                              A 408
        CALL GMPRD (NST,M3,CDTFO,SMAT,N,N,1)                            A 409
        DO 44 I=1,N                                                     A 410
44      CDTFO(I)=SMAT(I)+INH1(I)                                        A 411
C       **********                                                      A 412
C       FIND DTBM                                                       A 413
C       **********                                                      A 414
        CALL AVE (N,CDTFO,DTBM,NNT,IX)                                  A 415
        DTBM=DTBM*DTHI+TA+SS/UL                                         A 416
```

```
      TBM=SNGL(DTBM)                                                    A 417
C     ********************                                              A 418
C     FIND DTPI MEAN VALUES                                             A 419
C     ********************                                              A 420
      FAC=(DCOSH(NP)-1.0D+0)/NP/DSINH(NP)                               A 421
      SUMP=0.0D+0                                                       A 422
      DO 45 I=1,IX                                                      A 423
      TP(I)=FAC*(CDTFO(I)+CDTFO(I+1))                                   A 424
45    SUMP=SUMP+TP(I)                                                   A 425
      IF (NNT.NE.2) GO TO 46                                            A 426
      TPR=FAC*(2.0D+0*CDTFO(N))/(1.0D+0+DLTE)                           A 427
46    CONTINUE                                                          A 428
      DFAC=AE*DSINH(NE)/NE+DCOSH(NE)                                    A 429
      GFAC=(AE*(DCOSH(NE)-1.0D+0)/NE**2)/DFAC                           A 430
      FFAC=GFAC+DSINH(NE)/(NE*DFAC)                                     A 431
      TT=SS*(1.0D+0/UL-1.0D+0/ULE)*(FFAC-1.0D+0)/DTHI-SS*GFAC/ULE/DTHI  A 432
      TPL=TT+FFAC*CDTFO(1)                                              A 433
      IF (NNT.NE.1) GO TO 47                                            A 434
      TPR=TT+FFAC*CDTFO(N)                                              A 435
47    CONTINUE                                                          A 436
      IF (NNT.NE.3) GO TO 48                                            A 437
      TPR=0.0D+0                                                        A 438
48    CONTINUE                                                          A 439
C     ********************                                              A 440
C     FIND DTPM                                                         A 441
C     ********************                                              A 442
      WD=W-D                                                            A 443
      WD2=WD/2.0D+0                                                     A 444
      WD3=WD2*(1.0D+0+DLTE)                                             A 445
      IF (NNT.NE.3) GO TO 49                                            A 446
      SYM3=2.0D+0                                                       A 447
      GO TO 50                                                          A 448
```

```
49    CONTINUE                                                                  A 449
      SYM3=1.0D+0                                                               A 450
50    CONTINUE                                                                  A 451
      IF (NNT.EQ.1) GO TO 51                                                    A 452
      SYM=2.0D+0                                                                A 453
      GO TO 52                                                                  A 454
51    CONTINUE                                                                  A 455
      SYM=1.0D+0                                                                A 456
52    CONTINUE                                                                  A 457
      SUMB=0.0D+0                                                               A 458
      DO 53 I=1,IX                                                              A 459
53    SUMB=SUMB+CDTFO(I)                                                        A 460
      DTPM=(TPL*WD3+SUMP*WD+TPR*WD3+SUMB*D+CDTFO(N)*D/SYM3)/(WT/SYM)            A 461
      DTPI=(WT*DTPM-TPL*WD3*2.0D+00)/(W*(NT-1)+D)                               A 462
      DTPI=DTPI*DTHI+TA+SS/UL                                                   A 463
      DTPF=TPL*DTH1+TA+SS/UL                                                    A 464
      TPME=SNGL(DTPF)                                                           A 465
      TPMI=SNGL(DTPI)                                                           A 466
      DTPM=DTPM*DTHI+TA+SS/UL                                                   A 467
      TPMA=SNGL(DTPM)                                                           A 468
C     ********************                                                      A 469
C     EVALUATE PLATE TEMP. DIST.                                                A 470
C     ********************                                                      A 471
      IF (LDIST.EQ.0) GO TO 66                                                  A 472
      LOC=4                                                                     A 473
      LOCF=2                                                                    A 474
      REAL=LOC*1.0D+0                                                           A 475
      FREAL=LOCF*1.0D+0                                                         A 476
      LOCFE=LOCF+1                                                              A 477
      DO 54 J=1,LOCFE                                                           A 478
      I=J-1                                                                     A 479
54    DIV(J)=I/FREAL                                                            A 480
```

```
      JJ=1                                                              A 481
55    CONTINUE                                                          A 482
      DO 56 I=1,N                                                       A 483
56    EXPO(I)=DEXP(EIVAL(I)*DIV(JJ))                                    A 484
      CALL GMPRD (NST,M1,EXPO,CDTFO,N,N,1)                              A 485
      DO 57 I=1,N                                                       A 486
57    CDTFO(I)=CDTFO(I)+GF(I)                                           A 487
      CALL GMPRD (NST,M3,CDTFO,SMAT,N,N,1)                              A 488
      DO 58 I=1,N                                                       A 489
58    CDTFO(I)=SMAT(I)+INH1(I)                                          A 490
      LOCE=LOC+1                                                        A 491
      DO 59 J=1,LOCE                                                    A 492
      I=J-1                                                             A 493
      FACF(J)=(AE*DSINH(NE*I/REAL)/NE+DCOSH(NE*I/REAL))/DFAC            A 494
      FACG(J)=AE*DSINH(NE*(1.0D+0-I/REAL))/NE/DFAC                      A 495
      TT=SS*((1.0D+0/UL-1.0D+0/ULE)*(FACF(J)-1.0D+0)-FACG(J)/ULE)/DTHI  A 496
      TL(J)=(TT+FACF(J)*CDTFO(1))*DTHI+TA+SS/UL                         A 497
      IF (NNT.NE.1) GO TO 59                                            A 498
      TR(LOCE+1-J)=(TT+FACF(J)*CDTFO(N))*DTHI+TA+SS/UL                  A 499
59    CONTINUE                                                          A 500
      DO 60 I=1,IX                                                      A 501
      DO 60 JK=1,LOCE                                                   A 502
      J=JK-1                                                            A 503
60    TPD(I,JK)=((CDTFO(I+1)*DSINH(NP*J/REAL)+CDTFO(I)*DSINH(NP*(1.0D+0-  A 504
     1J/REAL)))/DSINH(NP))*DTHI+TA+SS/UL                                A 505
      IF (NNT.NE.2) GO TO 62                                            A 506
      LOC1=LOC/2+1                                                      A 507
      DO 61 I=1,LOC1                                                    A 508
      J=I-1                                                             A 509
61    TP(I)=(CDTFO(N)*(DSINH(NP*J/REAL)+DSINH(NP*(1.0D+0-J/REAL)))/DSINH  A 510
     1(NP))*DTHI+TA+SS/UL                                               A 511
62    CONTINUE                                                          A 512
```

```
      JL=JJ-1                                                          A 513
      WRITE (1,73) JL                                                  A 514
      WRITE (1,74) (TL(I),I=1,LOCE)                                    A 515
      DO 63 I=1,IX                                                     A 516
      WRITE (1,75) I,(TPD(I,J),J=1,LOCE)                               A 517
63    CONTINUE                                                         A 518
      IF (NN1.EQ.3) GO TO 65                                           A 519
      IF (NNT.EQ.2) GO TO 64                                           A 520
      WRITE (1,74) (TR(I),I=1,LOCE)                                    A 521
      GO TO 65                                                         A 522
64    CONTINUE                                                         A 523
      WRITE (1,76) (TR(I),I=1,LOC1)                                    A 524
65    CONTINUE                                                         A 525
      IF (JJ.EQ.LOCFE) GO TO 66                                        A 526
      JJ=JJ+1                                                          A 527
      GO TO 55                                                         A 528
66    CONTINUE                                                         A 529
      RETURN                                                           A 530
C                                                                      A 531
67    FORMAT (/,13HNON-SYMMETRIC)                                      A 532
68    FORMAT (/,9HSYMMETRIC)                                           A 533
69    FORMAT (/,27HNTH EIGENVECTOR ELEMENT = 0)                        A 534
70    FORMAT (/,16HEIGENVALUE ERROR)                                   A 535
71    FORMAT (1X,13H     TFD LOCAL)                                    A 536
72    FORMAT (1X,I2,3H   ,D23.8)                                       A 537
73    FORMAT (/,10HY LOCATION,2X,I2,/)                                 A 538
74    FORMAT (/,21HEDGE PLATE TEMP DISTR,/,5D23.7)                     A 539
75    FORMAT (/,14HINTERNAL PLATE,1X,I2,1X,10HTEMP DISTR,/,5D23.7)     A 540
76    FORMAT (/,25HSYM HALF-WIDTH TEMP DISTR,/,5D23.7)                 A 541
      END                                                              A 542
      SUBROUTINE AVE (N,CDTFL,DTA,NNT,IX)                              P   1
      IMPLICIT REAL*8 (A-H,O-Z)                                        P   2
```

```
      DIMENSION CDTFO(N)                                                B   3
      SUM=0.0D+0                                                        B   4
      DO 1 I=1,IX                                                       B   5
1     SUM=SUM+CDTFO(I)                                                  B   6
      RTTEMP=CDTFO(N)                                                   B   7
      IF (NNT.NE.3) GO TO 2                                             B   8
      SYM=2.0D+0                                                        B   9
      NT=2*N-1                                                          B  10
      GO TO 3                                                           B  11
2     CONTINUE                                                          B  12
      NT=N                                                              B  13
      SYM=1.0D+0                                                        B  14
3     CONTINUE                                                          B  15
      SUM=SYM*SUM+RTTEMP                                                B  16
      DTA=SUM/(1.0D+0*NT)                                               B  17
      RETURN                                                            B  18
      END                                                               B  19
      REAL FUNCTION KD*8(I,J)                                           C   1
      KD=0.0D+00                                                        C   2
      IF (I.NE.J) GO TO 1                                               C   3
      KD=1.0D+00                                                        C   4
1     CONTINUE                                                          C   5
      RETURN                                                            C   6
      END                                                               C   7
```

VITA

Clifford Keith Rice was born in Farmville, Virginia, on August 8, 1952. He graduated from Crewe High School in Crewe, Virginia, in June 1970.

In September of 1970, Mr. Rice became a student at Virginia Polytechnic Institute and State University. He graduated with distinction in June 1974 with a B.S. degree in Nuclear Science.

In the fall of 1974, he began graduate work at the same institution and received an M.S. degree in Nuclear Science and Engineering in July 1976. He then began his studies for the Ph.D. degree in Mechanical Engineering.

Mr. Rice is married to the former Judith Kay Fowlkes of Burkeville, Virginia, and presently resides in Oak Ridge, Tennessee.

Clifford Keith Rice

Clifford Keith Rice

ANALYTICAL METHODS FOR EVALUATING TWO-DIMENSIONAL EFFECTS IN FLAT-PLATE SOLAR COLLECTORS

by

Clifford Keith Rice

(ABSTRACT)

Presently, there exist significant discrepancies between experimental and theoretical predictions of flat-plate solar collector performance. There is a need to identify both those areas of analysis which need improvement as well as those which are already adequate.

Two new methods of absorber-plate thermal analysis which can be used within the framework of existing theory were developed. The first method used the separation of variables technique in a unique manner to solve exactly for the coupled axial and transverse temperature distributions in an absorber plate-tube assembly. The conventional assumption of an overall uniform loss coefficient U_L was used in the analysis. The first method is practical only for parallel-flow collectors. The second method used two sectionally uniform loss coefficients -- U_{LI} for internal collector sections and U_{LE} for edge sections -- to evaluate collector performance. The second method is applicable for both parallel-flow and serpentine configurations.

The validity of two assumptions commonly made in flat-plate collector analysis was investigated using the new methods. The first assumption that was investigated involved the approximate treatment

of the effect of axial conduction on the absorber-plate temperature distributions. Results from the first new method were graphically compared to the predictions of approximate analytical treatments given by Whillier and Phillips. The comparisons showed that, for conventional flat-plate designs, the method given by Phillips yields values of the heat removal factor F_R accurate to within 1 per cent. The more commonly used method given by Whillier is accurate to within 10 per cent for conventional designs. The second assumption that was investigated dealt with the manner in heat losses from the collector peripheral area are taken into account. Results from the second new method indicated that, for typical collector designs, the conventional edge loss treatment yields values of instantaneous collector efficiency η_c accurate to within 3 per cent absolute and 15 per cent relative. Analysis of the net effect of the two improvements indicated that approximate axial and edge-loss treatments are not the primary source of error between experimental and theoretical results for typical collectors.

The solution technique developed in the first new method has potential applications to a number of conduction-convection problems. The second new method has the inherent capability to better evaluate performance and design questions related to edge effects.

Convenient relations between the mean plate and fluid temperatures and the heat removal factor F_R were obtained. The relations apply for parallel-flow analysis under the assumption of a uniform loss coefficient U_L.